8-2016

Molecular Docking, Synthesis and Evaluation of Pyrrolo[2,1-c][1,4]benzodiazepines Derivatives as Non-β-lactam β-lactamases Inhibitors

Joseph Osamudiamen Osazee
East Tennessee State University

Molecular Docking, Synthesis and Evaluation of Pyrrolo[2,1-*c*][1,4]benzodiazepines Derivatives as Non-β-lactam β-lactamases Inhibitors

---

A thesis

presented to

the faculty of the Department of Chemistry

East Tennessee State University

in partial fulfilment

of the requirements for the degree

Master of Science in Chemistry

---

by

Joseph Osamudiamen Osazee

August 2016

Dr. Abbas G. Shilabin, Chair

Dr. Marina Roginskaya

Dr. Aleksey Vasiliev

Dr. Dhirendra Kumar

Keywords: Antibiotic resistance, β-Lactamases inhibitors, Pyrrolo[2,1-*c*][1,4]benzodiazepines (PBD), Lipinski's rule, Molecular docking, Enzyme kinetics.

ABSTRACT

Molecular Docking, Synthesis, and Evaluation of Pyrrolo[2,1-*c*][1,4]benzodiazepines Derivatives as Non-β-lactam β-lactamases Inhibitors.

by

Joseph O. Osazee

Our research aim was to design, synthesize, and study the competitive enzyme inhibition kinetics of pyrrolo[2,1-c][1,4]benzodiazepine (PBD) derivatives as potential non-β-lactam β-lactamase inhibitors. All compounds (**1-13**) passed the Lipinski's rule of 5 test and were docked into the active site of TEM-1 β-lactamase. PBD derivatives **1-7** were synthesized in high yields and tested for their potency against TEM-1 and P99 β-lactamases. Kinetic data showed that compounds **1, 4, 5,** and **7** possessed inhibitory activity against TEM-1 ranging from 4-34 %. Docking results revealed significant interactive spanning of the active site of TEM-1 by PBDs. The limited inhibitory activity of the compounds, **1-7** could be attributed to the lack of solubility and bulky nature of the molecules, thus limiting the optimal ligand-enzyme interactions. 1,2,4-Oxadiazolinones (**8-13)** were further synthesized to reduce the steric hindrance of the PBD scaffolds while promoting the electrophilicity of the potentially active lactam and also evaluated for potency.

DEDICATION

This work is dedicated to the Almighty God for His sustenance, protection, and guidance, my lovely wife, Mrs. Stacy Ehinomen Joseph-Osazee, my parents, Engr. Goodluck O. Osazee and Mrs. Esther Osazee, and my siblings.

ACKNOWLEDGEMENTS

My sincere thanks to God Almighty for His protection, sustenance, care, abundant grace, and love throughout my study.

I would also like to express my deepest gratitude to my advisor, Dr. Abbas G. Shilabin for his excellent guidance, patience, encouragement and providing me with an excellent atmosphere throughout this research work.

Thanks to Dr. Marina Roginskaya, Dr. Aleksey Vasiliev, and Dr. Dhirendra Kumar for serving as committee members and also Dr. Reza Mohseni for his assistance with instrumentation for this work.

I use this opportunity to express my profound gratitude to the Chair of the Department of Chemistry, Dr. Cassandra Eagle creating an enabling environment and enforcing safety policies which are important for doing proper research in the Chemistry.

I also want to thank the graduate coordinator of the Chemistry Department, Dr. Scott Kirkby for his assistance with questions at research scrum and help in understanding some of the computational chemistry parts of my work.

I am also grateful to all the faculty members of the Department of Chemistry, ETSU for their help and support. I also wish to appreciate the ETSU start-up grant for funding this research and graduate school staffs especially Ms. Queen Brown (the graduate office manager) for all her support and advice.

I also thank my wife, my parents and my family for their unceasing encouragement, support, and attention.

Finally, I wish to express my gratitude to all past and present graduate students of the Department of Chemistry, ETSU and my friends (particularly Ms. Constance Warden, Ms. Opeyemi Adetola, Mr. Joel Annor-Gyamfi, Mrs Pushpa Reddy, Mr. Chris Acquach, Mr. Isaac Addo and Mr. Emmanuel Onobun to mention but a few) for their support throughout my study.

TABLE OF CONTENTS

Page

LIST OF TABLES

LIST OF FIGURES

LIST OF SCHEMES

LIST OF ABBREVIATIONS

µL	microliter
Ala	Alanine
Arg	Arginine
Asn	Asparagine
DMSO	Dimethyl sulfoxide
DNA	Deoxyribonucleic acid
FT-IR	Fourier Transform Infra-Red
GC-MS	Gas Chromatography Mass Spectrometer
h	hours
K_2CO_3	Potassium carbonate
KBr	Potassium bromide
Kcal	kilocalories
Lys	Lysine
$MgSO_4$	Magnesium sulfate
min	minutes
mL	milliliter

mmol	millimoles
MOPS	(3-(*N*-morpholino)propanesulfonic acid)
$Na_2S_2O_3$	Sodium thiosulfate
Na_2SO_4	Sodium sulfate
NaCl	Sodium chloride
$NaHCO_3$	Sodium bicarbonate
nm	nanometer
nM	nanomolar
NMR	Nuclear Magnetic Resonance
ORTEP	Oak Ridge Thermal Ellipsoid Plot Program
PBDs	Pyrrolo[2,1-*c*][1,4]benzodiazepines
RT	Retention time
rt	Room temperature
rx	reflux
Ser	Serine
TLC	Thin Layer Chromatography
UV/Vis	Ultraviolet/Visible

CHAPTER 1

INTRODUCTION AND LITERATURE REVIEW

History of β-lactam Antibiotics

β-lactam antibiotics have continued to be the most popular drug for treating bacterial infections since their discovery in 1928 by Fleming and their introduction as antibacterial agents in the early 1950.[1] Most commonly used β-lactam drugs today stem from the original discovery and development of natural products from microorganisms like penicillin, cephalosporin, and other β-lactam based antibiotics (Figure 1).[1,2] However, soon after its commercialization, β-lactamases secreting penicillin resistant strains of *Staphylococcus aureus* were isolated.[3] The introduction of methicillin (a β-lactamase-insensitive semi-synthetic penicillin), to curb the resistance problem resulted in the evolution of another resistant strain known as methicillin-resistant Staphylococcus aureus (MRSA).[4]

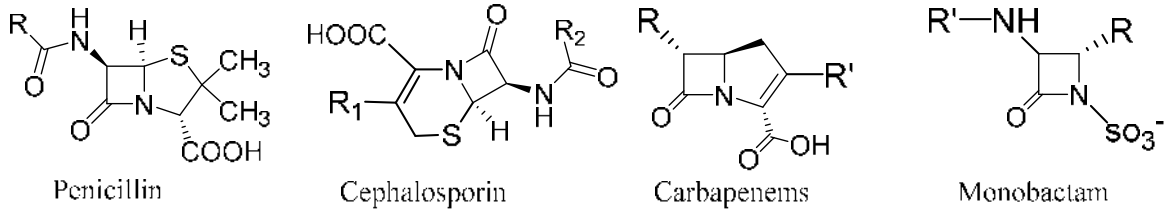

Figure 1: Some β-lactam Antibiotics

Resistance to β-lactams was easy for bacteria as all β-lactams shared the same mode of action which was the inhibition of bacterial cell wall synthesis by forming a stable covalent adduct with the active site serine residues of penicillin-binding proteins (PBPs). The PBPs are often divided into two classes: the high molecular weight PBPs (HMW-PBPs) and the low-

molecular weight PBPs (LMW-PBPs). The HMW-PBPs are further divided into two classes, A and B while the LMW-PBPs are divided into four subclasses based on their tertiary structures.[5]

The major target of the β-lactams are the HMW-PBPs as they are important for cell survival. Class A HMW-PBPs catalyze the formation of the glycan chains (trans-glycosylation) and both class A and class B PBPs catalyze the cross-linking of peptidoglycan stem-peptides (transpeptidation) on the external side of the cytoplasmic membrane.[5]

The reduced toxicity and high specificity of peptidoglycan synthesis-inhibiting drugs to humans also made β-lactams more preferable in bacterial inhibition as compared to other antibiotics.[5]

Thus, there is a need for more research into finding non-β-lactams drugs that also display high specificity for the target site, low toxicity to human cells, and are unhydrolysable by β-lactamases.

Bacteria have succeeded over the years in developing various mechanisms to resist β-lactams. These strategies or mechanisms include:

1. Production of β-lactamases, which catalyze the hydrolysis of the β-lactam rings in β-lactams and subsequent transfer of plasmids, encoded with β-lactamases genes amongst related and unrelated species. This is the most vital resistance mechanism in Gram-negative bacteria e.g. *Neisseria gonorrhoeae* and *Haemophilus influenza*e.[6-9]
2. Another important mechanism in Gram-positive bacteria is the production of low-affinity PBPs which catalyze the transpeptidation reaction even in the presence of high concentrations of β-lactam antibiotics. Most bacteria achieve this by mutations of residues surrounding the active sites of the PBPs thus lowering the affinity of PBPs to β-

lactam. This is mostly observed in non-β-lactamase producing Gram-negative bacteria and most Gram-positive bacteria (e.g. *Streptococcus pneumoniae* and MRSA).[5,7,10]

3. Target site accessibility also plays a key role in β-lactam drug action; the effectiveness of β-lactams is dependent on their ability to cross the outer membrane and this is facilitated by the outer membrane proteins (OMPs). However, bacteria further develop resistance to β-lactam drugs by decreasing the production of such OMPs that facilitates the transport of the β-lactams through the outer membrane of the cell, thus lowering their effectiveness and increasing the minimum inhibitory concentration of such antibiotics. This is often combined with another resistance mechanism such as β-lactamase expression.[11,12]
4. Decreasing the effective concentration of drugs in their periplasm is also exhibited by Gram-negative bacteria through efflux pumps that facilitate the export of β-lactams outside the cells.[12]

β-Lactamases

The β-lactamase enzyme was first identified and isolated by E. P. Abraham and E. Chain from *Bacillus* (*Escherichia*) *coli* and they described it as *B. coli* "penicillinase".[13] This occurred before the clinical use of penicillin. β-lactamases were not thought to be clinically relevant as of that time since penicillin was targeted to treat staphylococcal and streptococcal infections, as researchers then were unable to isolate the enzyme from these Gram-positive organisms. [13,14,15] Kirby *et. al.* successfully isolated these penicillinases from *Staphylococcus aureus* in 1944 and this signaled the emergence of a major clinical problem as these enzymes would in some years later become one of the leading causes of antibacterial resistance worldwide.[16]

The ever expanding number of β-lactam antibiotics has since increased the selective pressure on bacteria, promoting the survival of organisms with multiple β-lactamases.[17,18] Over 850 β-lactamases have been identified and it is speculated that high mutation frequency, rapid recombination, and replication rates are responsible for bacteria being able to adapt to novel β-lactams by evolution of these β-lactamases.[19]

Classification of β-lactamases

There are two major classification schemes that are used for categorizing β-lactamase enzymes:

1. The Ambler Classes A through D, based on amino acid sequence homology, and
2. The Bush-Jacoby-Medeiros groups 1 through 4, based on substrate and inhibitor profile.[20,21]

Classes A, C, and D serine-β-lactamase are known to share a lot of structural similarities which make them hydrolyze β-lactams similarly. However, Class B β-lactamases are metallo-β-lactamases (MBLs) and they possess either a single Zn^{2+} ion or a pair of Zn^{2+} ions coordinated to His/Cys/Asp residues in the active site.[22]

The Ambler classification scheme has been used in this literature review.

Class A Serine β-lactamase

Generally, most class A enzymes are susceptible to the commercially available most β-lactamase inhibitors like clavulanate, however, the *K. pneumoniae* carbapenemase (KPC) may be an important exception to this generalization as they are resistant to clavulanate.[23]

Class A Extended-spectrum β-lactamases (ESBLs)

They are known to hydrolyze many of the oxyimino-cephalosporins, monobactam (aztreonam) (but not cephamycins or carbapenems), and penicillin conferring resistance to bacteria that possess them. This class is also well known to be inhibited by clavulanate.[24,25]

Class A Serine Carbapenemases

Class A serine carbapenemases include the *nonmetallo c*arbapenemase of class A (NMC-A), IMI, SME, and KPC. Carbapenems as well as cephalosporins, penicillins, and aztreonam can be hydrolyzed by members of this group. This class of β-lactamases has been observed to occur in *Enterobacter cloacae*, *Serratia marcescens*, and *K. pneumoniae* and are also susceptible to clavulanate. [26]

Class B Metallo-β-lactamases

These enzymes are Zn^{2+} dependent β-lactamases and they hydrolyze β-lactam antibiotics in with a mechanism different from the other classes of β-lactamases (A, C, and D). They hydrolyze and thus exhibit resistance to cephalosporins, carbapenems, penicillins, and the clinically available β-lactamase inhibitors. An example is the New Delhi Metallo-β-lactamases [21,27]

Class C Serine Cephalosporinase

Class C serine cephalosporinase accounts for an array of β-lactamase enzymes that are mostly encoded in the *bla* gene of bacterial chromosomes. Organisms expressing this β-lactamase are typically resistant to penicillins, β-lactam β-lactamase inhibitor combinations, and

cephalosporins, including cefoxitin, cefotetan, ceftriaxone, and cefotaxime. However, AmpC enzymes are known to be inhibited by cloxacillin, oxacillin, and aztreonam.[21,28]

Class D Serine Oxacillinases

They were at first termed "oxacillinases" due to their ability to hydrolyze oxacillin at a rate of at least 50%, in contrast to the relatively slow hydrolysis of oxacillin by classes A and C. They are capable of conferring resistance to carbapenems, cephalosporins, and penicillins. [29]

Evolution of β-lactam and non-β-lactam β-lactamase inhibitors

Due to the prevailing β-lactam resistance, the need for more effective inhibitors of β-lactamases and bacterial growth has become more pertinent. The trend of antibiotic misuse and overuse, including their utilization as growth promoters in animals, has further enhanced bacterial resistance in recent times.[30]

Since 1970, various β-lactamase inhibitors (clavulanic acid, tazobactam, and sulbactam, [Figure 2]) have been introduced into clinical medicine. They all possess a four-membered β-lactam ring and are inactivators or "suicide inhibitors" of class A β-lactamases. They significantly reduce MICs against various bacteria when combined with β-lactam-antibiotics. Examples of such synergistic drug combinations include Augmentin™ (amoxicillin and clavulanate), Unasyn™ (ampicillin and sulbactam) and Zosyn™ (piperacillin/tazobactam). Notwithstanding the efficacy of these antibiotics, resistance was still observed after several years of employing these combinational therapies for the treatment of bacterial infections. This resistance was observed to be resulting from the production of inhibitor-resistant β-lactamases or enzyme hyper production. During the last 40 years, numerous β-lactamase inhibitors, β-lactams,

and non-β-lactams have been developed to try to curb this scourge (antimicrobial resistance).[6,31,32]

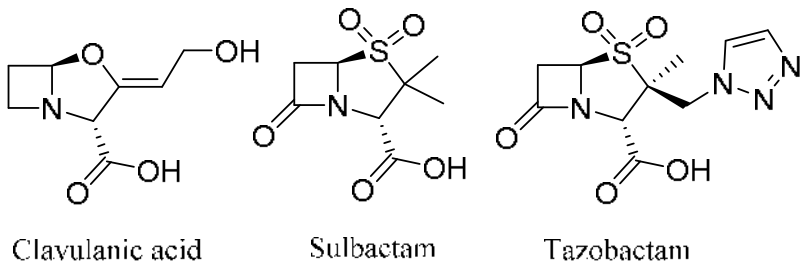

Figure 2: β-lactam based β-lactamases inhibitors

Non-β-lactam Inhibitors

Aside the regular β-lactams based drugs and their derivatives, more scientists have focused their attention on the synthesis and isolation of effective non-β-lactam based PBP inhibitors which are also able to evade β-lactamase hydrolysis.

NXL104 (avibactam) (Figure 3) is a non-β-lactam that inhibits serine β-lactamases. In combination with extended-spectrum cephalosporins and aztreonam, it is potent against Gram-negative infections (including *Klebsiella*).[33–35] NXL104 has been the first β-lactamase inhibitor to be studied in clinical trials since the introduction of tazobactam.[36]

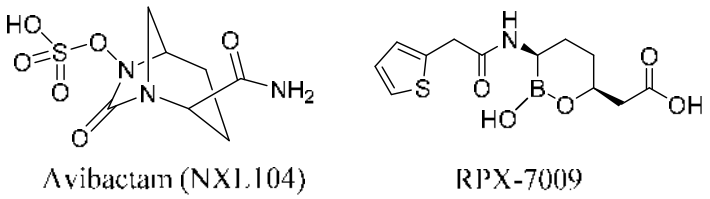

Figure 3: Non β-lactam based β-lactamases inhibitors

The non β-lactam based PBP inhibitors can be classified into three major groups:

1. Transition state analogs
2. Substrate analogs and
3. Non-covalent inhibitors

1. Transition State Analog: Transition State Analog (TSA) inhibitors have been found to be efficient serine β-lactamases and protease inhibitors.[6,37,38] TSA inhibitors like boronic acid, carbonyl compounds, and phosphonates have been identified as potent inhibitors of PBPs. Boronic acid binds preferentially to the LMW-PBPs.[5,39] Boronic acid compounds form reversible, covalent bonds with serine proteases and inhibits these enzymes by assuming tetrahedral reaction intermediates.[40,41]

Carbonyl compounds [peptide aldehydes Boc-L-Lys(Cbz)-D-Ala-H (K_i = 60 μM) and Boc-L-Lys(Cbz)-L-Ala-H (K_i = 79 μM)] have also been identified as inhibitors of *N. gonorrhoea* PBP3.[42]

Phosphonates are also known to be strong inhibitors of serine proteases which in some ways are related to β-lactamase. The clinical potential of phosphonates has been limited by their poor stability in aqueous solution and susceptibility to phosphodiesterases.[6,43]

2. Substrate Analogs: Substrate analogs react as suicide substrates by acylation of the PBP active serine, similarly to acylation by β-lactams.[5] Bicyclic pyrazolidinones and the lactivicins (LTV) have been shown to exhibit clinically relevant levels of antibacterial activities and PBP inhibitors.[44-46]

Bicyclic pyrazolidinones (Figure 4) compounds with strong electron withdrawing groups in C3 positions were shown to have better *in vitro* activities compared to others.[44]

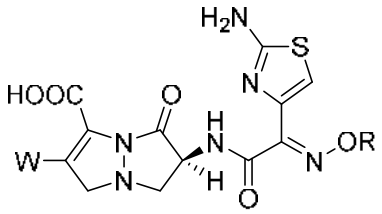

W = $COCH_3$, R = Me
W = SO_2Me, R = Me
W = SO_2Me, R = $C(CH_3)COOH$

Figure 4: Bicyclic pyrazolidinones[44]

Lactivicin (LTV) (Figure 5) was the first natural PBP inhibitor without a β-lactam ring to be isolated in 1986 from bacterial strains (*Empedobacter lactamgenus* and *Lysobacter albus*) by the Takeda Research group.[47-52]

It possesses a unique ring structure comprising a functionalized L-cycloserinyl ring linked to a γ-lactone ring. Its spectra of activity span a wide range of Gram-negative and Gram-positive bacteria; however, its relatively strong toxicity was a setback. LTV derivatives have been synthesized to increase its antibacterial activity against Gram-negative bacteria and minimize its toxicity.[45,47-52]

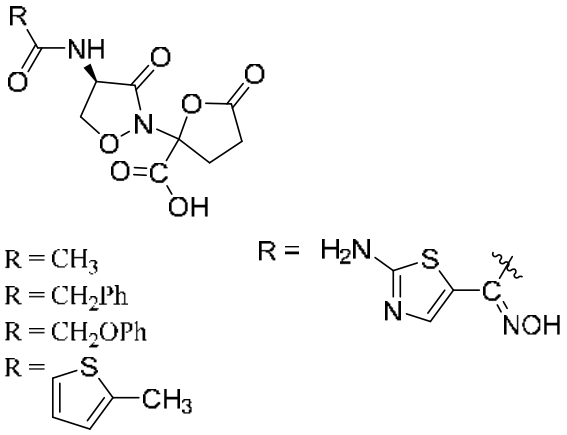

Figure 5: Lactivicin analogs[45]

3. Non-covalent Inhibitors: Non-covalent inhibitors bind tightly to the active site of PBPs without acylation, thus making them highly effective inhibitors. They do not require the unfavorable conformational changes in the active site of PBP2a of MRSA that is required for acylation.[53,54] Examples of non-covalent inhibitors are arylalkylidene rhodanines, arylalkylidene iminotriazolidenes (inhibitors of class C β-lactamases in the micromolar range), aminothiadiazole and *ortho*-phenoxyldiphenylurea derivatives, naphthalene sulfonamides, anthranilic acids, Cibacron Blue and Erie Yellow, cyclic peptides, and quinolones. 4-Quinolones were found to be noncovalent inhibitors of PBPs of *E. coli* and *B. subtilis* however, all active 4-quinolones had no *in vitro* antibacterial activities against *E. coli* or *B. subtilis* on their own.[55-60]

Pyrrolo[2,1-*c*][1,4]benzodiazepines (PBDS)

Pyrrolo[2,1-*c*][1,4]benzodiazepines (PBDs) are a group of natural products found in actinomycetes commonly possessing a pyrrolo[1,4]benzodiazepine ring system. The first PBD to be isolated and studied was Anthramycin from *Streptomyces refuineus*. It was first successfully synthesized in a laboratory setting by Leimgruber *et al.* in 1965.[61]

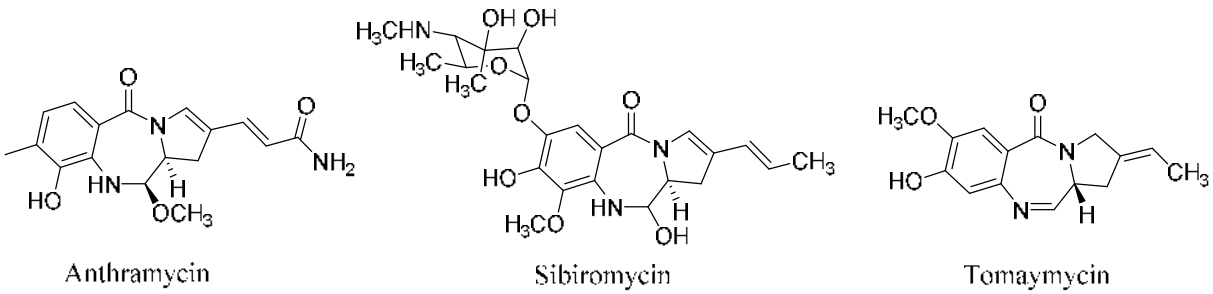

Figure 6: Examples of biologically active pyrrolobenzodiazepines

PBDs such as tomaymycin, anthramycin, and sibromycin (Figure 6) which have been isolated and developed over the years exert potent antibacterial activity against human pathogens through their ability to bind to DNA. This is done through the formation of covalent bond through their N10-C11 imine/carbinolamine moieties to the C2-amino position of a guanine residue within the minor groove of DNA (Figure 7). Monomers of PBDs (e.g. Anthramycin) span three DNA base pairs with a preference for Pu-G-Pu (where Pu = purine and G = guanine; reactive guanine emboldened) sequences and block transcription through RNA polymerase inhibition.[61-64]

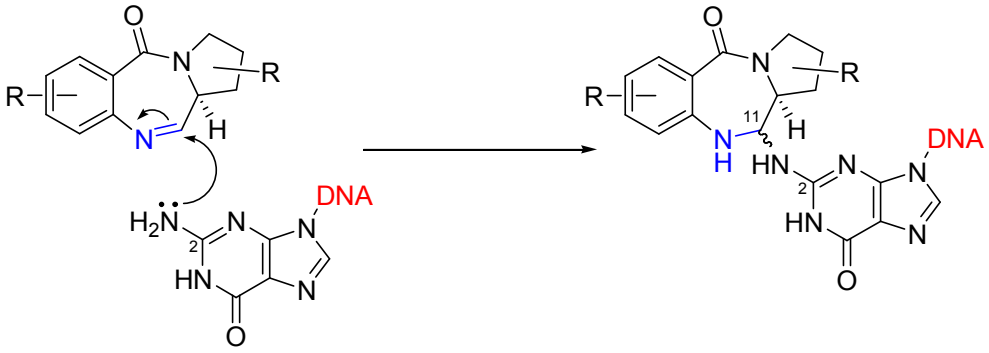

Figure 7: Mechanism of PBD binding to the N2 of guanine in the DNA minor groove.

Tethering of two PBD units through an inert propyldioxy [-O-(CH2)3-O-diether] or pentyldioxy [-O-(CH2)5-O-diether] linker via their C8/C8′ positions to form dimers (e.g. ELB-21) has also been shown to enhance potency, binding affinity, and sequence specificity of PBDs. These dimers are capable of cross-linking appropriately separated guanines on opposing DNA strands.[65]

High degree of cytotoxicity over the years have, however, rendered PBDs unattractive as antibacterial antibiotics when compared to other classes of antimicrobial compounds even if some PBDs have potentials as cancer chemotherapeutics. Notwithstanding, increasing evolution of multidrug-resistant pathogens capable of a rapid and efficient horizontal transmission of genes encoding antibiotic resistance determinants has led to the erosion of most of the front-line antibacterial chemotherapeutic agents of therapeutic value in a relatively short time frame. This has led to the reconsideration of PBDs and other possibly cytotoxic antibiotics as possible lead compounds for the production of better antibacterial agents by many research groups.[66,67] More recently, Colistin, a polymyxin antibiotic which was deemed too toxic for non-topical use is now widely used systemically due to the limited therapeutic options available for these infections.[68]

ELB-21 (Figure 8) is a pyrrolo[2,1-c][1,4]benzodiazepine (PBD) dimer that shows potent in vitro bactericidal activity against a wide range of Gram-positive clinical isolates, including methicillin-resistant strains of *Staphylococcus aureus* (MRSA) and vancomycin-resistant enterococci (VRE).[69]

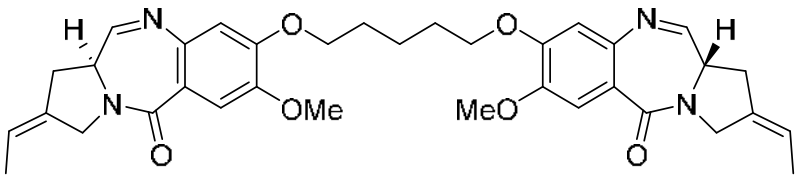

Figure 8: Structure of the pyrrolobenzodiazepine dimer ELB-21

Justification of Research

One of the major reason for trying to exploit PBDs as possible β-lactamase inhibitors stemmed from the fact that PBDs have regions in their structure that are similar to the active region of regular β-lactam β-lactamase inhibitors. In theory, by breaking a bond in regular β-lactam β-lactamase inhibitors, we could arrive at PBD analogs that bear the same sites of activity as regular β-lactam β-lactamase inhibitors as shown in Figure 9 below. Thus, our aim was to make PBD analogs which retained that activity units/regions and to evaluate them as possible non-β-lactam β-lactamase inhibitors. Secondly, the attack on the carbonyl carbon initiated by the Ser-OH of the active sites of Ser β-lactamases could possibly lead to the formation of a very stable covalent bond that could lead to the PBDs being suicide inhibitors of the β-lactamases. Figure 10 shows the mode of action of clavulanic acid (a classic β-lactam β-lactamase inhibitor) in relation to the possible mechanism of action in Figure 11.

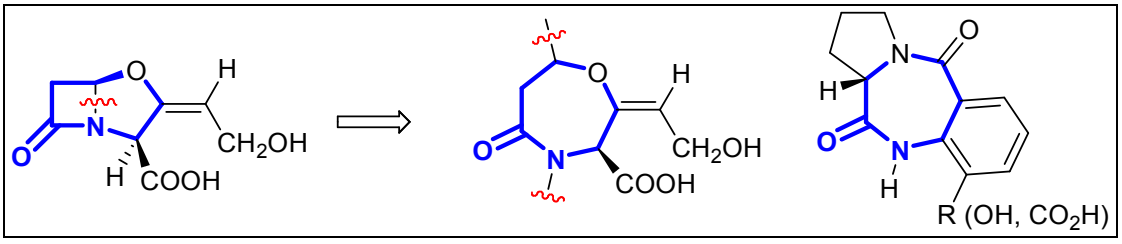

Figure 9: The structure-based relationship between β-lactam β-lactamase inhibitors and PBDs.

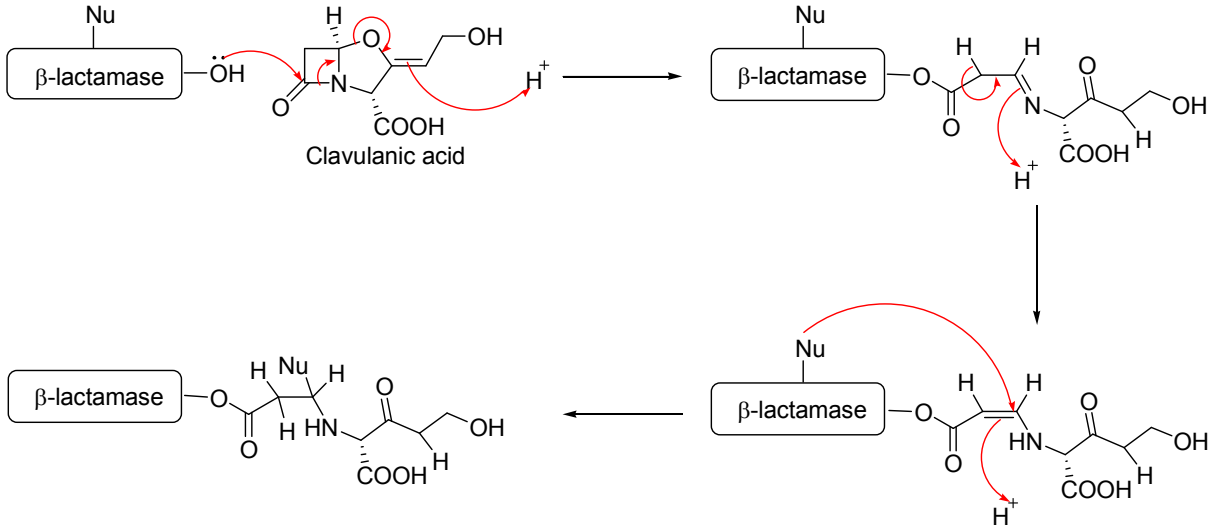

Figure 10: Mechanism of action of β-lactam β-lactamase inhibitors (suicide inhibitors) (Adapted from http://wizard.pharm.wayne.edu/medchem/betalactam.html).

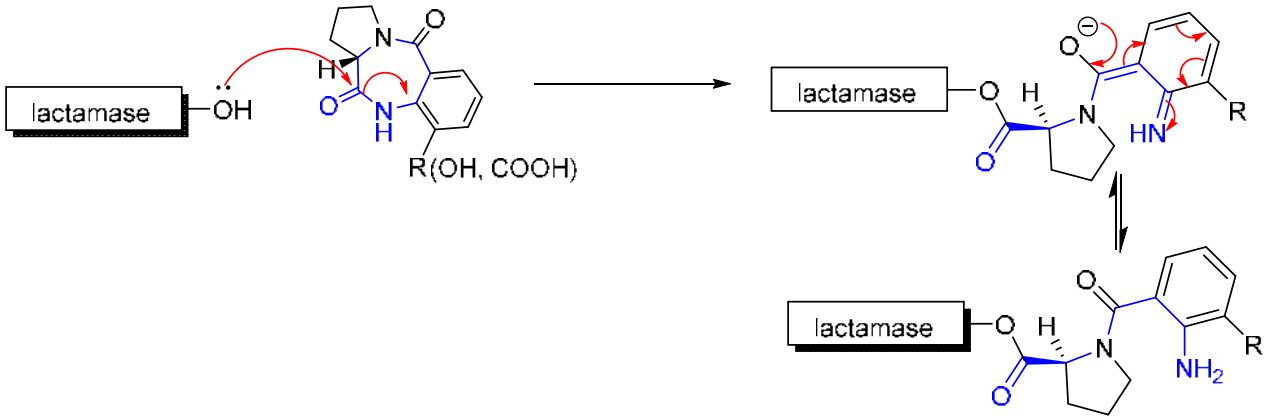

Figure 11: Proposed mechanism of action of PBD derivatives as β-lactamase inhibitors

PBD-dilactam (**1**) is a natural product from *Isatis indigotica* and can also be easily synthesized in the laboratory. The capability of natural product **1** and its synthetic analogs (*e.g.*

2-**6**) to interact with the DNA of bacterial cells is linked to their ability to cross the outer membrane of microorganisms thus making them promising candidates for new non-β-lactam β-lactamase inhibitors.[70-72] PBD dilactam (1) is a natural product from *Isatis indigotica* and can also be easily synthesized in the laboratory.[72]

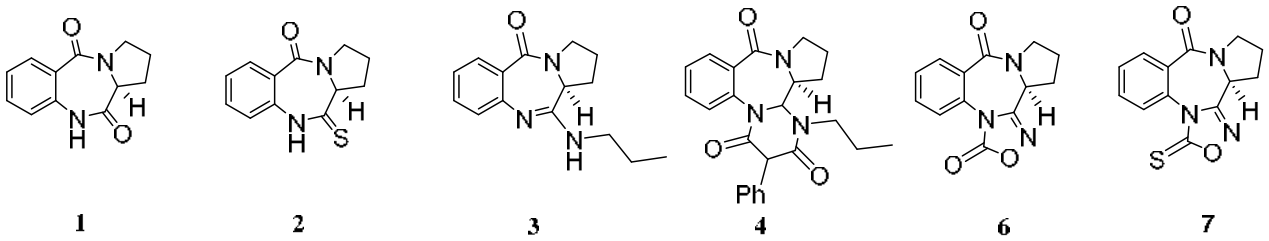

Figure 12: Examples of Pyrrolo[2,1-*c*][1,4]benzodiazepines derivatives synthesized during research.

Still in line with making further derivatives of PBDs that will serve as inhibitors of β-lactamase, we also made some smaller derivatives using *N*-phenylacetamide as our starting material. *N*-phenylacetamide derivatives have been known to have numerous biological activities ranging from antileishmanial[73], analgesic[74], antipyretic[75-77], antiviral[78], anti-parasitic,[79] and antibacterial activities (antitubercular[80]) to anticancer[81] properties depending on the derivation. By taking a cue from the justification of PBDs mentioned above, *N*-phenylacetamide can be also modified to form active regions that could possibly interact with the active site of β-lactamases, in the same manner, we suggested for PBDs. Thus, we also attempted to make *N*-phenylacetamide derivatives some of which are shown in Figure 14 below to also be evaluated as potential non β-lactam β-lactamase inhibitors.

Another reason for the synthesis of the *N*-phenylacetamide derivatives was to reduce the size of the PBD structure while keeping the suspected active region to increase its availability to the active site of the enzyme. In PBDs, proper interaction or binding to the active site appears to be hindered due to the seeming bulkiness of the PBDs.

In addition to the above-mentioned reasons, oxadiazoles have recently been discovered to inhibit PBPs (a close relative of β-lactamases) in MRSA. A good example of such oxadiazole is 5-(4-fluorophenyl)-3-(4-(4-(trifluoromethyl)phenoxy)phenyl)-1,2,4-oxadiazole (Figure 13). It has been shown to inhibit PBP2a with IC_{50} of 8 μg/mL.[82]

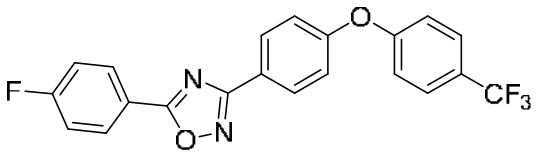

Figure 13: 5-(4-fluorophenyl)-3-(4-(4-(trifluoromethyl)phenoxy)phenyl)-1,2,4-oxadiazole[82]

This implies that there is a high possibility of the oxadiazoles (**6**, **7**, **12** and **13**) that we intended to make during the course of this study stood a high chance of being inhibitory to β-lactamases.

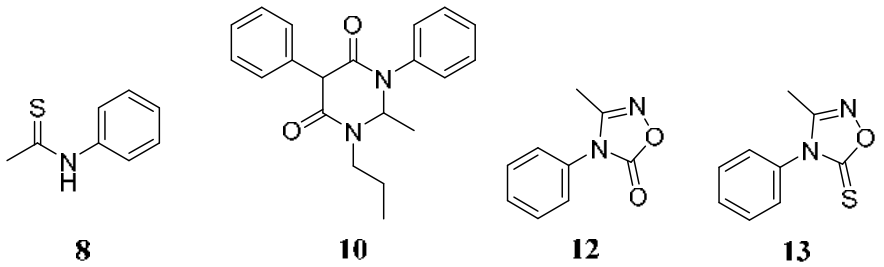

8 **10** **12** **13**

Figure 14: *N*-phenylacetamide derivatives made during this research work

Specific Aims

In this research, we aimed to study the molecular interaction of PBD derivatives and the active site residues of TEM-1 β-lactamase using the docking software Sanjeevini ParDOCK.[83] After molecular docking, derivatives that exhibited promising attributes of being efficient inhibitors were synthesized using PBD-dilactam (**1**) and *N*-phenylacetamide as the starting materials. Enzyme inhibition kinetics studies using the TEM-1 and P99 β-lactamase was done using Nitrocefin as the substrate to ascertain the efficacy of synthesized PBD and *N*-phenylacetamide derivatives as β-lactamase inhibitors. Clavulanic acid was used as the positive control in both molecular modeling and enzyme inhibition kinetics.

CHAPTER 2

EXPERIMENTAL SECTION (MATERIALS AND METHODS)

Prediction of Drug-likeness of PBD derivatives

All PBD derivatives synthesized during this work were first subjected to the Lipinski's rule of 5 which helps to distinguish between a drug-like and a non-drug-like compound. It is used to predict the high probability of success or failure of a compound as a drug due to its drug-likeness.[84] This rule as named was formulated by Christopher A. Lipinski in 1997 based on the fact that most drugs that are administered orally are moderately lipophilic and relatively small molecules. [84,85]

The Lipinski's rule of 5 evaluates if a chemical compound with certain biological or pharmacological activity has properties that would most likely make it an orally active drug in humans. Molecular properties of compounds described by the rule include their absorption, distribution, metabolism, and excretion in the human body. However, as important as the Lipinski's rule of 5 is in its determination of drug-likeness, it doesn't predict if a compound would be pharmacologically active.[85,86]

To qualify for a high probability of success, molecules have to comply with 2 or more of the Lipinski's rules. They must possess less than 5 hydrogen bond donors and less than 10 hydrogen bond acceptors, have a molecular mass less than 500 Dalton, possess molar refractivity between 40–130, and have a high lipophilicity (expressed as LogP less than 5). [84-86]

The Lipinski's rule of 5 parameters for all compounds was calculated using the Sanjeevini Drug Design Software by SCFBio, India.

Molecular Docking using ParDOCK

ParDOCK by Sanjeevini Supercomputer Facility, India is an all-atom energy based Monte Carlo docking procedure tested on a dataset of 226 protein-ligand complexes.[83]

The structural inputs for ParDOCK are a reference complex (target protein bound to a reference ligand) and a candidate molecule. The ParDOCK protocol consists of four main steps:

(a) identification of the best possible grid/translational points in a radius of 3 Å around the reference point (center of mass);

(b) generation of protein grid and preparation of energy grid in and around the active site of the protein to pre-calculate the energy of each atom in the candidate ligand;

(c) Monte Carlo docking and intensive configurational search of the ligand inside the active site;

(d) identification of the best-docked structures based on an energy criterion and prediction of the binding free energy of the complex.[83]

Figure 15 shows the flowchart of docking methodology adopted in ParDOCK.

ParDOCK is a docking software that was developed for the purpose of finding the binding mode of the ligand to its receptor to a known binding site and not for the purpose of predicting all possible binding sites. The reference complex, therefore, helps in initiating the search. For the sake of efficiency, a portion of the receptor enclosing the binding site is considered and this simplification is accounted for in atomic level energy calculations. ParDOCK, a Monte Carlo based docking protocol was used because it is able to reproduce the crystal conformation to an average root-mean-square deviation (RMSD) of 0.53 in 98% of the cases.[83]

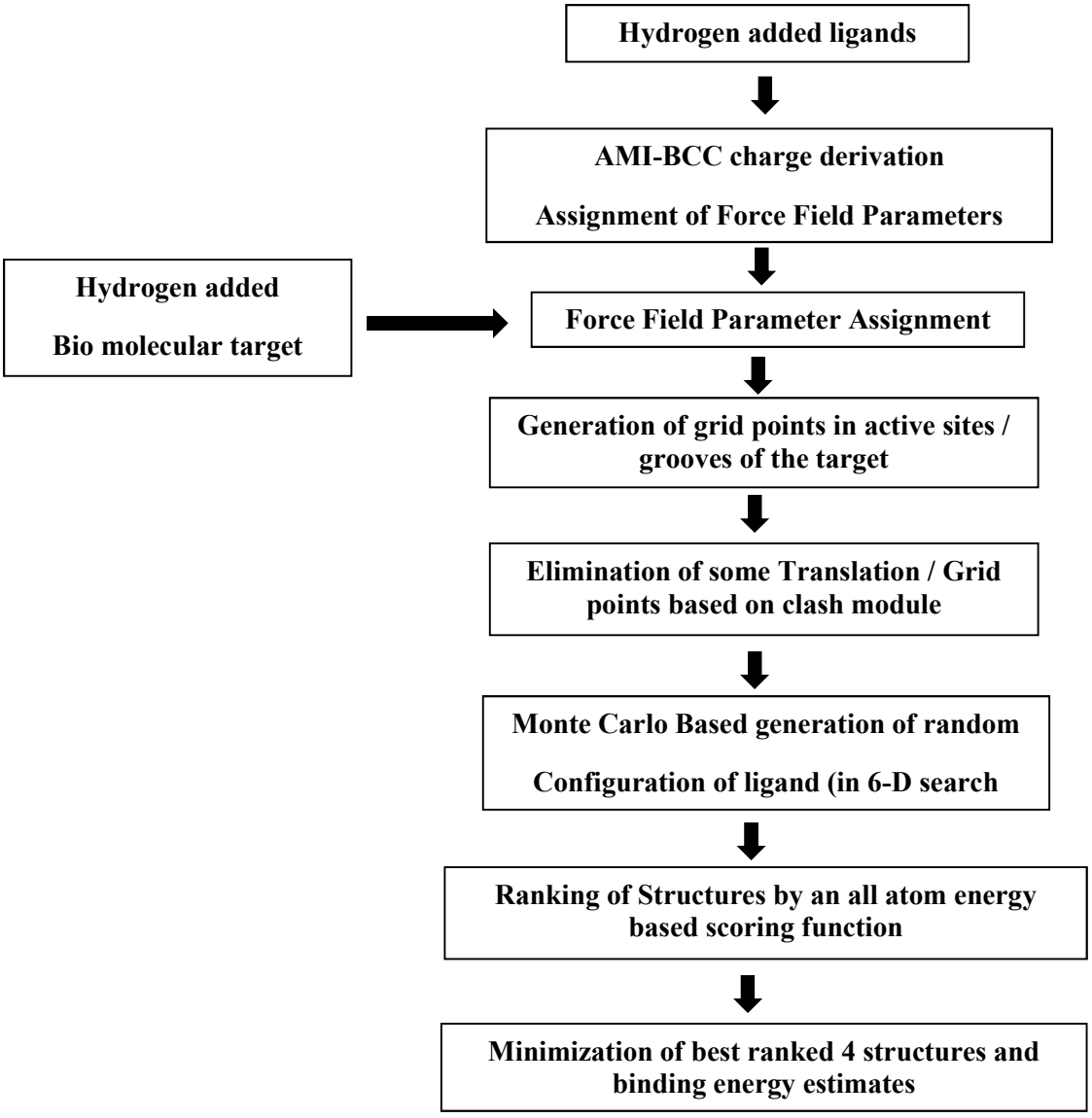

Figure 15: A computational flowchart for docking methodology (Adapted from Gupta*, et al*. *Protein and Peptide Letters*, **2007**, *14*, *7*, 632-646)[83]

Docking studies of PBD derivatives were performed using this software. Crystal structure of TEM-1 (PDB ID: 1LI0) was downloaded from Research Collaboratory for Structural Bioinformatics (RCSB) Protein Data Bank. All the structures of PBD derivatives were prepared by using Accelrys Discovery Studio Visualizer 4.5 from Biovia and saved in protein data bank (pdb) file format before used in docking procedure.

Syntheses of PBD Derivatives

Materials

Starting materials isatoic anhydride, L-proline and *N*-phenylacetamide were purchased from Alfa Aesar Chemical company. Deuterated solvents ($CDCl_3$-d and DMSO-d_6) were obtained from Sigma-Aldrich Chemical Company. Solvents (dichloromethane DCM, absolute ethanol, 95% ethanol, ethyl acetate, hexane, diisopropyl ether, diethyl ether, chloroform, acetone, dimethylformamide (DMF), methanol, toluene, propylamine, nitromethane, 2-propanol, anhydrous tetrahydrofuran (THF), anhydrous dioxane), salts ($MgSO_4$, $Na_2S_2O_3$, $NaHCO_3$, K_2CO_3 Na_2SO_4, NaCl, $HgCl_2$, hydroxylamine hydrochloride [$NH_2OH{\cdot}HCl$], MOPS buffer) and other reagents (Lawesson's reagent, 1,1 carbonyl diimidazole (CDI), 1,1 thionyl diimidazole (TDI), ammonia gas, polyphosphoric acid (PPA), ammonium hydroxide (NH_3 aq), nitroethane, aniline) were purchased from Alfa Aesar Chemical Company. Nitrocefin (NCF) and bovine serum albumin (BSA) used for enzyme kinetics assay were purchased from BioVision Incorporated. Enzymes TEM-1 β lactamase and P99 β lactamase were purchased from Invitrogen and Sigma-Aldrich Chemical Company, respectively.

Instrumentation

A Shimadzu IR Prestige-21 FTIR spectrometer was used for Infra-Red studies and a Jeol 400 MHz Nuclear Magnetic Resonance Spectrometer was used for ^{1}H NMR and ^{13}C NMR. An Agilent Technologies Cary 8454 UV/Vis spectrometer with a PCB 1500 water Peltier system by Agilent Technologies and quartz 1000 μL cuvettes with a path length of 1 cm were used for UV/Vis Absorbance and kinetic studies. Melting point was determined using a Thermo Scientific

Electrothermal Digital Melting Point Apparatus IA9100 series and molecular weight determination was done using a Shimadzu GC-MS – QP 2010 Plus.

The ^{1}H and ^{13}C NMR spectra were recorded in DMSO-d_6 and $CHCl_3$-d on a JEOL Eclipse 400 MHz NMR Spectrometer operating at 400 MHz for ^{1}H and 100 MHz for ^{13}C NMR. Chemical shift (δ) values are expressed in parts per million (ppm) and are referenced to the residual solvent signals of DMSO-d_6 and $CDCl_3$-d at δ_H/δ_C 2.50/39.5 and 7.25/76.8 ppm, 77.1 ppm, and 77.4 ppm respectively. Optical rotations were measured with a JASCO DIP-310 digital polarimeter.

Chemistry

General procedure for the preparation of the (S)-1,2,3,11a-tetrahydro-5H-benzo[e]pyrrolo[1,2-a][1,4]diazepine-5,11(10H)-dione (**1**): In a 250 mL one-neck round bottom flask, a suspension of isatoic anhydride (20.0 g, 122.68 mmol) and L-proline (14.12 g, 122.6 mmol) in DMF (60 mL) was heated to 155 ˚C for 5 h. The solvent was removed *in vacuo* and the residue was taken up in cold water. The precipitate was collected and dried to give the dilactam. The resultant solid was purified by recrystallization through slow evaporation in acetone/DMF (10:1) to afford pure colorless crystals in very good yield.

Yield: 24.78 g (93.6 %). **m.p.**: 223 – 225 °C. $[\alpha]_{D}^{25}$ = + 512 º (c = 0.5, CH_3OH).

^{1}H-NMR (400 MHz, DMSO-d_6): δ = 1.76–2.00 (m, 4H), 3.42–3.48 (m, 1H), 3.56–3.61 (m, 1H), 4.10 (d, 1H), 7.11–7.13 (dd, 1H), 7.20–7.24 (m, 1H), 7.49–7.51 (m, 1H), 7.77–7.79 (dd, 1H), 10.51 (s, 1H, NH). **^{13}C-NMR** (100 MHz, DMSO-d_6): δ = 23.6, 26.3, 40.4, 56.7, 121.8, 124.4, 127.1, 130.8, 132.6, 136.9, 165.0 (CO), 171.3 (CO). **IR** (KBr): $\tilde{\nu}$ (cm^{-1}) = 3222 (NH), 3206,

2955, 2918, 2850, 1691 (CO), 1680 (CO), 1621, 1551, 1536, 1479, 1443, 1412, 1385, 1285, 1259, 1179, 759, 701, 615. **UV** λ_{max} (MeOH): 198, 274 nm. **GC-MS** (70 eV) *m/z* (%): 216 (10) [M^+], 119 (14), 92 (20), 70 (100), 64 (10).

General procedure for the preparation of (S)-11-thioxo-1,2,3,10,11,11a-hexahydro-5H-benzo[e]pyrrolo[1,2-a][1,4]diazepin-5-one (**2**): In a 250 mL one neck round bottom flask, a mixture of dilactam (2.15 g, 10 mmol) and Lawesson's reagent (4.04 g, 10 mmol) in THF (100 mL) was stirred for 24 h at room temperature. Evaporation of solvent *in vacuo* gave a yellow solid residue which was purified by dissolving in toluene and filtered off by gravity. The solid was further washed with cold toluene to obtain pure yellow solid. Recrystallization through slow evaporation in acetone/DMF (20:1) to afford pure yellowish crystals in very good yield.

Yield: 2.03 g (88.0%). **m.p.**: 272-274 °C. $[\alpha]_{D}^{25}$ = + 762 ° (c = 0.5, $CHCl_3$)

^{1}H-NMR (400 MHz, DMSO-d_6): δ = 1.98-1.83 (m, 1H), 1.98–2.15(m, 2H), 2.88 (d, J=5.9 Hz, 1H), 3.42–3.48 (m, 3H), 3.56–3.61 (m, 1H), 4.28 (d, J=6.2 Hz, 1H), 7.27–7.29 (dd, J=8.1 Hz, 1H), 7.33–7.37 (m, 1H), 7.55–7.60 (ddd, J=7.7, 1.2 Hz, 1H), 7.82–7.84 (dd, J=7.7, 1.5 Hz, 1H), 8.13 (s, 1H, NH). **^{13}C-NMR** (100 MHz, DMSO-d_6): δ = 23.2, 29.5, 47.4, 60.3, 122.3, 126.2, 128.3, 130.8, 132.7, 137.0, 164.7 (CO), 202.5 (CS). **IR** (KBr): $\tilde{\nu}$ (cm^{-1}) = 3125 (N-H), 3094, 3063, 3024, 2974, 1620 (C=O), 1579, 1523, 1478, 1452, 1418, 1381, 1272, 1193, 1166, 1145, 1103, 1069, 1055, 887, 833, 817, 786, 755, 695, 664, 625. **UV** λ_{max} (MeOH): 194, 274 nm. **GC-MS** (70 eV) *m/z* (%): 232 (7) [M^+], 108 (6), 70 (100), 68 (6).

General procedure for the preparation of (S)-11-(propylamino)-1,2,3,11a-tetrahydro-5H-benzo[e]pyrrolo[1,2-a][1,4]diazepin-5-one (**3**): To a stirred suspension of monothiolactam (5.78 g, 25.0 mmol) and propylamine (20 mL) was added $HgCl_2$ (7.14 g, 26.25 mmol) at 60 ˚C. The mixture was stirred for a further 1 h at this temperature. After cooling to room temperature, the mixture was filtered through a plug of celite and eluted with CH_2Cl_2. The filtrate was washed with sat. $Na_2S_2O_{3(aq)}$ and after extraction with CH_2Cl_2, the combined organic layer was dried over $MgSO_4$, filtered, and the solvent and excess amine were evaporated under reduced pressure. The resultant solid was purified by recrystallization in nitromethane to afford pure colorless crystals in very good yield.

Yield: 5.64 g (88%). **m.p.:** 159-161 ^{o}C. $[\alpha]_{D}^{25}$ = + 1106 º (c = 0.5, $CHCl_3$)

^{1}H-NMR (400 MHz, $CDCl_3$-d_6): δ = 0.96–0.99 (t, J=7.5 Hz, 3H), 1.64-1.69 (m, 2H), 1.99-2.12 (m, 2H), 2.20-2.25 (m, 2H), 3.37-3.38 (d, J=4.8 Hz, 2H), 3.50-3.60 (m, 1H), 3.84-3.88 (m, 1H), 4.01-4.03 (t, J=4.9 Hz, 1H), 4.68 (s, 1H), 7.03–7.05 (m, 1H), 7.07–7.11 (m, 1H), 7.36–7.38 (ddd, J=8.6, 6.8, 1.3 Hz,1H), 7.91–7.93 (dd, J=7.7, 1.5 Hz, 1H). **^{13}C-NMR** (400 MHz, $CDCl_3$): δ = 11.7, 22.3, 23.9, 26.8, 43.3, 46.5, 54.4, 122.2, 126.5, 126.9, 130.1, 131.6, 146.7, 156.2 (CN), 166.8 (CO). **IR** (KBr): $\tilde{\nu}$ (cm^{-1}) = 3851, 3798, 3745, 3356 (N-H), 3319 (N-H), 3287, 3061, 2941, 2880, 2815, 2359, 2328, 1826, 1791, 1731, 1605 (C=O), 1554, 1531, 1506, 1456, 1406, 1383, 1336, 1256, 1215, 1150, 1096, 1067, 1035, 991, 918, 835, 761, 703, 635. **UV** λ_{max} (MeOH): 198, 273 nm. **GC-MS** (70 eV) *m/z* (%): 257 (21) [M^+], 146 (23), 119 (23), 90 (21), 70 (100).

Synthesis of (14aS)-3-phenyl-1-propyl-1,12,13,14,14a,14b-hexahydro-2H,10H-benzo[e]pyrimido[2,1-c]pyrrolo[1,2-a][1,4]diazepine-2,4,10(3H)-trione (**4**): A mixture of **3** (1

mmol, 0.257 g) and bis(2,4,6-trichlorophenyl) 2-phenylmalonate (1 mmol, 0.539 g) was heated at 190 ºC for 10 minutes in a *Zincke* apparatus under high vacuum. The residue was treated with diethyl ether to give a dark brown precipitate which was collected by filtration and washed with diethyl ether. Recrystallization was done in DMF/Water, 95% ethanol and 2-propanol.

Yield: 300 mg (75 %) **m.p.**: 230 – 233 °C. $[\alpha]_{D}^{25}$ = 0 º (c = 0.5, $CHCl_3$)

^{1}H-NMR (400 MHz, $CDCl_3$): δ = 0.77–0.81 (t, J=7.3 Hz, 3H), 1.31–1.39 (m, 2H), 2.04–2.17 (m, 1H), 2.21–2.28 (m, 1H), 2.62–2.71 (m, 1H), 2.77–2.82 (dd, J=14.6, 6.2 Hz, 1H), 2.96–3.03 (m, 1H), 3.96–4.11 (m, 2H), 4.17–4.25 (m, 1H), 4.71 (s, 1H), 7.28–7.30 (m, 2H), 7.36–7.45 (m, 5H), 7.54–7.59 (td, J=7.8, 1.6 Hz, 1H), 8.02–8.04 (m, 1H). **^{13}C-NMR** (100 MHz, $CDCl_3$): δ = 11.2, 20.6, 21.5, 29.6, 48.4, 49.5, 59.1, 118.0, 125.5, 127.5, 128.2, 128.4, 130.8, 131.3, 132.3, 133.3 (CO), 139.8 (CO), 167 (CO). **IR** (KBr): $\tilde{\nu}$ (cm^{-1}) = 2957, 2918, 2860, 2355, 1958, 1728, 1683 (C=O), 1633 (C=O), 1576, 1487, 1453, 1352, 1297, 1252, 1221, 1185, 1150, 899, 800, 753, 719, 698, 665, 631. **UV** λ_{max} (AcO): 194, 274 nm. **GC-MS** (70 eV) *m/z* (%): 401 (66) [M^+], 215 (11), 187 (29), 118 (100), 90 (46).

General procedure for the preparation of (S)-11-(hydroxyamino)-1,2,3,11a-tetrahydro-5H-benzo[e]pyrrolo[1,2-a][1,4]diazepin-5-one (**5**): Hydroxylamine hydrochloride (800 mg, 11.51 mmol) and potassium carbonate (6 g, 43.5 mmol) was added to a solution of monothiolactam (1.74 g, 7.5 mmol) in absolute ethanol (40 mL) and stirred for 48 hours at room temperature. The initial yellow mixture decolorized and H_2S was released. The mixture was taken up in dichloromethane (120 mL) and washed with water (80 mL). The organic layer was further washed with brine and dried over Na_2SO_4. The solvent was removed *in vacuo*. The crude

residue was dissolved in a mixture of diethyl ether/hexane (1:1), filtered and further washed in 20 mL of the solvent mixture to obtain 1.63 g (94% yield) of the pure solid. Recrystallization was done in nitromethane to yield off-white crystals.

Yield: 1.63 g (94%). **m.p.**: 150 – 153 °C. $[\alpha]_{D}^{25}$ = + 488 º (c = 0.5, $CDCl_3$)

^{1}H-NMR (400 MHz, DMSO-d_6): δ = 1.86–2.03 (m, 3H), 2.56–2.60 (m, 1H), 3.47–3.61 (m, 4H), 4.31–4.33 (m, 1H), 7.03–7.06 (t, J=7.5 Hz, 1H), 7.25–7.27 (dd, J=16.8, 7.7 Hz, 1H), 7.37–7.41 (t, J=7.7 Hz, 1H), 7.66–7.68 (d, J=7.7 Hz, 1H), 8.75 (s, 1H, N-H), 10.08 (s, 1H, OH). **^{13}C-NMR** (100 MHz, $CDCl_3$-d_6): δ = 23.4, 25.9, 47.4, 54.4, 120.5, 123.5, 125.8, 131.6, 132.6, 136.9, 151.2, 166.2 (CO). **IR** (KBr): $\tilde{\nu}$ (cm^{-1}) = 3788, 3716, 3281, 2965, 2911, 2878, 2806, 2351, 1724, 1689, 1658, 1612, 1573, 1552, 1530, 1480, 1453, 1425, 1396, 1273, 1227, 1201, 1162, 1108, 1040, 997, 957, 933, 884, 847, 807, 787, 756, 701, 663. **UV** λ_{max} (MeOH): 198, 313 nm. **GC-MS** (70 eV) *m/z* (%): 231 (20) [M^+], 144 (37), 90 (35), 70 (100).

Synthesis of (S)-11,12,13,13a-tetrahydro-3H,9H-benzo[e][1,2,4]oxadiazolo[3,4-c]pyrrolo[1,2-a][1,4]diazepine-3,9-dione (**6**): In a nitrogen atmosphere, **5** (231 mg, 1 mmol) dissolved in anhydrous dioxane (8 mL) was added to 1,1 carbonyl diimidazole (486.45 mg, 3.3 mmol). The reaction mixture was refluxed for 12 hours and the solvent removed *in vacuo* afterward. The residue was taken up in dichloromethane and washed three times with water. The organic layer was dried over Na_2SO_4 and the solvent removed *in vacuo*. The crude residue was purified by flash column chromatography to obtain a white solid which was recrystallized to get crystals used for x-ray crystallography.

Yield: 226.16 mg (88 %). **m.p.**: 180 – 182 °C. $[\alpha]_{D}^{25}$ = + 142 º (c = 0.5, $CDCl_3$)

^{1}H-NMR (400 MHz, $CDCl_3$-d_6): δ = 1.58 (d, J=12.1 Hz, 2H), 2.10-2.23 (m, 2H), 2.30-2.39 (m, 1H), 2.82-2.87 (tt, J=9.9, 3.4 Hz, 1H), 3.67-3.74 (m, 1H), 3.90-3.95 (m, 1H), 4.58-4.61 (dd, J=8.4, 2.9 Hz, 1H), 7.49–7.53 (m, 1H), 7.64–7.68 (td, J=7.8, 1.6 Hz, 1H), 7.83-7.85 (d, J=7.3 Hz, 1H), 8.02–8.04 (dd, J=7.9, 1.6 Hz, 1H). **^{13}C-NMR** (100 MHz, $CDCl_3$): δ = 23.4, 25.6, 47.9, 51.2, 122.4, 128.6, 128.6, 128.7, 132.8, 156.3 (CN), 158.0 (CO), 164.2 (CO). **IR** (KBr): $\tilde{\nu}$ (cm^{-1}) = 3623, 3335, 3044, 2956, 2918, 2875, 2851, 2381, 2349, 2296, 2199, 2105, 1981, 1838, 1787, 1728, 1710, 1690, 1657, 1640, 1599, 1551, 1468, 1451, 1410, 1301, 1267, 1167, 1081, 1025, 990, 761, 702, 662, 608. **UV** λ_{max} (MeOH): 198, 274 nm. **GC-MS** (70 eV) *m/z* (%): 257 (22) [M^+], 144 (100),116 (38), 90 (33), 44 (33), 41 (24).

X-ray crystallography study of **6**: A large colorless prism was cut (0.10 x 0.15 x 0.23 mm^3) and centered on the goniometer of a Rigaku Oxford Diffraction Gemini E diffractometer operating with MoKα radiation. The data collection routine, unit cell refinement, and data processing were carried out with the program CrysAlisPro.[87] The Laue symmetry and systematic absences were consistent with the monoclinic space groups *I*2 and *I*2/*m*. As the sample was known to be enantiomerically pure, the acentric space group, *I*2, was chosen to give Z=4 and Z'=1. The absolute configuration could not be determined from the anomalous dispersion effects. The structure was solved using SHELXS-2014[88] and refined using SHELXL-2014 via Olex2.[89] The final refinement model involved anisotropic displacement parameters for non-hydrogen atoms and a riding model for all hydrogen atoms.

Synthesis of (S)-3-thioxo-11,12,13,13a-tetrahydro-3H,9H-benzo[e][1,2,4]oxadiazolo[3,4-c]pyrrolo[1,2-a][1,4]diazepin-9-one (**7**): In a nitrogen atmosphere, **5** (231 mg, 1 mmol) dissolved

in anhydrous dioxane (8 mL) was added to 1,1 thionyl diimidazole (486.45 mg, 3.3 mmol). The reaction mixture was refluxed for 12 hours and the solvent removed *in vacuo* afterward. The residue was taken up in dichloromethane and washed three times with water. The organic layer was dried over Na_2SO_4 and the solvent removed *in vacuo*. The crude residue was purified by flash column chromatography to obtain a pale yellow solid. This was recrystallized using Hexane: Ethyl acetate 1:1

Yield: 245.7 mg (90 %). **m.p.**: 216 – 218 °C. $[\alpha]_D^{25}$ = + 34 º (c = 0.5, $CDCl_3$).

^{1}H-NMR (400 MHz, $CDCl_3$): δ = 1.17–1.27 (m, 1H), 2.06–2.29 (m, 2H), 2.32–2.47 (m, 1H), 2.84–2.90 (m, 1H), 2.88 (tt, J=9.9, 3.3 Hz, 1H), 3.65–3.72 (m, 1H), 3.90–3.95 (m, 1H), 4.57–4.60 (dd, J = 8.6, 2.7 Hz, 1H), 7.55–7.59 (td, J=7.6, 0.9 Hz, 1H), 7.67–7.72 (m, 1H), 8.01–8.04 (dd, J=8.1, 1.5 Hz, 1H), 8.27–8.29 (dd, J=8.2, 0.9 Hz, 1H). **^{13}C-NMR** (100 MHz, $CDCl_3$): δ = 23.5, 26.5, 47.6, 51.0, 124.7, 129.8, 131.8, 132.2. **IR** (KBr): $\tilde{\nu}$ (cm^{-1}) = 3788, 3716, 3281, 2965, 2911, 2878, 2806, 2351, 1724, 1689, 1658, 1612, 1573, 1552, 1530, 1480, 1453, 1425, 1396, 1273, 1227, 1201, 1162, 1108, 1040, 997, 957, 933, 884, 847, 807, 787, 756, 701, 663. **UV** λ_{max} (MeOH): 198, 276 nm. **GC-MS** (70 eV) *m/z* (%): 273 (70) [M^+], 146 (42), 102 (75), 90 (65), 69 (44), 43 (100).

General procedure for the preparation of N-phenylethanethioamide (**8**): In a 250 mL one-neck round bottom flask, a mixture of 0.5 M solution of acetanilide (6.75 g, 50 mmol) in dichloromethane (DCM) (100 mL) and 0.25 M Lawesson's reagent (10.1 g, 25 mmol) in DCM (100 mL) was stirred for 5 hours at room temperature. Evaporation of solvent *in vacuo* gave a yellow solid residue which was purified by column chromatography using DCM.

Yield: 7.02 g (93 %). **m.p.**: 74 - 76 °C. $[\alpha]_D^{25}$ = 0 º (c = 0.5, $CDCl_3$)

^{1}H-NMR (400 MHz, $CDCl_3$): δ = 2.16 (s, 3H), 7.08–7.11 (t, 1H), 7.28–7.32 (t, 2H), 7.48–7.50 (d, J=7.7 Hz, 1H), **^{13}C-NMR** (100 MHz, $CDCl_3$): δ = 24.7, 120, 124.4, 129.1, 139, 169.6 (CO), **IR** (KBr): $\tilde{\nu}$ (cm^{-1}) = 3184, 3164, 3002, 2957, 2920, 2359, 1595, 1533, 1495, **UV** λ_{max} (MeOH): 198, 277 nm

GC-MS (70 eV) *m/z* (%): 151 (43) [M^+], 110 (54), 93 (100), 77 (100), 59 (76).

Synthesis of (E)-N'-phenyl-N-propylacetimidamide (**9**): To a stirred suspension of **8** (755 mg, 5 mmol) and propylamine (20 ml, 59.11 mmol) was added $HgCl_2$ (1.42 g, 5.25 mmol) at 60 ˚C. The mixture was stirred for a further 1 hour at this temperature. After cooling to room temperature, the mixture was filtered through a plug of celite and eluted with CH_2Cl_2. The filtrate was washed with sat. $Na_2S_2O_3$(aq) and after extraction with CH_2Cl_2, the combined organic layer was dried over $MgSO_4$, filtered, and the solvent and excess amine were evaporated under reduced pressure. The resultant solid was purified by fractional distillation to yield a brownish liquid which solidifies on refrigeration.

Yield: 619.5 mg (70 %). **m.p.**: 180 - 182 °C. $[\alpha]_D^{25}$ = 0 º (c = 0.5, $CDCl_3$)

^{1}H-NMR (400 MHz, $CDCl_3$): δ = 0.96–1.00 (m, 3H), 1.19 (s, 1H), 1.57–1.66 (m, 2H), 1.77 (s, 3H), 3.28–3.32 (t, J=4.4 Hz, 2H), 6.75–6.77 (m, 2H), 6.94–6.97 (d, J=6.6 Hz,1H), 7.21–7.29 (m, 2H). **^{13}C-NMR** (100 MHz, $CDCl_3$): δ = 14.3, 21.5, 30.4, 60.5, 122.6, 128.8, 131, 171.3, 207.2. **IR** (KBr): $\tilde{\nu}$ (cm^{-1}) = 3419, 3282 (NH), 2961, 2929, 2872, 2362, 1626, 1592, 1542, 1487, 1382, 1261, 1223, 1168, 1070, 900, 800, 743, 699. **UV** λ_{max} (MeOH): 194, 274 nm. **GC-MS** (70 eV) *m/z* (%): 176 (19) [M^+], 133 (16), 118 (73), 93 (96), 77 (100), 59 (30), 42 (56).

Synthesis of 2-methyl-1,5-diphenyl-3-propyldihydropyrimidine-4,6(1H,5H)-dione (**10**): A mixture of **9** (1 mmol, 176 mg) and bis(2,4,6-trichlorophenyl) 2-phenylmalonate (1 mmol, 0.539 g) was heated at 100 ºC for 10 minutes in a *Zincke* apparatus under high vacuum. The residue was treated with diethyl ether to give a dark brown precipitate which was collected by filtration and washed with diethyl ether. Recrystallization was done in DMF/water, 95% ethanol and 2-propanol.

Yield: 194 mg (60 %). **m.p.**: 257–259 °C. $[\alpha]_{D}^{25}$ = 0 º (c = 0.5, $CDCl_3$)

^{1}H-NMR (400 MHz, $CDCl_3$): δ = 1.03–1.06 (m, 3H), 1.59 (s, 1H), 1.78–1.87 (m, 2H), 2.41 (d, J=4.4 Hz, 2H), 4.08–4.12 (m, 2H), 7.12–7.15 (m, 1H), 7.22–7.27 (m, 2H), 7.27–7.31 (m, 1H), 7.48–7.52 (m, 2H), 7.52–7.57 (m, 2H), 7.77–7.79 (dd, J=8.4, 1.1 Hz, 2H). **^{13}C-NMR** (100 MHz, $CDCl_3$): δ = 24.7, 120, 124.4, 129.1, 139, 169.6 (CO). **IR** (KBr): $\tilde{\nu}$ (cm^{-1}) = 2962, 2930, 2875, 2362, 2341, 1643 (CO), 1595, 1549, 1482, 1442, 1379, 1338, 1274, 1158, 988, 775, 752, 696, 678, 620. **UV** λ_{max} (MeOH): 198, 273 nm. **GC-MS** (70 eV) *m/z* (%): 321 (15) [M^+], 277 (15), 249 (14), 145 (19), 118 (20), 90 (100), 77 (35), 41 (27).

Synthesis of (E)-N-hydroxy-N'-phenylacetimidamide (**11**): Hydroxylamine hydrochloride (1.05 mg, 15 mmol) and sodium carbonate (1.5 g, 10 mmol) was added to a solution of **8** (1.5 g, 10 mmol) in dioxane (40 mL) and stirred for 48 hours at 50 ºC. The initial yellow mixture decolorized and H_2S was released. The mixture was taken up in DCM (30 mL) and washed with water twice (40 mL). The organic layer was dried over Na_2SO_4. The solvent was removed in vacuo. The crude residue was purified using column chromatography using a solvent mixture of

ethyl acetate /hexane (4:1). The white product collected after evaporation of the solvent was then recrystallized from water to give white crystals.

An alternative synthesis of **11**: A mixture of nitroethane (12.5 mmol) and aniline (10 mmol) in PPA (20 g, 86 % P_2O_5) was vigorously stirred. The reaction mixture was heated for 5 hours at 110 ºC. The mixture was cooled down to 80 ºC and diluted with water (50 mL) after TLC confirmed total consumption of starting material. 20 % aqueous ammonia was used to neutralize the mixture (to pH~9), heated to reflux, and filtered. The filtrate was cooled down to 0 ºC, to form a crystalline precipitate which was collected by suction filtration recrystallized from water.

Yield: a. 825 mg (55 %). b. 1.17 g (78 %) **m.p.**: 120 °C. $[\alpha]_D^{25} = 0$ º (c = 0.5, $CDCl_3$)

^{1}H-NMR (400 MHz, $CDCl_3$): δ = 1.97 (s, 3H), 7.06–7.07 (dd, J=8.4, 1.1 Hz, 2H), 7.12–7.15 (m, 1H), 7.29-7.34 (m, 2H). **^{13}C-NMR** (100 MHz, $CDCl_3$): δ =16.1, 123.9, 124.7, 129.3, 139.0, 150.7 (CO). **IR** (KBr): $\tilde{\nu}$ (cm^{-1}) = 3435, 3182, 3091 (OH), 2999, 2878, 2813, 1611, 1465, 1411, 1343, 758. **UV** λ_{max} (MeOH): 198, 245 nm. **GC-MS** (70 eV) *m/z* (%): 150 (15) [M^+], 133 (33), 118 (30), 93 (100), 77 (74), 65 (35), 51 (24).

Synthesis of 3-methyl-4-phenyl-1,2,4-oxadiazol-5(4H)-one (**12**): In a nitrogen atmosphere, **11** (150 mg, 1 mmol) dissolved in anhydrous dioxane (10 mL) was added to CDI (535.1 mg, 3.3 mmol). The reaction mixture was stirred at 50 °C for 24 hours and the solvent removed *in vacuo* afterward. The residue was taken up in DCM and washed three times with water. The organic layer was dried over Na_2SO_4 and the solvent removed *in vacuo*. The crude residue was purified by flash column chromatography to obtain a white solid, 106 mg (60 %).

The solid was further purified by recrystallization using hexane and ethyl acetate to obtain white crystals.

Yield: 106 mg (60 %). **m.p.**: 133–135 °C. $[\alpha]_D^{25}$ = 0 º (c = 0.5, $CDCl_3$)

^{1}H-NMR (400 MHz, $CDCl_3$): δ = 2.19 (s, 3H), 7.30–7.32 (d, J=2.9 Hz, 1H), 7.51-7.54 (m, 2H), 7.55–7.56 (m, 1H). **^{13}C-NMR** (100 MHz, $CDCl_3$): δ = 11.3, 126.8, 130.1, 130.2, 131.2, 156.2 (CO). **IR** (KBr): $\tilde{\nu}$ (cm^{-1}) = 3062, 2926, 1766, 1595, 1502, 1445, 1420, 1310, 1168, 1080, 1004, 885, 756, 692, 623. **UV** λ_{max} (MeOH): 197, 274 nm. **GC-MS** (70 eV) *m/z* (%): 176 (34) [M^+], 131 (54), 91 (83), 77 (100), 64 (62), 51 (56).

Synthesis of 3-methyl-4-phenyl-1,2,4-oxadiazole-5(4H)-thione (**13**): In a nitrogen atmosphere, **11** (150 mg, 1 mmol) dissolved in anhydrous dioxane (10 mL) was added to TDI (587.9 mg, 3.3 mmol). The reaction mixture was stirred at 50 °C for 12 hours and the solvent removed *in vacuo* afterward. The residue was taken up in DCM and washed three times with water. The organic layer was dried over Na_2SO_4 and the solvent removed *in vacuo*. The crude residue was purified by flash column chromatography to obtain a pale yellow solid, 150 mg (78 % yield). The solid was further purified by recrystallization using hexane and ethyl acetate.

Yield: 145 mg (78 %). **m.p.**: 135–137 °C. $[\alpha]_D^{25}$ = 0 º (c = 0.5, $CDCl_3$)

^{1}H-NMR (400 MHz, $CDCl_3$): δ = 2.20 (s, 3H), 7.32–7.35 (td, J=3.8, 1.8 Hz, 2H), 7.57–7.62 (m, 3H). **^{13}C-NMR** (100 MHz, $CDCl_3$): δ = 10.4, 124.9, 127.5, 128.5, 130.4, 130.9, 132.6, 167.1 (CN), 186.7 (CS). **IR** (KBr): $\tilde{\nu}$ (cm^{-1}) = 2956, 2914, 1591, 1495, 1348, 1294, 1141. **UV** λmax (MeOH): 198, 274 nm. **GC-MS** (70 eV) *m/z* (%): 192 (40) [M^+], 123 (56), 91 (70), 77 (100), 64 (70), 51 (56).

Enzyme Inhibition Kinetics

β-lactamase activity, % inhibition and enzyme residual activity determination

Enzyme activity quantitation was performed by spectrophotometric measurement of the hydrolysis of NCF at 485 nm and at 30°C ($\Delta\varepsilon$ = 20,500 M^{-1} cm^{-1}). NCF which is a chromogenic substrate is known to absorb light at 385 nm displaying an orange yellowish color but its hydrolyzed product absorbs at a much higher wavelength, 485 nm (pinkish red color) (Scheme 1).

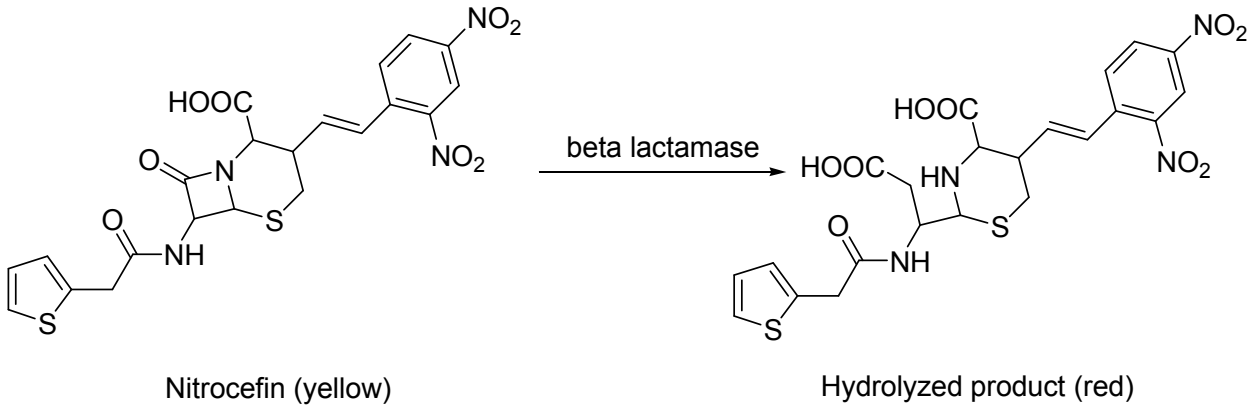

Nitrocefin (yellow) Hydrolyzed product (red)

385 nm 485 nm

Scheme 1: Hydrolysis of NCF by β-lactamase enzyme

Preparation of MOPS stock solution (0.1M)

8.372 g MOPS was dissolved in 500 mL of water. 0.02 M solution was then made by diluting 40 mL of the stock to 200 mL of water.

Preparation of BSA (1 % and 0.1 %) in buffer (MOPS)

100 mg of BSA was dissolved in 10 mL of MOPS buffer. 1 % BSA was used for the dilution of the enzymes. 0.1 % BSA was also made by diluting 1 mL of 1 % BSA in the MOPS buffer in 9 mL of MOPS buffer. 0.1 % BSA was used for actual enzyme kinetics assay.

Substrate (NCF) Preparation (5 mM)

2.582 g of NCF was dissolved in 1 mL of 0.02 M MOPS buffer and further diluted to 100 μM in enzyme mixture.

Enzyme Preparation (TEM-1 β-lactamase)

Commercially available enzyme (TEM-1) with a concentration of 0.56 mg/mL and molecular weight of 29.3 kDa from Invitrogen was diluted to 47.5 nM using 1 % BSA and 3 μL was used for the assay to get the final enzyme concentration to be 0.25 nM.

Enzyme Preparation (P99 β-lactamase)

1.4 mg of commercially available enzyme (P99) with a molecular weight of 39 kDa from Sigma-Aldrich was dissolved in 1 mL of 1 % BSA in MOPS buffer to make a stock solution of 100 mM. The stock solution was further diluted and used for enzyme kinetics assay.

In enzyme kinetic assay mixture, NCF was present at 100 μM, TEM-1 was at 0.25 nM, and P99 was at 0.2 nM in 20 mM MOPS buffer, pH 7.5, with 0.1 % BSA in MOPS buffer in a final volume of 600 μL. Clavulanate was used as the positive control at a final concentration of 120 nM for the inhibition assay.

Initial rates were monitored for 5 minutes on an Agilent Technologies Cary 8454 UV-Vis spectrophotometer. Percentage enzyme inhibition was calculated by the formula below:

$$\%\ \text{enzyme inhibition} = \frac{Initial\ rate\ of\ enzyme + inhibitor}{Initial\ rate\ of\ enzyme\ without\ inhibitor} \text{x } 100\ \%$$

Enzyme residual activity was calculated as:

$$Enzyme\ Residual\ Activity\ (\%) = 100\ \% - \%\ enzyme\ inhibition$$

CHAPTER 3

RESULTS AND DISCUSSION

Lipinski's Rule of 5 for Drug-likeness

All compounds designed and synthesized during the course of this research were first tested for conformity to at least two of the 5 Lipinski's rules for drug-likeness.[84,85] As shown in Table 1, most compounds (**1-6** and, **10-13**) conformed to at least 2 of all 5 rules with respect to drug-likeness.

Table 1: Lipinski's rule of 5 data for compounds **1-6** and, **10-13**.

	PBD DERIVATIVES										
LIPINSKI RULE OF 5 PARAMETERS	**1**	**2**	**3**	**4**	**5**	**6**	**10**	**11**	**12**	**13**	**Clavulanic acid**
Mass (Daltons) [<500]	216	232	257	403	231	259	325	150	176	192	201
High lipophilicity (cLOGP) [<5]	1.243	2.044	2.334	2.999	1.212	1.092	1.776	1.614	1.977	2.334	-4.057
Hydrogen bond donor [<5]	1	1	1	0	2	1	2	2	0	0	3
Hydrogen bond acceptors [<10]	4	3	4	6	5	6	3	3	4	2	5
Molar Refractivity [40-130]	59.13	66.72	75.89	112.96	62.67	66.34	94.70	44.28	48.51	53.33	40.42

Drug-likeness, as described by the Lipinski's rule of 5, are based on a number of factors and it is a qualitative concept used in drug design to ascertain how drug-like a compound is with regards to its bioavailability.

Lipophilicity of a compound which is a key factor of drug-likeness is the ability of a compound to be soluble in fat. This is relevant because all orally administered drugs need to first pass through the intestinal lining after consumption, be carried in the blood which is aqueous and also penetrate the lipid-based membrane of the cell to reach inside the cell. Lipophilicity is

usually measured experimentally using a model system or computationally as it was done in this work where it is termed cLOGP.[90]

Solubility in water can be estimated from the number of hydrogen bond donors (HBDs) in a molecule. Low amount of hydrogen bond donors translates to low water solubility which in turn leads to slow absorption into the blood and action. On the other hand, high amount of HBDs leads to low fat solubility thus making it difficult for molecules to penetrate the cell membrane to reach inside the cell. [84,91]

The effect of molecular weight stems from the fact that the smaller the molecule, the better because this directly affects the diffusion of the molecules. Thus, drugs which are less than 500 Daltons in size are known to be usually more efficient in terms of easy diffusion into the cell.[90]

As shown in Table 1, all compounds were observed to have low to moderate cLOGP, molecular weights ranging from 150-403, low HBDs, moderate hydrogen bond acceptors (HBAs), and molar refractivity ranging from 44.28 – 94.70.

With these positive data in mind, we went ahead to dock the molecules using Sanjeevini ParDocK. [83]

Molecular Docking Results

To gain an insight into the binding mode of some of the PBD derivatives (e.g. **1**–**13**), ligands made using the free Accelrys Discovery Studio were docked on to TEM-1 β-lactamase (PDB code: 1LI0) using ParDock[83] software from SCFBio, India. To validate the results, known TEM-1 β-lactamase inhibitor, Clavulanate was also docked onto the enzyme using ParDock.

Results from molecular docking revealed the interaction of ligands with different amino acid residues of the active site of TEM-1 β-lactamase are as shown in Table 1 below.

Table 2. Predicted binding affinity, hydrogen bond distances, and active site residues of TEM-1 β-lactamase interacting with ligands.

	Predicted distances (Å) of ligands from active site residues										
Predicted active site residues and predicted binding affinity energies	**1**	**2**	**3**	**4**	**5**	**6**	**10**	**11**	**12**	**13**	**Control (Clavulanate)**
Binding Affinity Energies (kcal/mol)	-5.10	-5.55	-5.81	-7.14	-6.86	-4.42	-6.51	-3.64	-3.03	-4.05	-4.73
SER45	2.66	2.71	3.73	3.75	-	1.76	-	2.10	3.48	3.41	2.66
SER105	2.75	2.69	3.21	2.50	-	1.71	-	-	3.59	-	2.66
SER210	-	-	-	-	1.55	-	1.89	-	-	-	-
LYS48	-	-	-	-	2.05	-	-	-	-	-	-
ASN107	-	-	-	2.20	-	-	-	2.48	2.25	-	-
ALA212	-	-	-	-	1.84	-	-	-	-	-	-
ARG218	-	-	-	-	-	-	1.94	-	-	-	2.79
LYS209	-	-	2.87	-	-	-	1.95	-	-	-	-
GLU141	-	-	-	-	-	-	-	2.14	-	-	-

From the data in Table 2, we were able to see the possible interactions between some of the PBD derivatives and the active site residues of the TEM-1 β-lactamase crystal structure obtained from the protein data bank. It was observed that the most important catalytic Ser70 (here seen as Ser45) for β-lactam hydrolysis as well as other serine active site residues (Ser105, Ser210) were found to be interacting with the docked PBD derivatives. Comparing the results obtained from the docked PBD ligands to the positive control clavulanate, most PBDs had better predicted binding affinity energies ranging from – 3.03 to – 7.14 kcal/mol compared to clavulanate which had a binding affinity energy of – 4.73 kcal/mol. Binding affinity energy was calculated based on the formation of simulated hydrogen bonding and other non-covalent interactions between the ligands (inhibitors) and active site residues. Similar active site residues

were observed to be interacting and forming hydrogen bonds at distances mostly < 3 Å as shown in Figure 16–20.

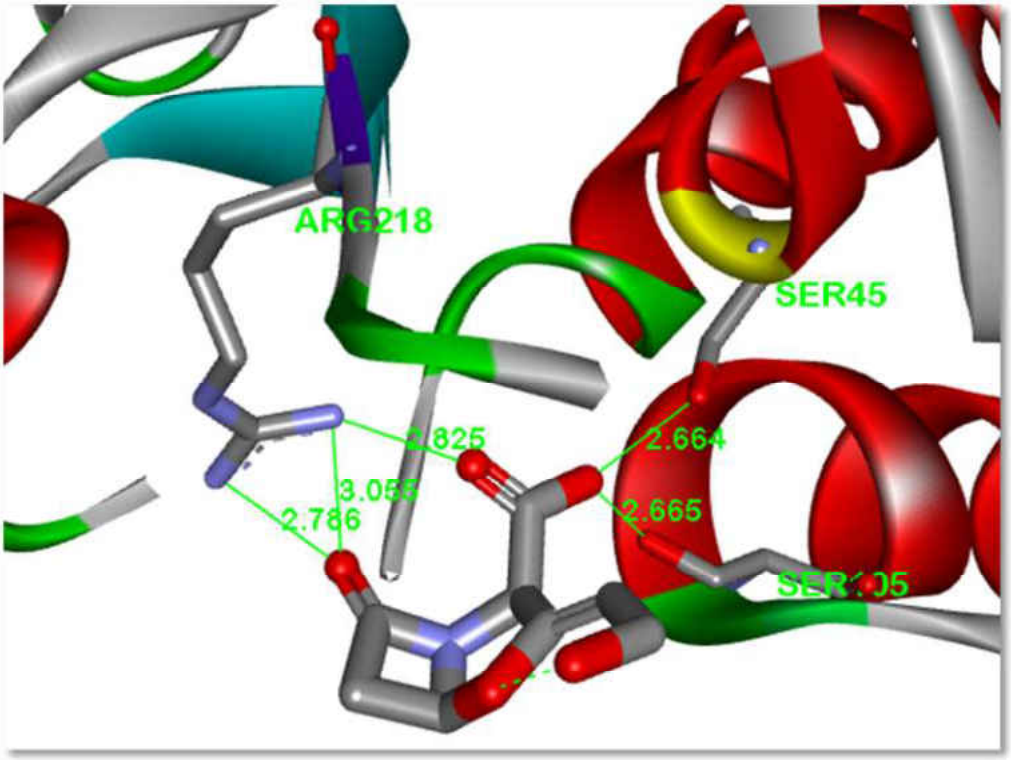

Figure 16: Interaction between TEM-1 β-lactamase active site residues and Clavulanic acid

Compound **5**, **6** and **11** had the best hydrogen bond distances (shortest) (1.55 and 2.10 Å respectively) in their interaction with important active site residue Ser 45. Compound **6** was also shown to interact with about the same closeness with Ser105 (1.71 Å). These bond distances were indicative of the relative closeness of these important active site residues to the ligand thus leading us to believe that these derivatives may interact more easily with active site residues. This is due to the non-covalent interactions (hydrogen bonding) observed during docking. Based on these potentially positive results due to the simulated binding affinity energies and interactions, all proposed PBD and *N*-phenylacetamide derivatives were synthesized.

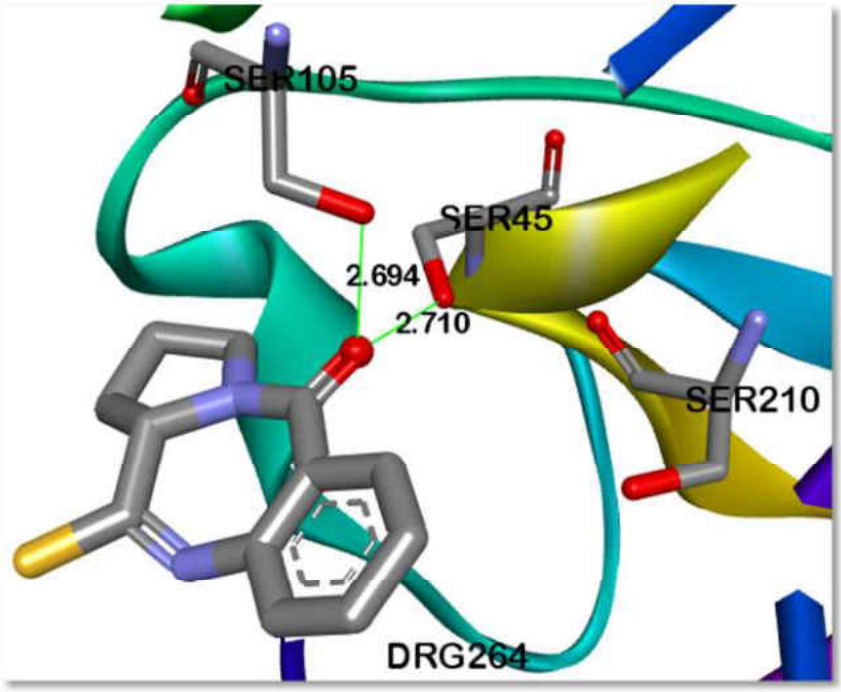

Figure 17: Interaction between TEM-1 β-lactamase active site residues and **2**

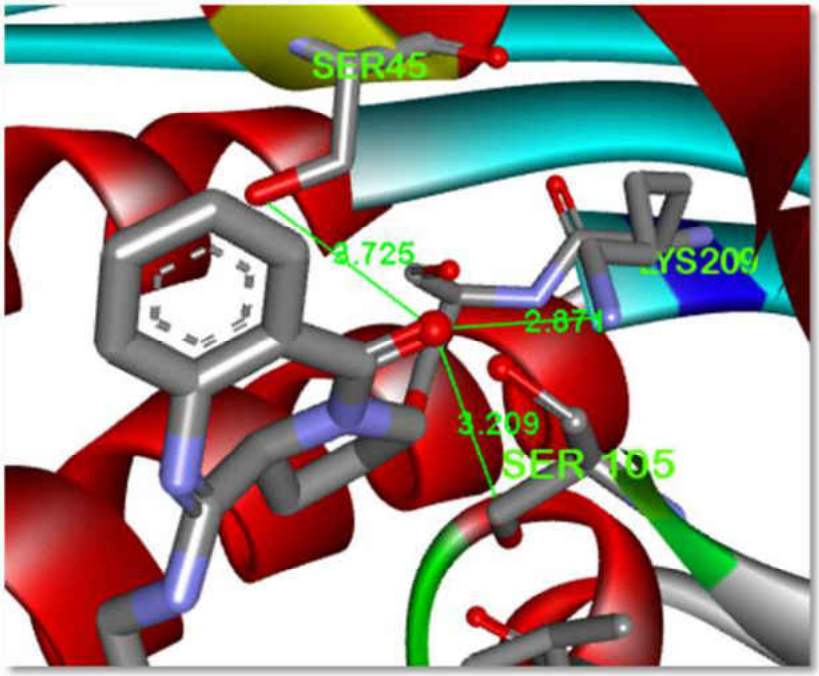

Figure 18: Interaction between TEM-1 β-lactamase active site residues and **3**

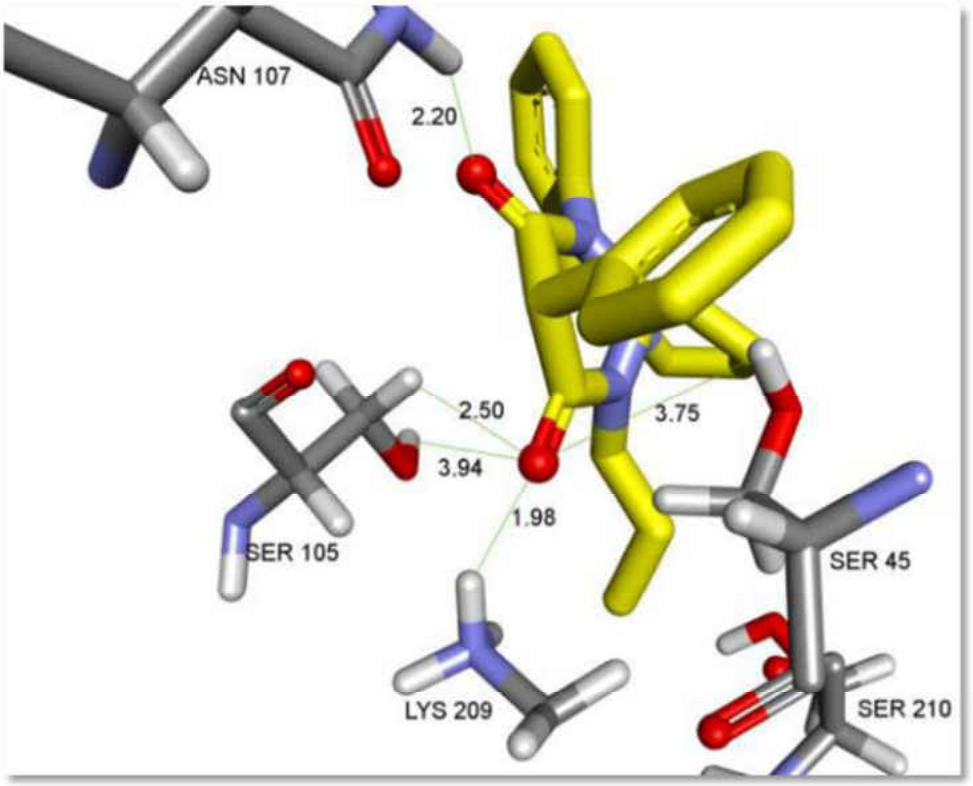

Figure 19: Interaction between TEM-1 β-lactamase active site residues and **4**

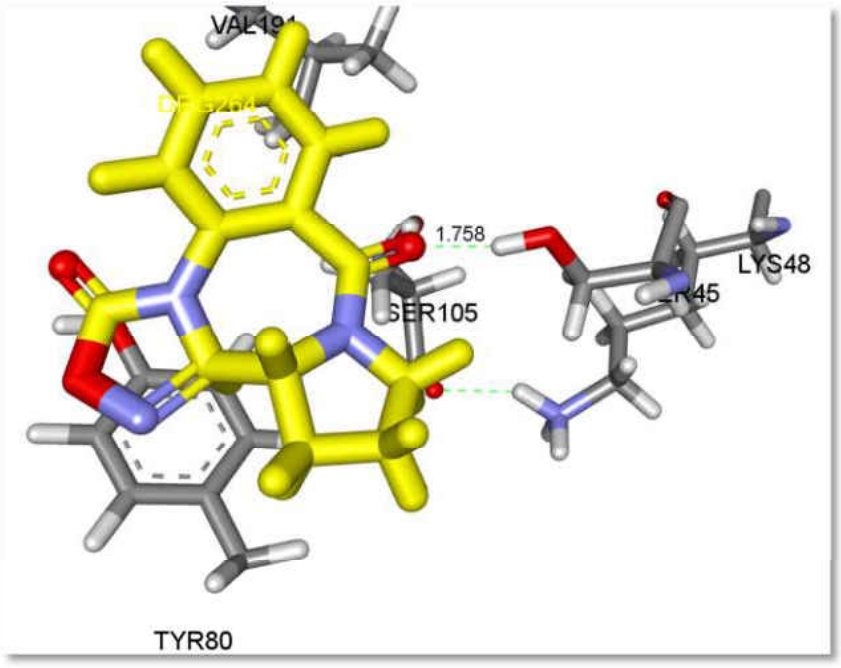

Figure 20: Interaction between TEM-1 β-lactamase active site residues and **6**

Syntheses of PBD derivatives

Synthesis of PBD Cyclic Amidine (**3**)

Pyrrolo[2,1-c][1,4]benzodiazepine natural product (**1**) (from *Isatis indigotica* [63]) was made as the starting material for all other derivatives by refluxing isatoic anhydride with (L)-proline in DMF following literature procedures (Scheme 1).[92,93] After recrystallization from Acetone/DMF (v/v 10:1) (yield = 82%), ^{1}H NMR in DMSO-d_6 showed six multiplets for the three (-CH_2) groups on the pyrrolidine ring (1.78–3.59 ppm), a doublet for the C-11a proton (4.10–4.13 ppm), two each of doublet-doublet and doublet-doublet-doublet for the aromatic protons (7.1–7.8 ppm) and a singlet representing the (–NH) group (10.51 ppm) (Appendix A1).

^{13}C NMR, IR, and GC-MS were also used to further confirm the structure of the product **1**. IR spectrum showed amide stretches at 1621 cm^{-1} and 1691 cm^{-1} confirming the presence of the two amide carbonyl groups present in **1**. Both amide carbonyl groups were also represented by peaks at 165.1 and 171.3 ppm in the ^{13}C NMR also helping to confirm that the product was PBD dilactam (**1**). In GC-MS, parent peak was observed at a retention time (R.T) of 13.4 minutes with a peak area of 99.69 % which indicated the exact molecular weight of the desired compound (**1**) (Appendix A2–A4).

Monothiolactam (**2**) was synthesized with a good yield by the thionation of **1** in THF at room temperature for 28 hours with 2,4-bis-(4-methoxyphenyl)-1,3-dithia-2,4-diphosphetane-2,4-disulfide (Lawesson's reagent).[94] Acetone/DMF (v/v 20:1) was used for the recrystallization of monothiolactam. ^{1}H NMR in DMSO-d6, ^{13}C NMR, IR, and GC-MS was used to confirm that the product was properly thionated (Appendix B1–B4). IR peak for one of the amide carbonyl was shown to have been removed (Appendix B4) indicating that the carbonyl of the amide at 1691 cm^{-1} had been thionated. Other characteristic features of **1** also present in **2** were observed

in the ^{1}H NMR and ^{13}C NMR, however with slightly different chemical shifts. Only one amide carbonyl was observed in the ^{13}C NMR at 164.8 ppm and the second peak at 202.6 ppm, which was indicative of the conversion of the C=O into a C=S thus confirming thionation (Appendix B1–B2). R.T and peak area of **2** in GC – MS was 14.6 and 99.30 %, respectively, also indicative of the molecular weight of the desired compound (**2**); although a little amount of the starting material (**1**) was observed to still be present in the sample. (Appendix B3).

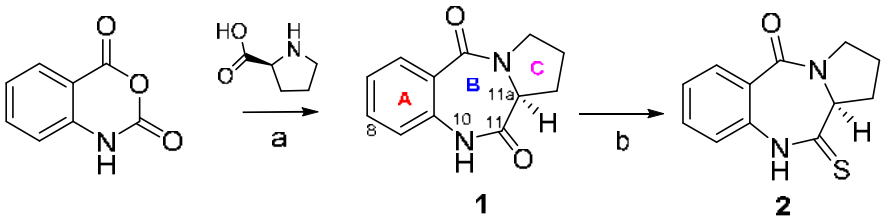

(a) L-proline, DMF, 155 °C, 5h;
(b) Lawesson's reagent, THF, rt, 24h

Scheme 2: Synthesis of PBD Dilactam (**1**) and Thiolactam (**2**)

The monothiolactam (**2**) was then reacted with an amine (propylamine) in the presence of mercury(II)chloride ($HgCl_2$) to the cyclic amidine **3** in high yields.

IR showed medium stretch (3356 cm^{-1}) for **3** indicating the replacement of the thio group in **2** by an amine (**3**) group (Appendix C4). ^{13}C NMR also showed the replacement of the thio (C=S) peak previously at 202.6 ppm with a new amino peak at about 43 ppm in **3**. The propyl group introduced were also observed as new peak at chemical shifts between 10–40 ppm in **3** (Appendix C2)

GC – MS showed a parent peak at an R.T. of 15.0 minutes and a peak area of 97.14 % for **3** (Appendix C3).

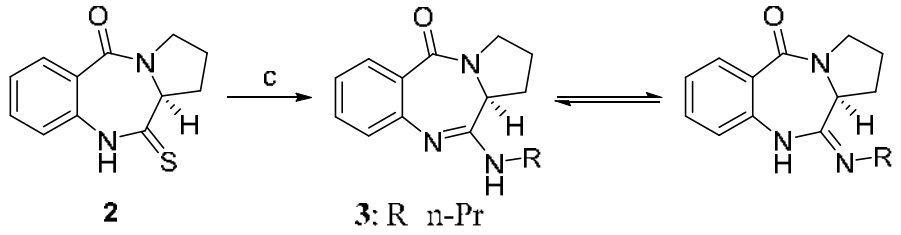

(c) R-NH_2, $HgCl_2$, THF, rx, 1h

Scheme 3: Synthesis of PBD propyl cyclo amidine (**3**)

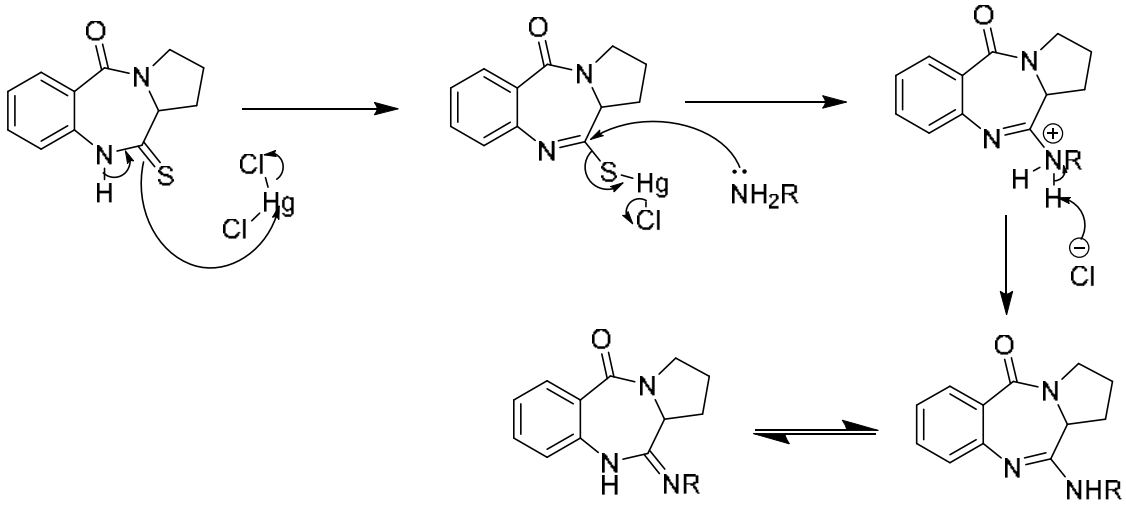

Scheme 4. Mechanism for synthesis of PBD cyclo amidine

Synthesis of PBD oxopyrimidine (**4**)

Neat reaction (without the use of solvent; performed in a Zincke apparatus) of the amidine **3** with bis(2,4,6-trichlorophenyl)-2-phenylmalonates resulted in the formation of the pyrimidine-annulated pyrrolobenzodiazepine **4** with the leaving group 2,4,6-trichlorophenol being distilled off during the reaction.[95]

^{1}H NMR in DMSO-d6 showed the introduction of a singlet proton at 4.91 ppm in **4** which is indicative of the phenylic proton from the malonic ester's introduction into the PBD (Appendix D1). Overlapping of duplicate aromatic protons indicating the presence of new aromatic protons were also observed from 7.30 to 8.05 ppm in **4**. The peak for the C11a proton which was present in **3** was absent in the ^{1}H NMR for **4** due to the presence of a double bond between C11 and C11a (Appendix D1).

^{13}C NMR also confirmed the presence of extra carbons (125.5–133.3 ppm for **4**) in the aromatic region of the ^{13}C NMR introduced due to the presence of the new phenyl ring from the malonic ester's introduction. New carbonyl carbons were also introduced (Appendix D2).

IR and GC-MS were also used to further confirm the structure of the product (**1**) (Appendix D3 – D4).

GC-MS showed R.T, molecular weight and peak area of **4** to be 29.1 minutes, 401 g mol^{-1}, and 99.34 %, respectively, indicating the formation of the desired product **4** (Appendix D3).

Results from previous studies have shown the possible existence of enolic partial structures in **4** in DMSO-d_6 and $CDCl_3$ at room temperature and hence the possibility of tautomers.[95]

In general, the reaction of *N*, *N′*-disubstituted amidines with bis(2,4,6-trichlorophenyl) malonates has been shown to result in the formation of pyridinium-4-olates. Ring closure by the loss of two molecules of trichlorophenol through a ketene intermediate as shown below is thought to be one of the possible explanation for the syntheses of these compounds mechanistically (Scheme 5).[95] To be taken into account is also the fact that this is the first time compound **4** has been synthesized and crystallized.

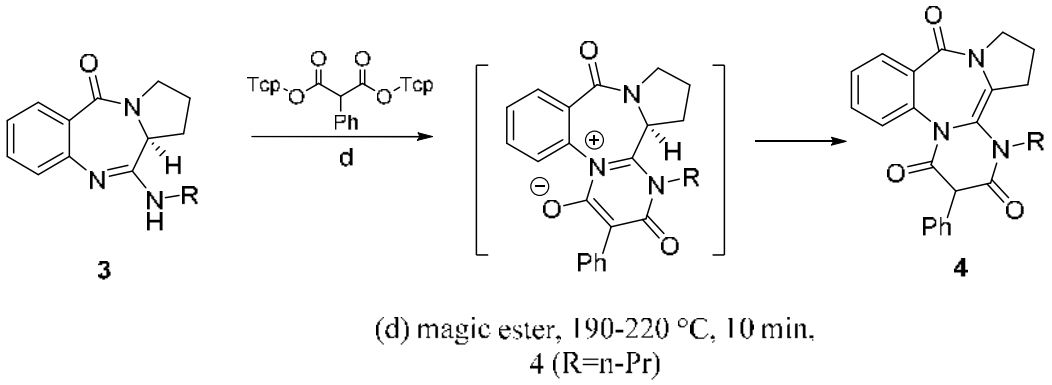

Scheme 5: Synthesis of PBD oxopyrimidine (**4**)

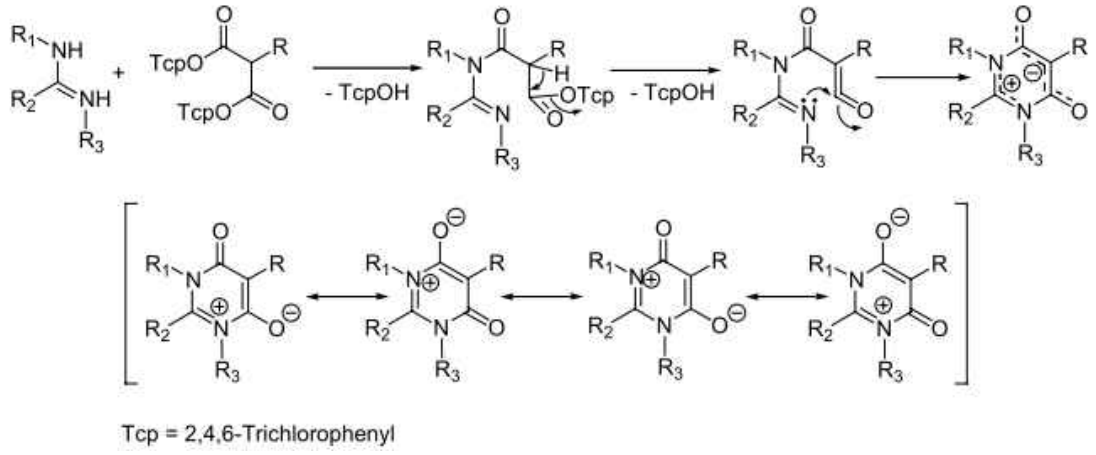

Scheme 6: Proposed mechanism for the formation of PBD oxo pyrimidine **4** (Adapted from Shilabin, 2005) [95].

Synthesis of PBD oxime (**5**)

A slight modification of the protocol used in Rekowski *et al*. 2010 and Bartsch *et al.* 1989 for the synthesis of **5** was employed. [96,97] Compound **5** was formed by a nucleophilic

substitution of **2** using $NH_2OH{\cdot}HCl$ under basic conditions. In place of triethylamine, K_2CO_3 was used in this reaction as the base. The product was formed after 24 hours of stirring at room temperature and further purified by flash column chromatography.

IR spectra confirmed the introduction of an OH group (3281 cm^{-1}) into the PBD as well as the presence of an OH proton in the proton NMR at 8.75 ppm. The presence of the newly introduced NH peak was also represented by a singlet at 10.08 ppm (Appendix E1 and E4).

GC-MS confirmed the desired product (**5**) with a molecular weight of 231 g mol^{-1} by an R.T. of 14.5 minutes and a peak area of 44.6 %. However, a possible reversion to **1** from some of the starting material **2** was observed as indicated by a molecular weight of 216 g mol^{-1} with a peak area of 49.8 % at R.T of 13.3 minutes which is the same R.T. for **1** (Appendix E3).

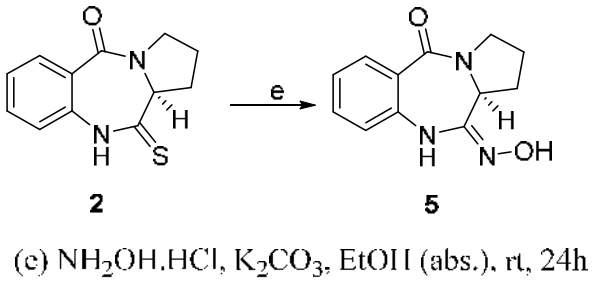

2 **5**

(e) $NH_2OH.HCl$, K_2CO_3, EtOH (abs.), rt, 24h

Scheme 7: Synthesis of PBD oxime (**5**)

The % yield of the reaction improved drastically from 76% reported in literature[97] to 94 % with the change in the base from triethylamine to K_2CO_3.

Synthesis of PBD oxadiazole (**6** and **7**)

PBD oxadiazole (**6**)[96] and thionyl oxadiazole (7) were formed through carbonylative and thionylative reactions, respectively. PBD oxime (**5**) was treated with 1,1-carbonyl diimidazole (CDI) and 1,1-thionyl diimidazole (TDI) and refluxed in dioxane for 12 hours respectively. The change in the solvent from THF to dioxane made the reaction faster and more efficient. The reaction with THF according to literature occurs in 24 hours and produces a yield of 84 %.[97] The modification leads to the formation of **6** and **7** in 12 hours with yields of 88 % and 90 %, respectively.

^{1}H NMR of **6** and **7** in $CDCl_3$-d revealed the retention of the aromatic protons as well all other protons present in the starting material **5** except the NH and OH peaks which were now absent in **6** and **7,** respectively, due to the introduction of the oxadiazolinone ring (Appendix F1 and G1). Formation of desired products **6** and **7** was also confirmed using IR which showed the introduction of a new C=O stretch at 1786 cm^{-1} in **6** replacing the OH stretch in **5** at 3281 cm^{-1}. This comes in addition to the previously present C=O stretch observed at 1612 cm^{-1} in **5** which is also represented by a stretch of 1640 cm^{-1} in **6**. The absence of the OH at 1612 cm^{-1} from **5** in **7** also indicates its possible replacement by a thione (C=S which is not observable in an IR spectra) as intended by the synthetic approach employed for the synthesis of **7.** This is also confirmed by the absence of the new C=O group introduced in **6** (Appendix F4 and G4). Characteristic molecular weights for compound **6** (257 g mol^{-1}) and **7** (273 g mol^{-1}) were observed in their respective GC-MS spectra at 14.9 minutes with a peak area of 62.94 % for **6** and 15.6 minutes with a peak area of 63.49 % for **7** (Appendix F3 and G3).

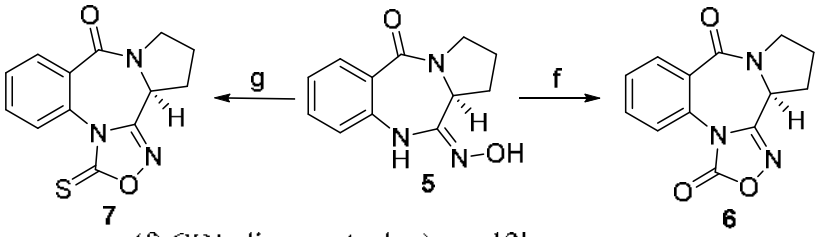

(f) CDI, dioxane (anhy.), rx, 12h,
(g) TDI, dioxane (anhy.), rx, 12h
CDI: carbonyldiimidazole, TDI: thionyldiimidazole

Scheme 8: Synthesis of PBD oxadiazole (**6**) and (**7**)

Crystals of compound **6** and **7** which have not been published in literature before now were also formed.

In order to gain additional insights into the structure of **6**, we tried to obtain single crystals for an X-ray analysis. We were finally successful in that: by slow evaporation of a concentrated solution of **6** in a 1:1 mixture of diisopropyl ether and ethyl acetate, we were able to crystallize **6**. The elemental cell contains one molecule of the PBD oxadiazole. The molecular structure and crystallographic numbering of **6** are shown in Figure 21 below.

The conformation adopted by **6** according to the X-ray diffraction ORTEP structure was a twisted conformation which is synonymous with 6:7:5 pyrrolobenzodiazepine ring systems. The 7 membered ring in this structure adopts a boat arrangement which is confirmed by bond angles of N(2)-C(8)-C(9) and C(8)-N(2)-C(7) which were determined to be 119.90 (19º) and 126.35 (2º), respectively. The C(8)-N(3) bond length is 128.8 pm which corresponds to an imino $C(sp^2)=N(sp^2)$ double bond. On the other hand, the N(2)-C(8) represents a single bond which has a bond length of 136.9 pm. The distinct C(8)-C(9) single bond present in the structure with a

bond length of 149.5 pm excludes the formation of an optically inactive tautomer of **6** (Appendix N1).

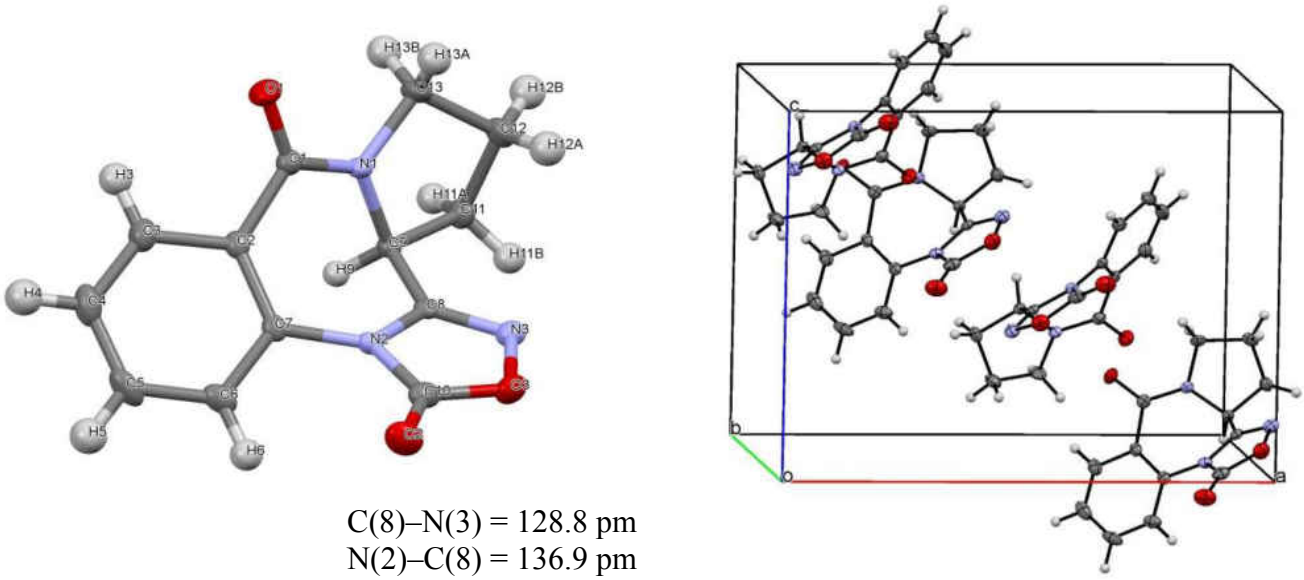

C(8)–N(3) = 128.8 pm
N(2)–C(8) = 136.9 pm

Figure 21: X-ray diffraction ORTEP structure and cell unit of compound **6**.

Synthesis of Thioacetamide (**8**) and *N*-phenylacetamide Cyclic Amidine (**9**)

N-phenylacetamide which is readily available was used as the starting material for the synthesis of other derivatives by the thionation in DCM at room temperature for 4 hours with Lawesson's reagent.[98]

^{1}H NMR in $CDCl_3$-d showed four sets of non-equivalent protons for the aromatic protons and the methyl group proton. The methyl protons were indicated by a singlet of 3H at 2.16 ppm and the aromatic protons were between 7.09–7.51 ppm (Appendix H1). Aromatic carbons were

indicated by chemical shifts between 120 to 138 ppm in ^{13}C NMR, while the methyl carbon, as well as the thioamide carbon, were represented by peaks at 24.7and 168.6 ppm, respectively (Appendix H2). IR indicated the absence of the carbonyl peak in the starting material (acetanilide) and the retention of the NH peak which could be seen at about 3175 cm^{-1} (Appendix I4). GC-MS further confirmed the structure of the product (**8**) with a parent peak of 151 g mol^{-1} at 9.7 minutes and a peak area of 96.6 % which is in correspondence with the molecular weight of the expected product (Appendix H3).

After thionation, thioacetamide (**8**) was reacted with propyl amine to yield (E)-*N*-phenyl-*N*'-propylacetimidamide (**9**) which was a liquid with a boiling point of about 150 °C. This reaction was accomplished after 3 different reaction conditions ranging from reflux temperature to 0 °C in the presence of mercury(II)chloride. The highest yield was obtained by carrying out the reaction at 0 °C.

^{13}C NMR showed the introduction of new carbon moieties from the propylamine into the structure of 9 with a new peak at chemical shifts between 11 and 68 ppm. The carbon positioned between the two nitrogen groups was very much deshielded thus showing a peak at about 207 ppm (Appendix I2). ^{1}H NMR in $CDCl_3$-d showed the introduction of three new sets of non-equivalent protons at chemical shifts 0.96-1, 1.57- 1.66, and 3.28-3.32 ppm, respectively, which was indicative of the newly introduced propyl chain. An extra proton at 1.19 ppm was observed and this was representative of the -NH proton. Every other proton as in starting material 8, were all accounted for but at different chemical shifts as they were in **8** (Appendix I1).

GC-MS confirmed the synthesis of the desired product, **9** with a parent peak of 176 g mol^{-1} at 9.3 minutes and a peak area of 96.84 % corresponding to the molecular weight of the desired product, **9** (Appendix I3).

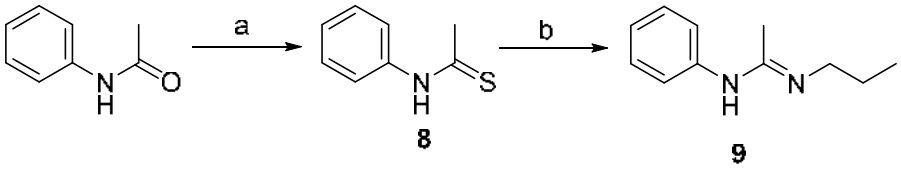

(a) Lawesson's reagent, DCM, rt, 4h,
(b) n-Pr-NH_2, $HgCl_2$, THF, 0 °C, 2h

Scheme 9: Synthesis of thioacetamide (**8**) and *N*-phenylacetamide cyclic amidine (**9**)

Synthesis of 2-methylene-1,5-diphenyl-3-propyldihydropyrimidine-4,6(1H,5H)-dione (**10**)

(E)-*N*-phenyl-*N*'-propylacetimidamide (**9**) was used to prepare **10,** using the same neat reaction (performed in a Zincke apparatus) used for the synthesis of PBD oxo pyrimidines (**4**). Bis(2,4,6-trichlorophenyl)-2-phenylmalonate was reacted with **9** leading to the formation of compound **10** with the 2,4,6-trichlorophenol being distilled off during the reaction.

^{13}C NMR showed the introduction of new carbonyl peaks as a result of the malonic ester introduction at chemical shifts of 150 and 168 ppm, respectively. Overlapping aromatic carbon peaks were also observed in aromatic carbon region represented by an increase in peak sizes (Appendix J2). ^{1}H NMR in $CDCl_3$-d confirmed the introduction of a singlet proton at 4.10 ppm and new aromatic protons at the aromatic region (Appendix J1). IR confirmed the introduction of the C=O groups with a very sharp C=O stretch at 1643 cm^{-1} (Appendix J4). Finally, GC-MS was also used to confirm the structure of the compound (**10**) obtained with a molecular peak at about 322 coming at retention times of 18.9 and 18.93 with peak areas of 55.5 % and 45.5 % (Appendix J3).

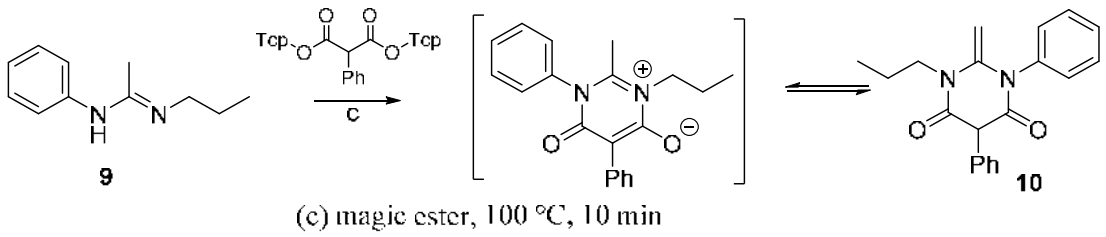

Scheme 10: Synthesis of **10**

Synthesis of (E)-*N*'-hydroxyl-*N*-phenylacetimidamide (**11**)

Two different synthetic routes were employed for the synthesis of **11**. The first route employed was similar to that used for the formation of compound **5**, where **11** is formed by nucleophilic substitution of **8** with $NH_2OH{\cdot}HCL$ in the presence of a mild base (Na_2CO_3).

The yield was fairly lower (55 % yield) when compared to the other synthetic procedure that had been reported in literature for the synthesis of **11**.[99]

In the second synthetic route, aniline was reacted with nitroethane in the presence of polyphosphoric acid (PPA). The reaction was quenched and neutralized after 5 hours using H_2O and then NH_3 (aq), respectively, and the final product, **11** recrystallized afterward from water. The yield for this procedure was 75 % which was similar to the yield gotten from literature.[99]

The mechanism for the second synthetic route occurs through an umpolung activated nitroalkane formed from the addition of the PPA to the nitroalkane to form an electrophilic phosphorylated aciform of the nitroalkane. This umpolung activated nitroalkane is then attacked by electron-rich arene (aniline).[99]

Oxime intermediates are formed after the subsequent elimination of H_3PO_4. It is rationalized that anilines can also be employed in a similar transformation as nitrogen-based

nucleophiles to produce imidamides as shown in Scheme 10, which can further be employed as convenient building blocks for the synthesis of heterocyclic compounds.[99]

^{1}H NMR, ^{13}C NMR, IR, and GC-MS were used to further confirm the structure of both products (**11**) (Appendix K1 – K4).

GC-MS showed a molecular peak of 150 coming at a retention time of 8.9 (Appendix K3).

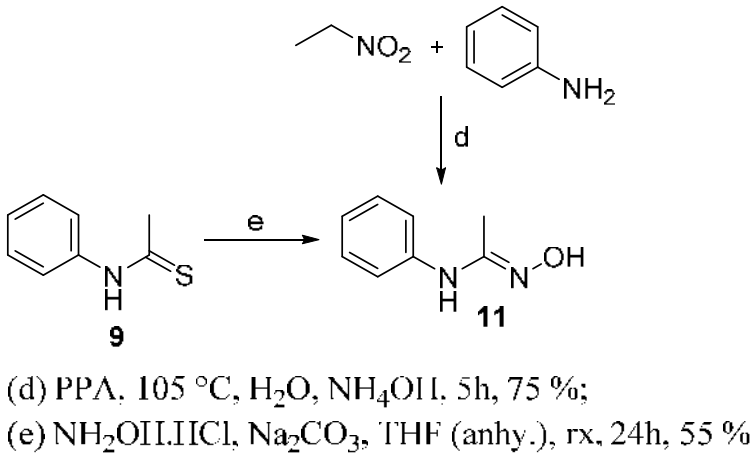

Scheme 11: Synthesis of (E)-*N*'-hydroxyl-*N*-phenylacetimidamide (**11**)

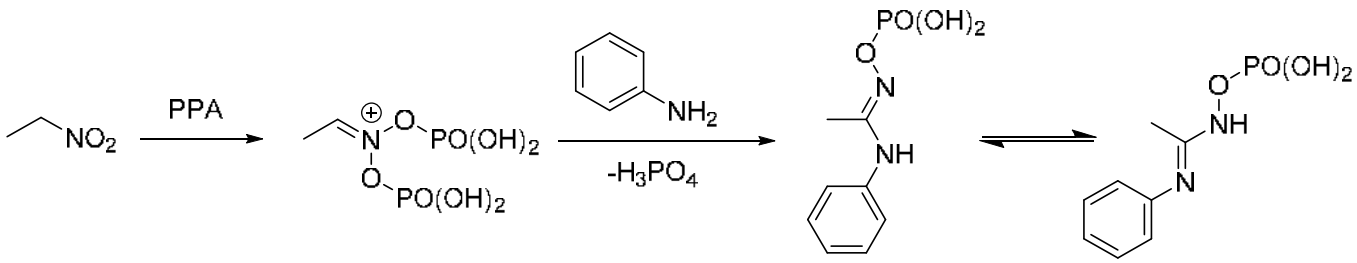

Scheme 12: Mechanism for the alternative synthesis of (E)-*N*'-hydroxyl-*N*-phenylacetimidamide (**11**) (Adapted from Aksenov *et al.* 2015).[99]

Synthesis of *N*-phenyl oxadiazoles (**12** and **13**)

N-phenyl oxadiazoles (**12** and **13**) were also formed through carbonylative and thionylative reactions, respectively, just like their PBD counterparts. In these reactions, however, dioxane was used as the solvent and the reaction temperature was reduced to 50 ^{o}C. Crystals of compound **12** and **13** were also recovered from a mixture of diisopropyl ether and ethyl acetate.

^{1}H NMR in $CDCl_3$-d showed aromatic protons as well as only the methyl group protons which were conserved in both **12** and **13**. The OH proton observed in **12** was no longer present showing that **12** and **13** were formed (Appendix L1 and M1). ^{13}C NMR reveals new C=O and C=S peaks for **12** and **13** at 156.2 and 186.7 ppm, respectively. (Appendix L2 and M2). IR confirmed the replacement of the OH in **11** by the removal of the OH stretch (Appendix K4, L4, and M4). GC – MS showed peaks at 10.1 and 12.3 minutes for **12** and **13,** respectively. Molecular peaks of 176 and 192 g mol^{-1} were also observed for **12** and **13** with peak areas of 96.26 % and 62.11 % (Appendix L3 and M3).

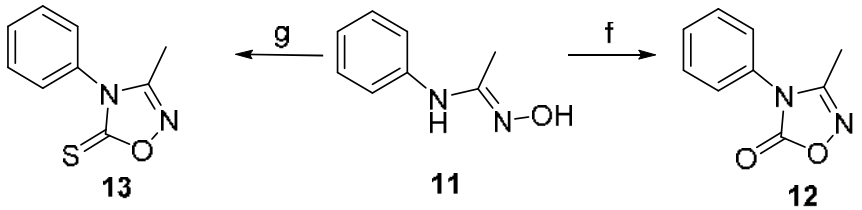

(f) CDI, dioxane (anhy.), 50 °C, 24h, 60 %;
(g) TDI, dioxane (anhy.), 50 °C, 12h, 78 %.
CDI: carbonyldiimidazole, TDI: thionyldiimidazole

Scheme 13: Synthesis of *N*-phenyl oxadiazole (**12**) and (**13**)

Enzyme Inhibition Kinetics

Enzyme inhibition kinetics to ascertain the percentage inhibition and residual activity of the enzymes TEM-1 and p99 lactamase was carried out in 20 mM MOPS buffer. 3 µL (final concentration = 0.25 and 0.20 nM for TEM-1 and P99 respectively) of enzymes was used for the assay. Percentage inhibition and residual activities of the enzymes after incubation with inhibitors (**1-13**) in the presence of chromogenic substrate NCF is shown in Tables 3 – 6 below.

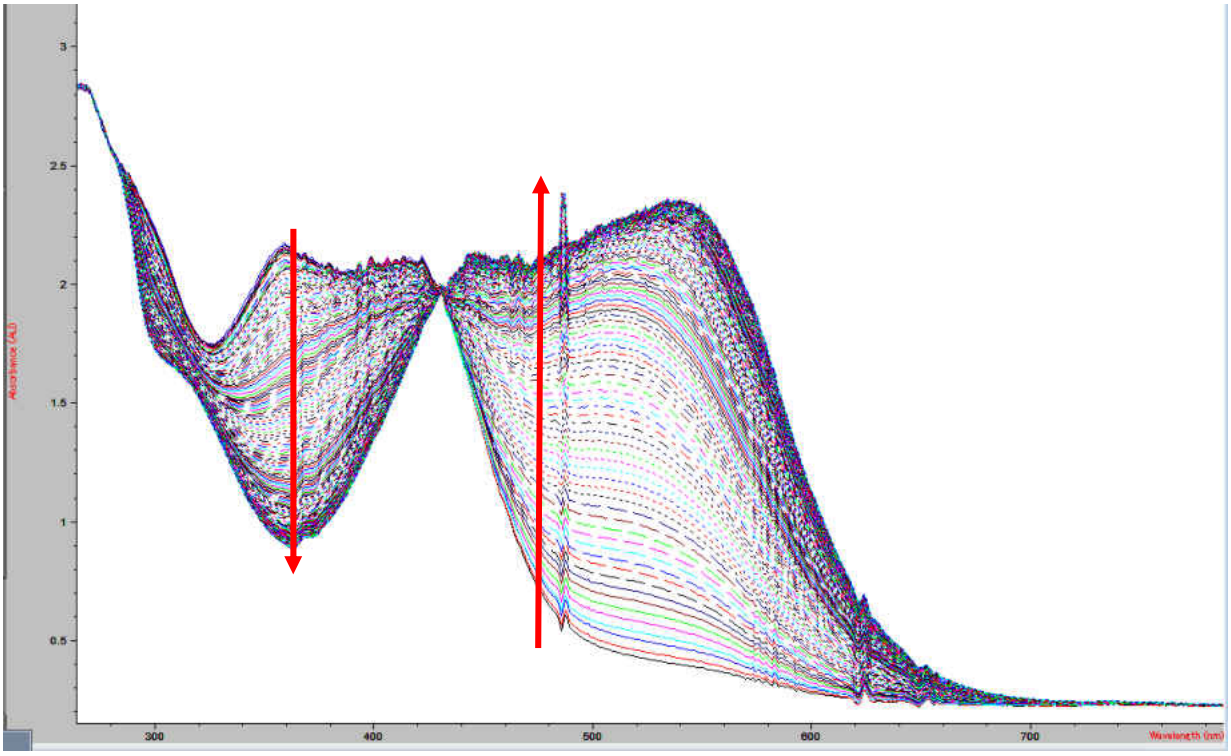

Figure 22: Typical hydrolysis of substrate, NCF by TEM-1 β-lactamase

Table 3: Residual Activity (%) and percent inhibition of TEM-1 after incubation with clavulanate and PBD derivatives for 5 minutes, 30 ^{o}C in DMF (3%).

Enzyme Inhibition Kinetics Conditions	$V_o \pm SD$ ($\Delta A, s^{-1}$) x 10^{-4}	$V_i \pm SD$ ($\Delta A, s^{-1}$) x 10^{-4}	Residual Activity (%)	% Inhibition
Clavulanate [#]	2.3721 ± 0.0179	0.6112 ± 0.0091	25.77	74.23
1	2.3721 ± 0.0179	1.5667 ± 0.01686	66.05	33.95
2	2.3721 ± 0.0179	2.5101 ± 0.08144	100	NI
3	2.3721 ± 0.0179	2.6475 ± 0.04724	100	NI
4	2.3721 ± 0.0179	2.0864 ± 0.01605	87.96	12.04
5	2.3721 ± 0.0179	1.5617 ± 0.01740	65.83	34.17
6	2.3721 ± 0.0179	2.1298 ± 0.02806	89.79	10.21
7	2.3721 ± 0.0179	2.1795 ± 0.02172	91.88	9.22

Table 4: Residual Activity (%) and percent inhibition of P99 after incubation with clavulanate and PBD derivatives for 5 minutes, 30 ^{o}C in DMF (3%).

Enzyme Inhibition Kinetics Conditions	$V_o \pm SD$ ($\Delta A, s^{-1}$) x 10^{-4}	$V_i \pm SD$ ($\Delta A, s^{-1}$) x 10^{-4}	Residual Activity (%)	% Inhibition
Clavulanate[#]	2.5743 ± 0.01647	2.277 ± 0.03676	88.45	11.55
1	2.5743 ± 0.01647	3.9885 ± 0.04783	100	NI
2	2.5743 ± 0.01647	3.802 ± 0.08103	100	NI
3	2.5743 ± 0.01647	3.4348 ± 0.01447	100	NI
4	2.5743 ± 0.01647	2.2329 ± 0.01290	86.74	13.36
5	2.5743 ± 0.01647	2.6279 ± 0.03439	100	NI
6	2.5743 ± 0.01647	2.2965 ± 0.02968	89.24	10.76
7	2.5743 ± 0.01647	2.4733 ± 0.02748	96.08	3.92

[#] Final concentration and volume of Clavulanate = 120 nM
Final concentration & volume of Enzyme (TEM-1) = 3 µL (0.25 nM)
Final concentration & volume of Enzyme (P99) = 3 µL (0.20 nM)
Substrate (NCF) = 12 µL (100 µM), Triton X100 = 3 µL (0.1 %), 0.1 % BSA in MOPS buffer = 562 µL (0.02 M, pH 7.5)
Inhibitor (in 3 % DMF) = 20 µL (400 µM), NI = No inhibition

Table 5: Residual Activity (%) and percent inhibition of TEM-1 after incubation with clavulanate and N-phenylacetamide derivatives for 5 minutes, 30 ^{o}C in DMF (3%).

Enzyme Inhibition Kinetics Conditions	$V_o \pm SD$ ($\Delta A, s^{-1}$) x 10^{-4}	$V_i \pm SD$ ($\Delta A, s^{-1}$) x 10^{-4}	Residual Activity (%)	% Inhibition
11	3.7575	4.2356	100	NI
12	3.7575	4.6721	100	NI
13	3.7575	3.3132	88.18	11.82

Final concentration & volume of Enzyme (TEM-1) = 3 µL (0.25 nM)
Final concentration & volume of Enzyme (P99) = 3 µL (0.20 nM)
Substrate (NCF) = 10 µL (50 µM), Triton X100 = 3 µL (0.1 %), 0.1 % BSA in MOPS buffer = 562 µL (0.02 M, pH 7.5)
Inhibitor (in 3 % DMF) = 20 µL (1 mM), NI = No inhibition

Table 6: Residual Activity (%) and percent inhibition of P99 after incubation with clavulanate and *N*-phenylacetamide derivatives for 5 minutes, 30 ^{o}C in DMF (3%).

Enzyme Inhibition Kinetics Conditions	$V_o \pm SD$ ($\Delta A, s^{-1}$) x 10^{-4}	$V_i \pm SD$ ($\Delta A, s^{-1}$) x 10^{-4}	Residual Activity (%)	% Inhibition
11	4.4748	4.5517	100	NI
12	4.4748	4.6837	100	NI
13	4.4748	5.0231	100	NI

Final concentration & volume of Enzyme (TEM-1) = 3 µL (0.25 nM)
Final concentration & volume of Enzyme (P99) = 3 µL (0.20 nM)
Substrate (NCF) = 10 µL (50 µM), Triton X100 = 3 µL (0.1 %), 0.1 % BSA in MOPS buffer = 562 µL (0.02 M, pH 7.5)
Inhibitor (in 3 % DMF) = 20 µL (1 mM), NI = No inhibition

From the enzyme kinetics results, it was observed that all derivatives of PBD and *N*-phenylacetamide had little or no inhibiting effects on the enzymes studied in this study. For PBDs, **5** has the highest percentage inhibition of 34.17 % for TEM-1 β-lactamase but had no effect on P99 at a final concentration of 400 µM. **4**, **6**, and **7** also showed percentage inhibition of TEM-1 β-lactamase of 12.04 %, 10.21 %, and 9.22 %, respectively. This relative inhibition was replicated in P99 β-lactamase; 13.36, 10.76, and 9.21 % for **4**, **6**, and **7** respectively. It is suspected that there might be issues with the solubility of the inhibitors in the buffer solution used for the enzyme kinetics reactions thus making the inhibitor unavailable to the active site.

There is also a possibility of steric interference being another setback preventing the active part of the molecules from interacting appropriately with the active site of the enzymes. We believe that incorporation of groups that enhance solubility (e.g. COOH, SO_3^-, OH) would be key to improving the inhibitory activity of the inhibitors against the enzymes. Derivatives **8-13** were made to try to tackle the possible steric hindrance problem and possibly increase electrophilicity and interaction between active site residues and the inhibitors. However, after *in vivo* assays, only **13** showed some activity against TEM-1 β-lactamase with a percentage inhibition of 11.82 % at a final concentration of 1 mM.

We believe that the attachment of a phenyl group to the nitrogen group as shown in **12** and **13** leads to the formation of very stable intermediates due to the resonance stabilization effected by the phenyl ring. This stabilization could thus prevent the OH nucleophile from the splitting of water to catalyze the remainder of the reaction of hydrolysis thus leading to the inhibitor being released from the active site of the enzymes. For future work, in addition to improving solubility by the addition of COOH, SO_3, and OH groups to the derivatives, we aim to also change the position the phenyl group in the latter derivatives (**8**-**13**) to allow better interaction of the active site residues (Ser 45 and Ser 105) with the oxadiazole ring particularly in **12** and **13** as well as reduce the resonance stabilizing effect of the phenyl ring on the derivatives **12** and **13**.

CHAPTER 4

CONCLUSION AND FUTURE WORK

Conclusion

In this project, various derivatives of PBD were synthesized, using commercially available starting materials like PBD dilactam (**1**) (formed from isatoic anhydride and L-proline) and *N*-phenylacetamide and evaluated for their efficacy as non-β-lactam β-lactamase inhibitor.

The PBD derivatives were: (S)-11-thioxo-1,2,3,10,11,11a-hexahydro-5H-benzo[e]pyrrolo[1,2-a][1,4]diazepin-5-one (**2**), **(S)-**11-amino-1,2,3,11a-tetrahydro-5H-benzo[e]pyrrolo[1,2-a][1,4]diazepin-5-one **(3a**), (S)-11-(propylamino)-1,2,3,11a-tetrahydro-5H-benzo[e]pyrrolo[1,2-a][1,4]diazepin-5-one (**3b)**, (14aS)-3-phenyl-12,13,14,14a-tetrahydro-2H,10H-benzo[e]pyrimido[2,1-c]pyrrolo[1,2-a][1,4]diazepine-2,4,10(3H)-trione **(4)**, 3-phenyl-1-propyl-1,12,13,14-tetrahydro-2H,10H-benzo[e]pyrimido[2,1-c]pyrrolo[1,2-a][1,4]diazepine-2,4,10(3H)-trione **(5)**, (S,E)-11-(hydroxyimino)-1,2,3,10,11,11a-hexahydro-5H-benzo[e]pyrrolo[1,2-a][1,4]diazepin-5-one **(6)**, (S)-11,12,13,13a-tetrahydro-3H,9H-benzo[e][1,2,4]oxadiazolo[3,4-c]pyrrolo[1,2-a][1,4]diazepine-3,9-dione **(7)** and (S)-3-thioxo-11,12,13,13a-tetrahydro-3H,9H-benzo[e][1,2,4]oxadiazolo[3,4-c]pyrrolo[1,2-a][1,4]diazepin-9-one **(8)**.

The *N*-phenylacetamide derivatives were**:** *N*-phenylethanethioamide **(9)**, (E)-*N*-phenyl-*N*'-propylacetimidamide (**10**), 2-methylene-1,5-diphenyl-3-propyldihydropyrimidine-4,6(1H,5H)-dione (**11**), (E)-*N*'-hydroxy-*N*-phenylacetimidamide (**12**), 3-methyl-4-phenyl-1,2,4-oxadiazol-5(4H)-one (**13**) and 3-methyl-4-phenyl-1,2,4-oxadiazole-5(4H)-thione (**14**).

Docking studies were also conducted to determine the possible interaction of PBD derivatives with active site amino acid residues revealed significant interactive spanning of the active site of TEM-1 β-lactamase by PBD-derivatives. This indicated the high possibility of being high potentials at being a new class of non-β-lactam β-lactamase inhibitors due to their non-covalent interactions with active site residues of the enzyme. Molecular docking results showed the possibility of some PBDs derivatives, particularly compounds **4, 5,** and **7** having the best potentials of being non-β-lactam β-lactamase inhibitors due to their interaction with the enzymes' active site residues and predicted binding affinity energies. Compound **4** displayed the best potential interaction in terms of the number of active site residues, as well as hydrogen bonding forces. However, possible steric hindrances to more efficient interactions were thought to be encountered during docking due to the bulky nature of the PBD molecules thus limiting optimal interactions. This was also observed in the percentage inhibition recorded during enzyme kinetics reaction with TEM-1 and P99 β-lactamases.

Based on the poor inhibitory activities of the PBD derivatives observed during the enzyme kinetics experiment, we proposed some possible reasons for this poor results The poor inhibitory activities of the PBD derivatives could have been as a result of poor solubility of the compounds in the solvent used that is DMF, thus availability of the inhibitor molecules to the enzymes. Another possible reason for the low inhibitory activities observed from compounds **1-13** could be the incubation time of the reaction which was 5 minutes. This could possibly not be sufficient enough time for the enzyme and inhibitors to interact appropriately to bring about maximum inhibition. In future work, we would also extend the incubation time of the inhibitor with the enzymes before the addition of the substrate, NCF.

The mechanism of action which we proposed at the beginning of the work could be different from the mechanism by which the inhibitor interacts with enzymes thus facilitating easy release of the inhibitor by the enzyme after initial interaction. This could imply that PBDs possibly do not for covalent interactions as in β-lactam based inhibitors like clavulanate but rather form non-covalent interactions which are readily susceptible to being reversible.

Optimization of enzyme kinetics assay parameters such as reaction temperature, solvent changes to enhance possible solubility and hence bioavailability of ligands to enzymes, reaction times as well as buffer change would also be done in the future to further rule out these possibilities as reasons for the poor inhibitory activities of the inhibitors.

The search for more elaborate PBD chemotypes which may have better activity as well as stronger affinity, exploiting fragment-based designing followed by synthesis and further *in vitro* evaluation against TEM-1 and P99 β-lactamases will be done in the future.

Future Work

1. Assay a library of compounds in search of better lead compounds for β-lactamase inhibition. This would be done to help get lead compounds that would spearhead the synthesis of new and better inhibitors.

2. The introduction of functional groups like carboxylic acid groups that will further enhance the solubility of the inhibitors in the enzyme assays solution to enhance further interactions.

3. Substituting the methyl group on the latter derivatives (**8**-**13**) with a phenyl group and the removal of the phenyl group from being attached to the amide group as shown in the Figure 23 below will further possibly enhance interactions of inhibitors with enzymes.

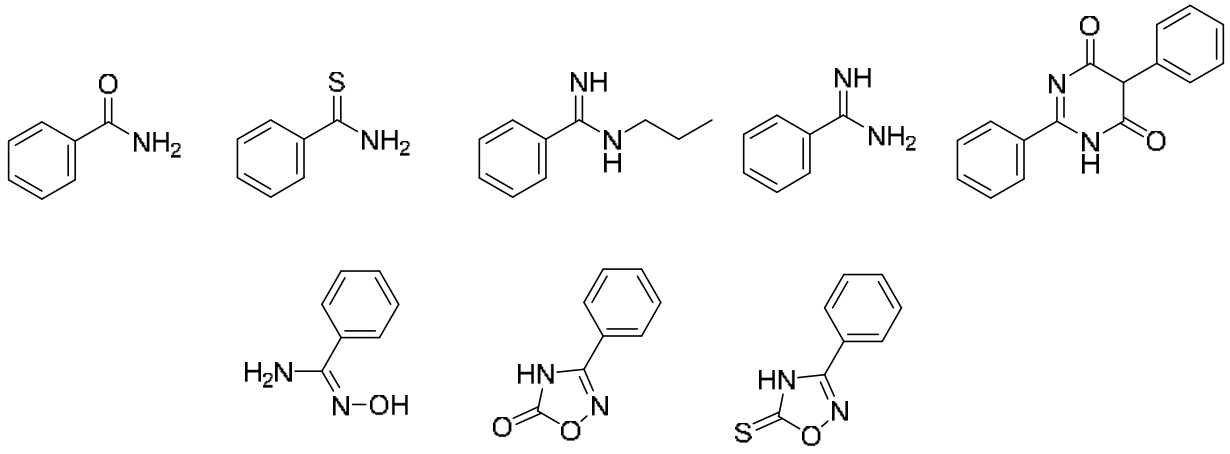

Figure 23: Proposed derivatives for future work

4. Depending upon the results of the assay, design and synthesize new β-lactamase inhibitors.

5. Check the efficacy of the PBD compounds and all other synthesized compounds on cytotoxic activity and inhibition of other enzymes (e.g. ACE) implicated in diseases and infections.

REFERENCES

1. Papp-Wallace, K. M.; Endimiani, A.; Taracila, M. A.; Bonomo, R. A. Carbapenems: Past, Present, and future. *Antimicrob. Agents Ch.* **2011**, *55*, 4943–4960.
2. Demain, A. L.; Sanchez, S. Microbial drug discovery: 80 Years of progress. *J. Antibiot.* **2009**, *62*, 5–16.
3. Rammelkamp, C. H.; Maxon, T. Resistance of *Staphylococcus aureus* to the Action of Penicillin. *Proc. Soc. Exp. Biol. Med.* **1942**, *51*, 386–389
4. Chambers, H. F. Methicillin resistance in Staphylococci: Molecular and biochemical basis and clinical implications. *Clin. Microbiol. Rev.* **1997**, *10*, 781–791.
5. Zervosen, A.; Sauvage, E.; Frère, J. M.; Charlier, P.; Luxen, A. Development of New Drugs for an Old Target — The Penicillin Binding Proteins. *Molecules* **2012**, *17*, 12478-12505
6. Drawz, S. M.; Bonomo, R. A. Three decades of beta-lactamase inhibitors. *Clin. Microbiol. Rev.***2010**, *23*, 160–201.
7. Barlow, M. What antimicrobial resistance has taught us about horizontal gene transfer. *Methods Mol. Biol.* **2009**, *532*, 397–411.
8. Brannigan, J. A.; Tirodimos, I. A.; Zhang, Q. Y.; Dowson, C. G.; Spratt, B.G. Insertion of an extra amino acid is the main cause of the low affinity of penicillin-binding protein 2 in penicillin-resistant strains of *Neisseria gonorrhoeae*. *Mol. Microbiol.* **1990**, *4*, 913–919.
9. Dabernat, H.; Delmas, C.; Seguy, M.; Pelissier, R.; Faucon, G.; Bennamani, S.; Pasquier, C. Diversity of beta-lactam resistance-conferring amino acid substitutions in penicillin-binding protein 3 of *Haemophilus influenzae*. *Antimicrob. Agents Ch.* **2002**, *46*, 2208–2218.

10. Pernot, L.; Chesnel, L.; Le Gouellec, A.; Croize, J.; Vernet, T.; Dideberg, O.; Dessen, A. A PBP2x from a clinical isolate of *Streptococcus pneumoniae* exhibits an alternative mechanism for reduction of susceptibility to beta-lactam antibiotics. *J. Biol. Chem.* **2004**, *279*, 16463–16470.
11. Doumith, M.; Ellington, M. J.; Livermore, D. M.; Woodford, N. Molecular mechanisms disrupting porin expression in ertapenem-resistant *Klebsiella* and *Enterobacter* spp. clinical isolates from the UK. *J. Antimicrob. Chemother.* **2009**, *63*, 659–667.
12. Livermore, D.M. Of Pseudomonas, Porins, Pumps and carbapenems. *J. Antimicrob. Chemother.* **2001**, *47*, 247–250.
13. Abraham, E. P.; Chain, E. An enzyme from bacteria able to destroy penicillin. *Nature,* **1940**, *146*, 837.
14. Abraham, E. P., E. Chain, C. M. Fletcher, H. W. Florey, A. D. Gardner, N. G. Heatley, and M. A. Jennings. Further observations on penicillin. *Lancet II,* **1941**, *238*, 177–189.
15. Bush, K., and P. A. Bradford. β-Lactamases: historical perspectives, p. 67–79. *In* R. A. Bonomo and M. E. Tolmasky (ed.), Enzyme-mediated resistance to antibiotics: mechanisms, dissemination, and prospects for inhibition. **2007**. ASM Press, Washington, DC.
16. Kirby, W. M. Extraction of a highly potent penicillin inactivator from penicillin-resistant staphylococci. *Science,* **1944**, *99*, 452–453.
17. Massova, I.; Mobashery, S. Kinship and diversification of bacterial penicillin-binding proteins and β-lactamases. *Antimicrob. Agents Chemother*. **1998**, *42*, 1–17.
18. Medeiros, A. A. Evolution and dissemination of β-lactamases accelerated by generations of β-lactam antibiotics. *Clin. Infect. Dis.* **1997**, *24;* S19–S45.

19. Perez, F.; Endimiani, A.; Hujer, K. M.; Bonomo, R. A. The continuing challenge of ESBLs. *Curr. Opin. Pharmacol.* **2007**, *7,* 459–469

20. Ambler, R. P.; Coulson, A. F.; Frere, J. M.; Ghuysen, J. M.; Joris, B.; Forsman, M.; Levesque, R. C.; Tiraby, G.; Waley, S. G. A standard numbering scheme for the class A β-lactamases. *Biochem. J.* **1991**, *276*, 269–270.

21. Bush, K.; Jacoby, G. A.; Medeiros, A. A. A functional classification scheme for β-lactamases and its correlation with molecular structure. *Antimicrob. Agents Chemother*. **1995,** *39*, 1211–1233.

22. Bush, K. Metallo-β-lactamases: a class apart. *Clin. Infect. Dis.* **1998**, *27*, S48–S53.

23. Papp-Wallace, K. M.; Bethel, C. R.; Distler, A.; Kasuboski, C.; Taracila, M.; Bonomo. R. A. Inhibitor resistance in the KPC-2 β-lactamase: a pre-eminent property of this class A β-lactamase. *Antimicrob. Agents Chemother*. **2009**, *54*, 890–897

24. Jacoby, G. A.; Medeiros, A. A. More extended-spectrum β-lactamases. *Antimicrob. Agents Chemother*. **1991**, *35*, 1697–1704.

25. Jacoby, G. A.; Munoz-Price, L. S. The new β-lactamases. *N Engl. J. Med.* **2005**, *352*, 380–391.

26. Rice, L. B.; Eckstein, E. C.; DeVente, J.; Shlaes, D. M. Ceftazidime-resistant *Klebsiella pneumoniae* isolates recovered at the Cleveland Department of Veterans Affairs Medical Center. *Clin. Infect. Dis.* **1996,** *23*, 118–124.

27. Walsh, T. R.; Toleman, M. A.; Poirel, L.; Nordmann, P. Metallo- β-lactamases: the quiet before the storm? *Clin. Microbiol. Rev*. **2005**, *18*, 306–325.

28. Philippon, A.; Arlet, G.; Jacoby, G. A. Plasmid-determined AmpC-type β-lactamases. *Antimicrob. Agents Chemother.* **2012**, *46*, 1–11.

29. Daniel, F.; Page, M. G.; Livermore, D. M. Class D β-lactamases, p. 163–194. *In* R. A. Bonomo and M. E. Tolmasky (ed.), Enzyme-mediated resistance to antibiotics: mechanisms, dissemination, and prospects for inhibition. 2007. ASM Press, Washington, DC.

30. Aarestrup, F. Sustainable farming: Get pigs off antibiotics. *Nature* **2012**, *486*, 465–466.

31. Bebrone, C.; Lassaux, P.; Vercheval, L.; Sohier, J.S.; Jehaes, A.; Sauvage, E.; Galleni, M. Current challenges in antimicrobial chemotherapy: Focus on beta-lactamase inhibition. *Drugs* **2010**, *70*, 651–679.

32. Pratt, R.F. Beta-lactamase inhibitors: Non-beta-lactams. In *Beta-lactamases*; Frére, J.-M., Ed.; Nova Science Publisher, Inc: Hauppauge, NY, USA, 2012; pp. 259–292.

33. Coleman, K. Diazabicyclooctanes (DBOs): A potent new class of non-beta-lactam beta-lactamase inhibitors. *Curr. Opin. Microbiol.* **2011**, *14*, 550–555.

34. Endimiani, A.; Choudhary, Y.; Bonomo, R. A. *In vitro* activity of NXL104 in combination with beta-lactams against *Klebsiella pneumoniae* isolates producing KPC carbapenemases. *Antimicrob. Agents Ch.* **2009**, *53*, 3599–3601.

35. Stachyra, T.; Levasseur, P.; Pechereau, M.C.; Girard, A. M.; Claudon, M.; Miossec, C.; Black, M.T. *In vitro* activity of the {beta}-lactamase inhibitor NXL104 against KPC-2 carbapenemase and Enterobacteriaceae expressing KPC carbapenemases. *J. Antimicrob. Chemother.* **2009**, *64*, 326–329.

36. Devasahayam, G.; Scheld, W. M.; Hoffman, P. S. Newer antibacterial drugs for a new century. *Expert Opin. Inv. Drugs* **2010**, *19*, 215–234.

37. Bebrone, C.; Lassaux, P.; Vercheval, L.; Sohier, J. S.; Jehaes, A.; Sauvage, E.; Galleni, M. Current challenges in antimicrobial chemotherapy: Focus on beta-lactamase inhibition. *Drugs* **2010**, *70*, 651–679.

38. Pratt, R. F. Beta-lactamase inhibitors: Non-beta-lactams. In *Beta-lactamases*; Frére, J.-M., Ed.; Nova Science Publisher, Inc: Hauppauge, NY, USA, 2012; pp. 259–292.

39. Pechenov, A.; Stefanova, M. E.; Nicholas, R. A.; Peddi, S.; Gutheil, W. G. Potential transition state analogue inhibitors for the penicillin-binding proteins. *Biochemistry* **2003**, *42*, 579–588.

40. Bone, R.; Shenvi, A. B.; Kettner, C. A.; Agard, D. A. Serine protease mechanism: structure of an inhibitory complex of alpha-lytic protease and a tightly bound peptide boronic acid. *Biochemistry* **1987***, 26*, 7609–7614.

41. Lindquist, R. N.; Terry, C. Inhibition of subtilisin by boronic acids, potential analogs of tetrahedral reaction intermediates. *Arch. Biochem. Biophys*. **1974**, *160*, 135–144.

42. Woon, E. C. Y.; Zervosen, A.; Sauvage, E.; Simmons, K. J.; Zivec, M.; Inglis, S. R.; Fishwick, C. W. G.; Gobec, S.; Charlier, P.; Luxen, A.; Schofield, C. J. Structure-Guided Development of Potent Reversibly Binding Penicillin Binding Protein Inhibitors. *ACS Med. Chem. Lett.* **2011**, *2*, 219–223.

43. Kraut, J. Serine proteases: Structure and mechanism of catalysis. *Annu. Rev. Biochem.* **1977**, *46*, 331–358.

44. Jungheim, L. N.; Ternansky, R. J. Non-beta-lactam mimics of beta-lactam antibiotics. In *The Chemistry of Beta-Lactams*; Page, M.I., Ed.; Chapman and Hall: London, UK, **1992**; pp. 306–324.

45. Baldwin, J. E.; Lynch, G. P.; Pitlik, J. Gamma-lactam analogues of beta-lactam antibiotics. *J. Antibiot.* **1991**, *44*, 1–24.

46. Marchand-Brynaert, J.; Ghosez, L. Non-beta-lactam analogs of penicillins and cephalosporins. In *Recent Progress in the Chemical Synthesis of Antibiotics*; Ohno, M., Lukais, G., Eds.; Springer-Verlag: Berlin, Germany, **1990**; pp. 729–794.

47. Harada, S.; Tsubotani, S.; Hida, T.; Ono, H.; Okazaki, H. Structure of Lactivicin, an antibiotic having a new nucleus and similar biological activities to β-lactam antibiotics. *Tetrahedron Lett.* **1986**, *27*, 6229–6232.

48. Nozaki, Y.; Katayama, N.; Harada, S.; Ono, H.; Okazaki, H. Lactivicin, a naturally occurring non-beta-lactam antibiotic having beta-lactam-like action: Biological activities and mode of action. *J. Antibiot.* **1989**, *42*, 84–93.

49. Nozaki, Y.; Katayama, N.; Ono, H.; Tsubotani, S.; Harada, S.; Okazaki, H.; Nakao, Y. Binding of a non-beta-lactam antibiotic to penicillin-binding proteins. *Nature* **1987**, *325*, 179–180.

50. Harada, S.; Tsubotani, S.; Hida, T.; Koyana, K.; Kondo, M.; Ono, H. Chemistry of a new antibiotic: Lactivicin. *Tetrahedron* **1988**, *44*, 6589–6606.

51. Natsugari, H.; Kawano, Y.; Morimoto, A.; Yoshioka, K.; Ochiai, M. Synthesis of lactivicin and its derivatives. *J. Chem. Soc. Chem. Commun.* **1987**, 62–63.

52. Tamura, N.; Matsushita, Y.; Kawano, Y.; Yoshioka, K. Synthesis and antibacterial activity of lactivicin derivatives. *Chem. Pharm. Bull.* **1990**, *38*, 116–122.

53. Macheboeuf, P.; Contreras-Martel, C.; Job, V.; Dideberg, O.; Dessen A. Penicillin binding proteins: key players in bacterial cell cycle and drug resistance processes. *FEMS Microbiol Rev*. **2006,** *30*: 673–691.

54. Lim, D.; Strynadka, N. Structural basis for the beta-lactam resistance of PBP2a from methicillin-resistant *Staphylococcus aureus*. *Nat. Struct Biol.* **2002,** *9*: 870–876.

55. Grant, E. B.; Guiadeen, D.; Baum, E. Z.; Foleno, B. D.; Jin, H.; Montenegro, D. A.; Nelson, E. A.; Bush, K.; Hlasta, D. J. The synthesis and SAR of rhodamines as novel class C beta-lactamase inhibitors. *Bioorg. Med. Chem. Lett.* **2000**, *10*, 2179–2182.

56. Miguet, L.; Zervosen, A.; Gerards, T.; Pasha, F. A.; Luxen, A.; Disteche-Nguyen, M.; Thomas, A. Discovery of new inhibitors of resistant *Streptococcus pneumoniae* penicillin binding protein (PBP) 2x by structure-based virtual screening. *J. Med. Chem.* **2009**, *52*, 5926–5936.

57. Zervosen, A.; Lu, W.P.; Chen, Z.; White, R.E.; Demuth, T.P., Jr.; Frere, J.M. Interactions between penicillin-binding proteins (PBPs) and two novel classes of PBP inhibitors, Arylalkylidene rhodamines, and aryl alkylidene iminothiazolidin-4-ones. *Antimicrob. Agents Chem.* **2004**, *48*, 961–969.

58. Turk, S.; Verlaine, O.; Gerards, T.; Zivec, M.; Humljan, J.; Sosic, I.; Amoroso, A.; Zervosen, A.; Luxen, A.; Joris, B.; Gobus, S. New noncovalent inhibitors of penicillin-binding proteins from penicillin-resistant bacteria. *PLoS One* **2011**, *6*, e19418.

59. Phichith, D.; Bun, S.; Padiolleau-Lefevre, S.; Guellier, A.; Banh, S.; Galleni, M.; Frere, J.M.; Thomas, D.; Friboulet, A.; Avalle, B. Novel peptide inhibiting both TEM-1 beta-lactamase and penicillin-binding proteins. *FEBS J.* **2010**, *277*, 4965–4972.

60. Shilabin, A. G.; Dzhekieva, L.; Misra, P.; Jayaram, B.; Pratt, R. F. 4-Quinolones as Noncovalent Inhibitors of High Molecular Mass Penicillin-Binding Proteins. *ACS Med. Chem. Lett.* **2012**, *3*, 592–595.

61. Leimgruber, W.; Stefanovic, V.; Schenker, F.; Karr, A. J. Isolation and characterization of anthramycin, a new antitumor antibiotic. *J. Amer. Chem. Soc.* **1965** ,*87*, 5791–5793.

62. Arima, K.; Kosaka, M.; Tamura, G.; Imanaka, H.; Sakai, H. Studies on tomaymycin, a new antibiotic. I. Isolation and properties of tomaymycin. *J. Antibiot. (Tokyo)*, **1972**, *25*, 437–444.

63. Brazhnikova, M. G.; Konstantinova, N. V.; Mesentsev, A. S. Sibiromycin: isolation and characterization. *J. Antibiot (Tokyo)* **1972**, *25*, 668–673.

64. Puvvada, M. S.; Forrow, S. A.; Hartley, J. A.; Stevenson, P.; Gibson, I.; Jenkins, T. C.; Thurston, D. E. Inhibition of bacteriophage T7 RNA polymerase in vitro transcription by DNA-binding pyrrolo[2,1-c][1,4]-benzodiazepines. *Biochem.* **1997**, *36*, 2478–2484.

65. Smellie, M.; Bose, D. S.; Thompson, A. S.; Jenkins, T. C.; Hartley, J. A.; Thurston, D. E. Sequence-selective recognition of duplex DNA through covalent interstrand cross-linking: kinetic and molecular modeling studies with pyrrolobenzodiazepine dimers. *Biochem.* **2003**, *42*, 8232–8239.

66. Levy, S. B.; Marshall, B. Antibacterial resistance worldwide: causes, challenges, and responses. *Nat. Med.* **2004**, *10*, S122–129

67. Davies, J.; Davies, G. Origins and evolution of antibiotic resistance. *Microbiol. Mol. Biol. Rev.* **2010**; 74: 417–33.

68. Li J.; Nation, R. L.; Turnidge, J. D.; Milne, R. W.; Coulthard, K.; Rayner, C. R.; Paterson, D. L. Colistin: the re-emerging antibiotic for multidrug-resistant Gram-negative bacterial infections. *Lancet Infect. Dis.* **2006**, *6*, 589–601.

69. Hadjivassileva, T.; Thurston, D. E.; Taylor, P. W. Pyrrolobenzodiazepine dimers: novel sequence-selective, DNA-interactive, cross-linking agents with activity against Gram-positive bacteria. *J. Antimicrob. Chemother.* **2005**, *56*, 513–518.

70. Rahman, K. M.; Rosado, H.; Moreira, J. B.; Feuerbaum, E. A.; Fox, K. R.; Stecher, E.; Howard, P. W.; Gregson, S. J.; James, C. H.; de la Fuente, M.; Waldron, D. E.; Thurston, D. E.; Taylor, P. W. Antistaphylococcal activity of DNA-interactive pyrrolobenzodiazepine (PBD) dimers and PBD-biaryl conjugates. *J. Antimicrob. Chemother.*, **2012**, *67*, 1683-1696.

71. Schmidt, S.; Shilabin, A, G.; Namyslo, J, C.; Nieger, M.; Hemmen, S. Pyrimidine-Annulated Pyrrolobenzodiazepines. A New Ring System Related to *Aspergillus* Alkaloids. *Eur. J. Org. Chem.* **2005**, *36*, 1781–1789.

72. Wu, X.; Liu, Y.; Sheng, W.; Sun, J.; Qin, G. Chemical constituents of *Isatis indigotica*. *Planta Med.* **1997,** *63*, 55-57.

73. Sahu, N. P.; Pal, C.; Mandal, N. B.; Banerjee, S.; Raha, M.; Kundu, A. P.; Basu, A.; Ghosh, M.; Roy, K.; Bandyopadhyay, S. Synthesis of a novel quinolone derivative, 2-(2-Methylquinolin-4-ylamino)-*N*-phenylacetamide – A Potential antileishmanial agent. *Bioorganic & Med. Chem.*, **2002**, *10*, 1687–1693

74. Cahn, A.; Hepp, P. *"Das Antifebrin, ein neues Fiebermittel", Centralbl. Klin. Med.* ***1886,*** *7,* 561–564.

75. Lester, D.; Greenberg, L. A. "Metabolic fate of acetanilide and other aniline derivatives. II. Major metabolites of acetanilide in the blood", *J. Pharmacol. Exp. Ther*. **1947**, *90*, 68, PMID 20241897.

76. Brodie, B. B.; Axelrod, J. The estimation of acetanilide and its metabolic products, aniline, N-acetyl p-aminophenol and p-aminophenol (free and total conjugated) in biological fluids and tissues. *J. Pharmacol. Exp. Ther*. **1948**, *94*, 22-28, *PMID 18885610*.

77. Brodie, B. B.; Axelrod, J. The fate of acetanilide in man. *J. Pharmacol. Exp. Ther*. **1948**, *94*, 29–38, PMID 18885611

78. Hedstrom, L. K.; Striepen, B. IMP dehydrogenase inhibitor for treating mammalian gastrointestinal parasitic infections. WO2007143557, 2007.

79. Tipparaju, S. K.; Muench, S. P.; Mui, E. J.; Ruzheinikov, S. N.; Lu, J. Z.; Hutson, S. L.; Kirisits, M. J.; Prigge, S. T.; Roberts, C. W.; Henriquez, F. L.; Kozikowski, A. P.; Rice, D. W.; McLeod, R. L. Identification and development of novel inhibitors of toxoplasma gondii enoyl reductase. *J. Med. Chem.* **2010**, *53*, 6287–6300.

80. Wei, A.; Yan-Ni, L.; Tao, Y.; Jian-Zhong, Y.; Wei-Yi, P.; Ying-Hong, Y.; You-Fu, L.; Yong; D.; Yu-Quan, W. Synthesis and biological evaluation of 2-(3-Fluoro-4-nitrophenoxy)-*N*-phenylacetamide derivatives as novel Potential affordable Antitubercular agents. *Molecules* **2012**, *17*, 2248-2258.

81. Sun, A.; Prussia, A.; Zhan, W. Q.; Murray, E. E.; Doyle, J.; Cheng, L. T.; Yoon, J. J.; Radchenko, E. V.; Palyulin, V. A.; Compans, R. W.; Liotta, D. C.; Plemper, R. K.; Snyder, J. P. Nonpeptide inhibitors of measles virus entry. *J. Med. Chem.* **2006**, *49*, 5080–5092.

82. O'Daniel, P. I.; Peng, Z.; Pi, H.; Testero, S. A.; Ding, D.; Spink, E.; Leemans, E.; Boudreau, M. A.; Yamaguchi, T.; Schroeder, V. A.; Wolter, W. R.; Llarrull, L. I.; Song, W.; Lastochkin, E.; Kumarasiri, M.; Antunes, N. T.; Espahbodi, M.; Lichtenwalter, K.; Suckow, M. A.; Vakulenko, S.; Mobashery, S.; Chang, M. Discovery of a New Class of

Non-β-lactam Inhibitors of Penicillin-Binding Proteins with Gram-Positive Antibacterial Activity. *J. Am. Chem. Soc*. **2014,** *136,* 3664–3672.

83. Gupta, A.; Gandhimathi, A.; Sharma, P.; Jayaram, B. ParDOCK: An All-Atom Energy Based Monte Carlo Docking Protocol for Protein-Ligand Complexes. *Protein and Peptide Letters*, **2007**, *14*, 632-646.

84. Lipinski, C. A.; Lombardo, F.; Dominy, B. W.; Feeney, P. J. Experimental-computational approaches to estimate solubility and permeability in drug discovery and development settings. *Adv. Drug Deliv. Rev.* **2001**, *46*, 3-26.

85. Lipinski, C. A. Lead- and drug-like compounds: the rule-of-five revolution. *Drug Discov. Today Technol.* **2004**, *1*, 337-341.

86. Leeson, P. D.; Springthorpe, B. The influence of drug-like concepts on decision-making in medicinal chemistry. *Nat. Rev. Drug Discov.,* **2007**, *6* (11): 881–90.

87. CrysAlisPro Software System, v1.171.37.35, Rigaku Oxford Diffraction, **2015**, Rigaku Corporation, Oxford, UK.

88. Sheldrick, G. M. "A short history of SHELX." *Acta Cryst.* **2008**, *A64*, 112-122.

89. Dolomanov, O.V.; Bourhis, L. J.; Gildea, R. J.; Howard, J. A. K.; Puschmann, H. *J. Appl. Cryst.* **2009**, *42*, 339–341

90. Uetrecht, J. "Idiosyncratic drug reactions: past, present, and future". *Chem. Res. Toxicol.,* **2008**, *21 (1): 84–92.*

91. Duffy, F. J.; Devocelle, M.; Shields, D. C. Computational approaches to developing short cyclic peptide modulators of protein-protein interactions". In Zhou, P., Huang, J. *Methods in Molecular Biology. Computational Peptidology*. New York: Humana Press. 2015; pp. 250–251

92. Kamal, A. Enzymic approach to the synthesis of the pyrrolo[1,4]benzodiazepine antibiotics. *J. Org. Chem*. **1991**, *56*, 2237-2240.

93. Wright Jr., W. B.; Brabander, H. J.; Greenblatt, E. N.; Day, I. P.; Hardy Jr., R. A. Derivatives of 1,2,3,11a-tetrahydro-5H-pyrrolo[2,1-c][1,4]benzodiazepine-5,11(10H)-dione as anxiolytic agents. *J. Med. Chem.,* **1978**, *21*, 1087-1089.

94. Kamal, A.; Howard, P. W.; Reddy, B. S. N.; Reddy, B. S. P.; Thurston, D. E. Synthesis of pyrrolo[2,1-*c*][1,4]benzodiazepine antibiotics: Oxidation of cyclic secondary amine with TPAP. *Tetrahedron* **1997**, *53*, 3223-3230.

95. Shilabin, A. G. Seven-Membered Ring Mesomeric Betaines: From Anti-Hückel Aromatics to Model Compounds of the Pyrrolobenzodiazepine Alkaloids-Circumdatin A and B. Ph.D. Dissertation. Technischen Universität Clausthal, Clausthal-Zellerfeld, 2005

96. Rekowski, M. von W.; Pyriochou, A.; Papapetropoulos, N.; Stöbel, A.; Papapetropoulos, A.; Giannis, A. Synthesis and biological evaluation of oxadiazole derivatives as inhibitors of soluble guanylyl cyclase. *Bioorg. & Med. Chem.*, **2010**, *18*, 1288–1296.

97. Bartsch, H.; Erker, T.; Neubauer, G. Untersuchungen zur Synthese neuer tricyclischer Heterocyclen aus 1,4-Benzoxazin- und 1,4-Benzothiazin-3-oximen (Studien zur Chemie O,N- und S,N-haltiger Heterocyclen, 7. Mitt.). *Monatsh. Chem.* **1989**, *120*, 81-84

98. Koduri, N. D.; Wang, Z.; Cannell, G.; Cooley, K.; Lemma, T. M.; Miao, K.; Nguyen, M.; Frohock, B.; Castaneda, M.; Scott, H.; Albinescu, D.; Hussaini, S. R. Enaminones via Ruthenium-Catalyzed Coupling of Thioamides and α-Diazocarbonyl Compounds. *Journal of Organic Chemistry*, **2014**, *79*, 7405-7414.

99. Aksenov, A. V.; Smirnov, A. N.; Aksenov, N. A.; Bijieva, A. S.; Aksenova, I. V.; Rubin, M. Benzimidazoles and benzoxazoles via the nucleophilic addition of aniline to nitroalkanes. *Org. Biomol. Chem*., **2015**, *13*, 4289 – 4295.

APPENDIX

Appendix A1: ^{1}H NMR Spectrum for Compound **1** in DMSO-d6

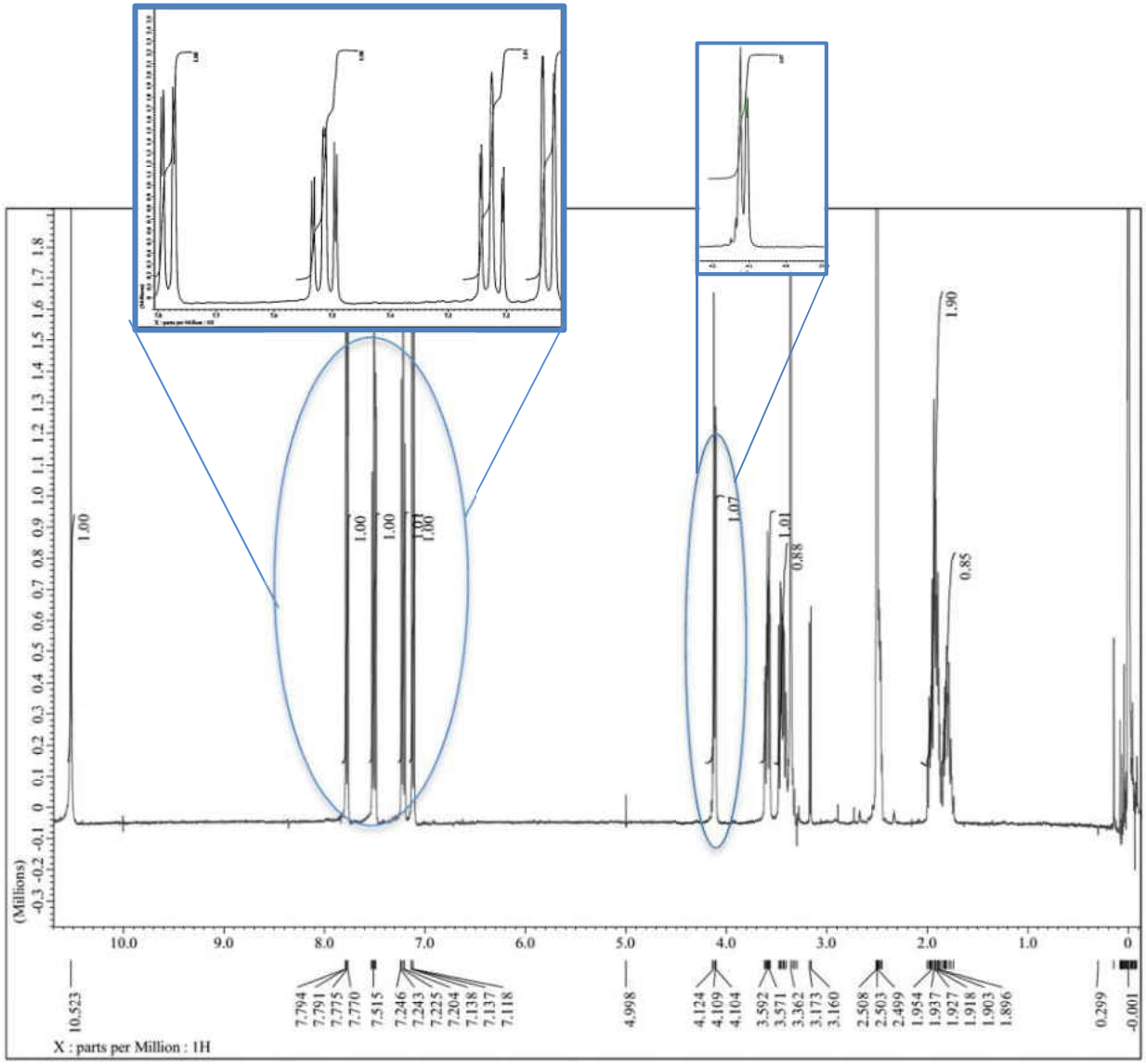

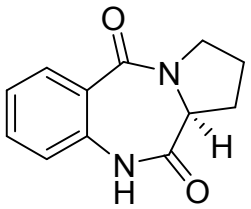

Appendix A2: ^{13}C NMR Spectrum for Compound **1** in DMSO-d6

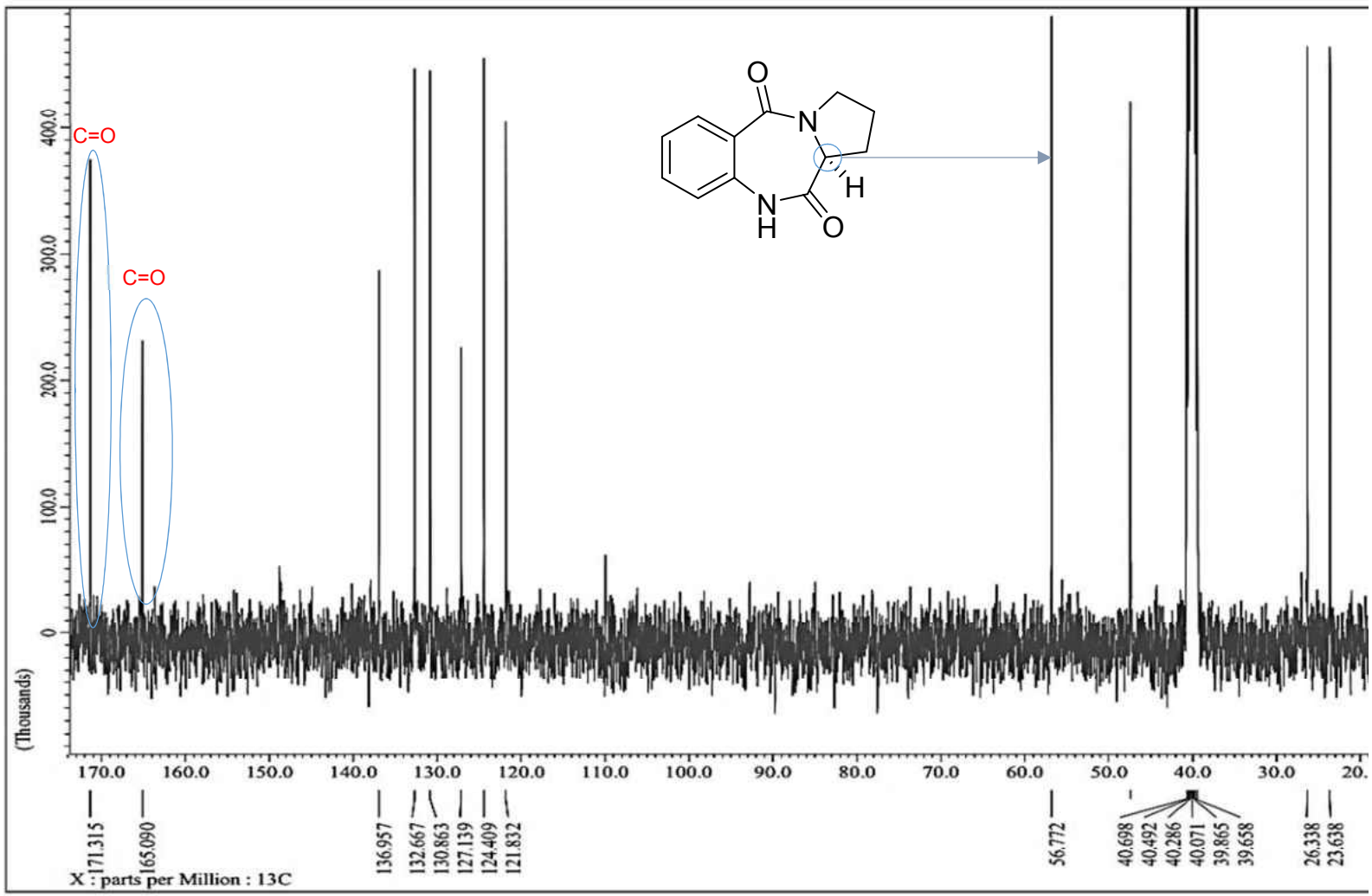

Appendix A3: GC-MS Spectrum for Compound **1** in Chloroform

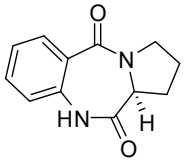

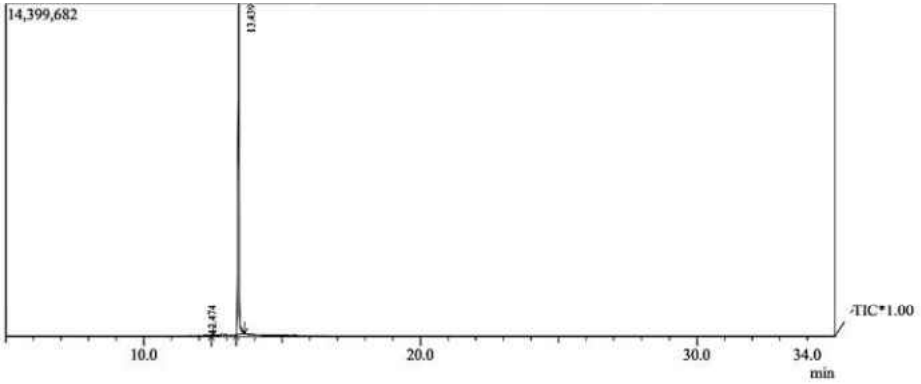

Peak Report TIC

Peak#	R.Time	I.Time	F.Time	Area	Area%	Height	Height%	A/H	Mark	Name
1	12.474	12.448	12.504	67054	0.13	43937	0.31	1.53		Tricyclo[4.2.2.0(2,5)]dec-7-ene,
2	13.439	13.337	13.645	49809273	99.87	14299056	99.69	3.48		Pyrrolidine[2,1-c]-2H,5H-1,4-be
				49876327	100.00	14342993	100.00			

Line#:2 R.Time:13.4(Scan#:1206)
MassPeaks:251
RawMode:Averaged 13.4-13.4(1205-1207) BasePeak:70(5604477)
BG Mode:Calc. from Peak Group 1 - Event 1

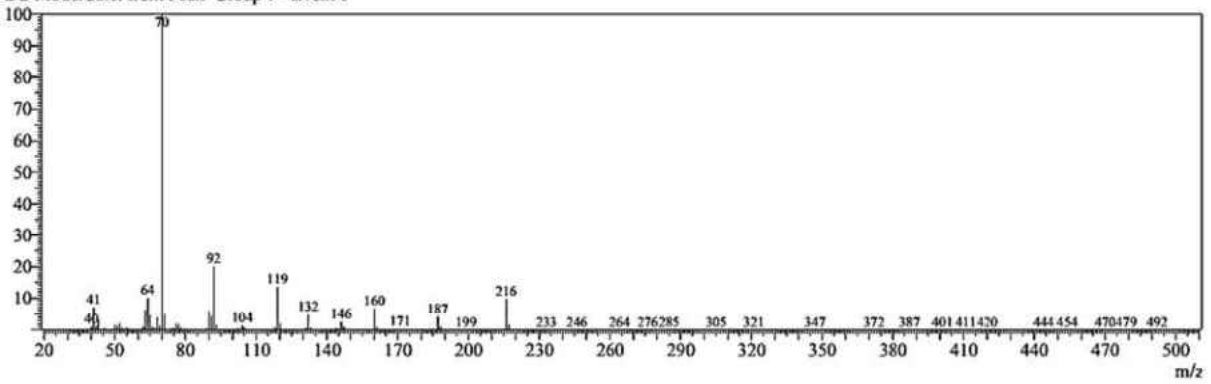

Appendix A4: IR Spectrum for Compound **1** in Chloroform

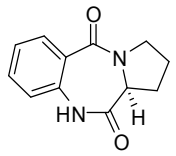

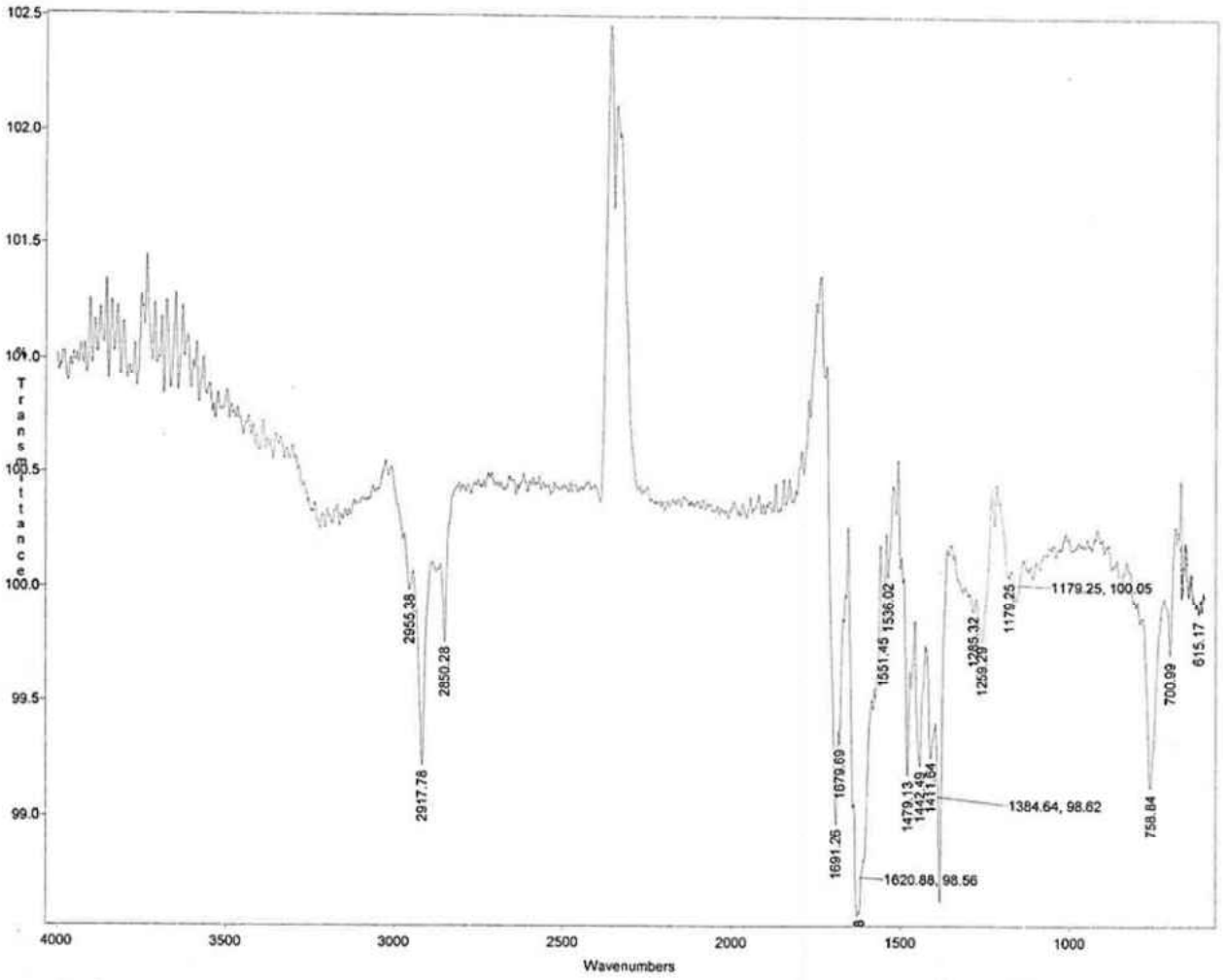

Appendix B1: ^{1}H NMR Spectrum for Compound **2** in DMSO-d6

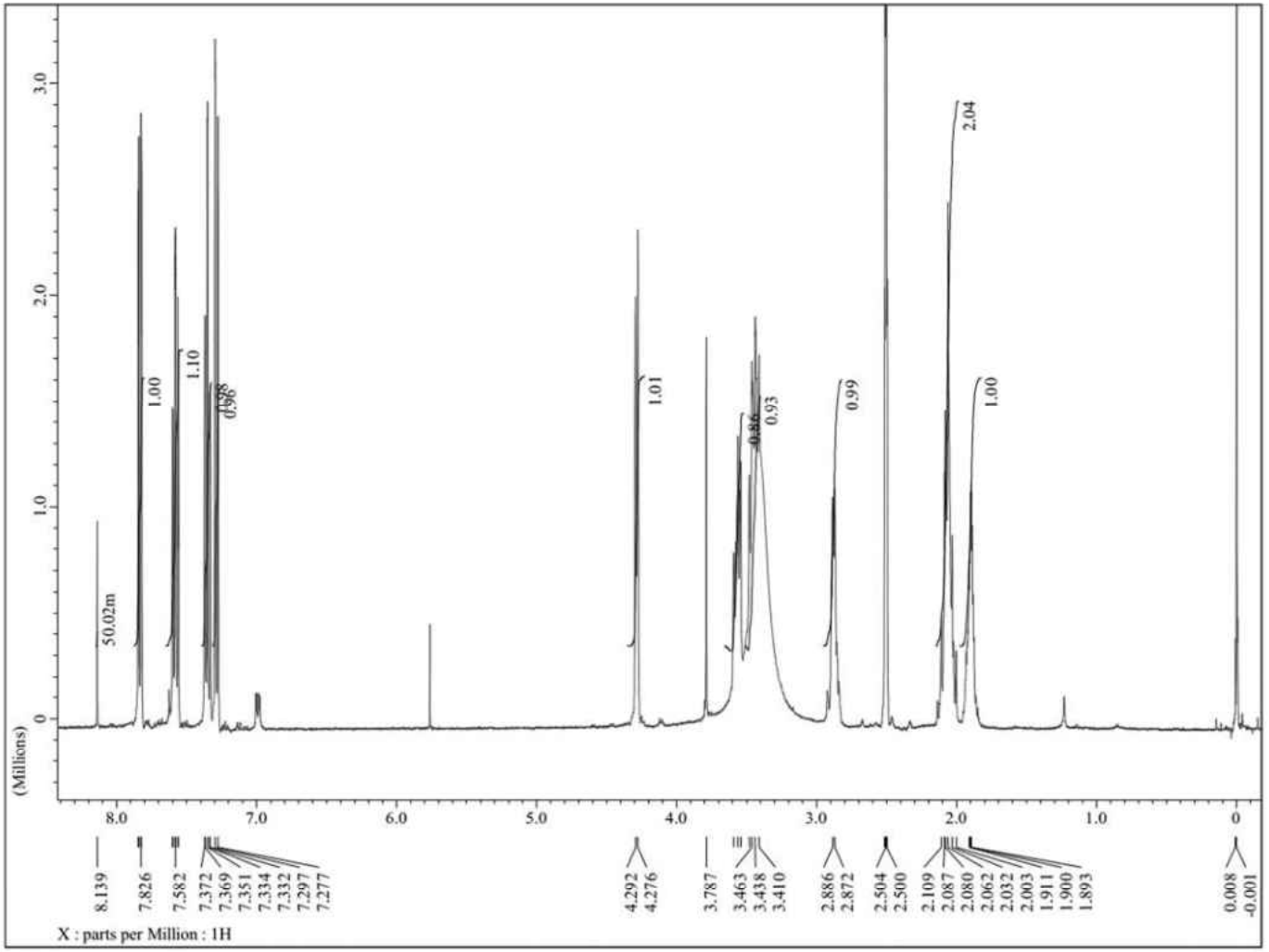

Appendix B2: ^{13}CNMR Spectrum for Compound **2** in DMSO-d6

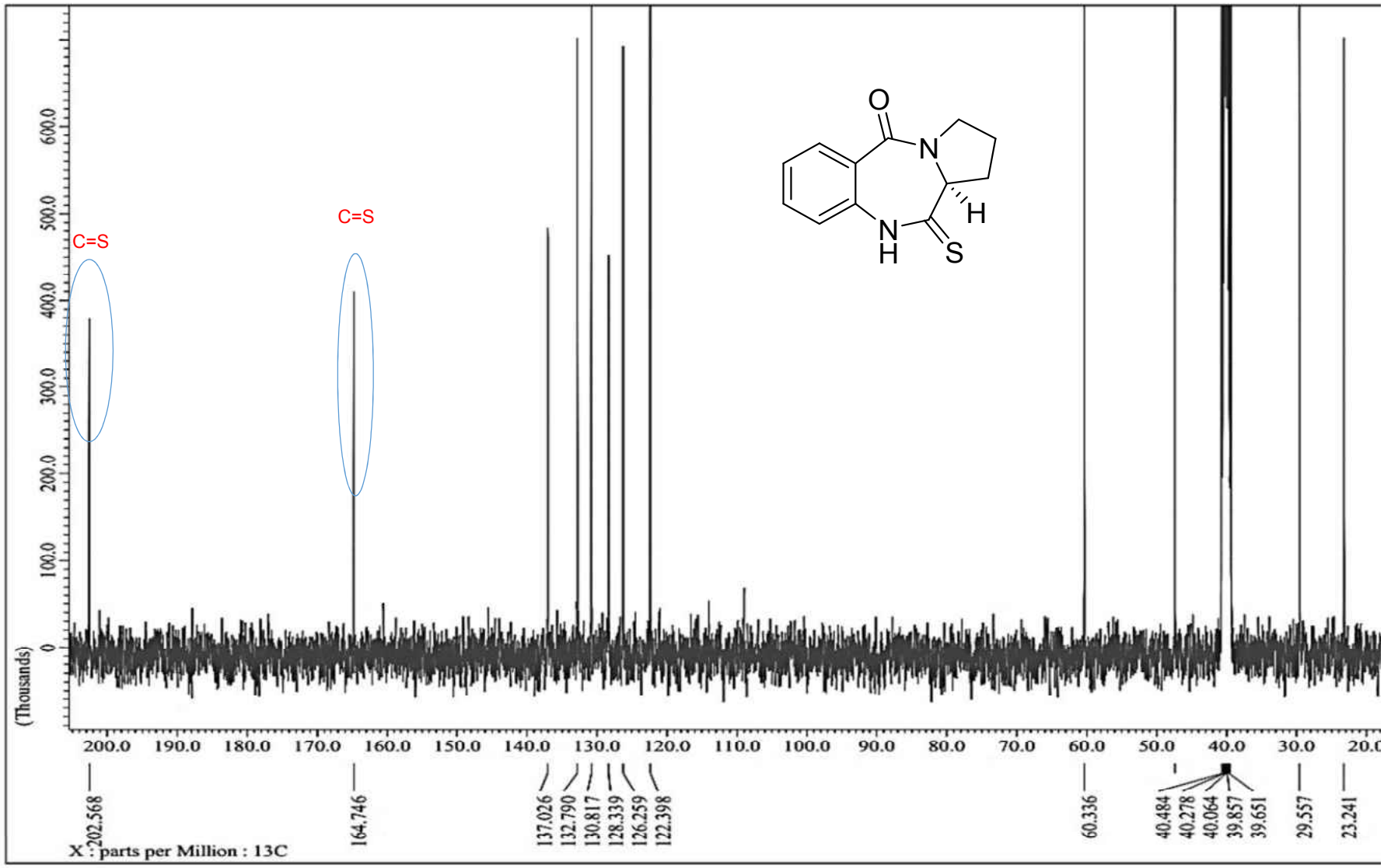

Appendix B3: GC-MS Spectrum for Compound **2** in Acetone

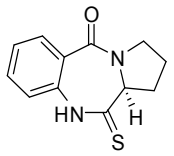

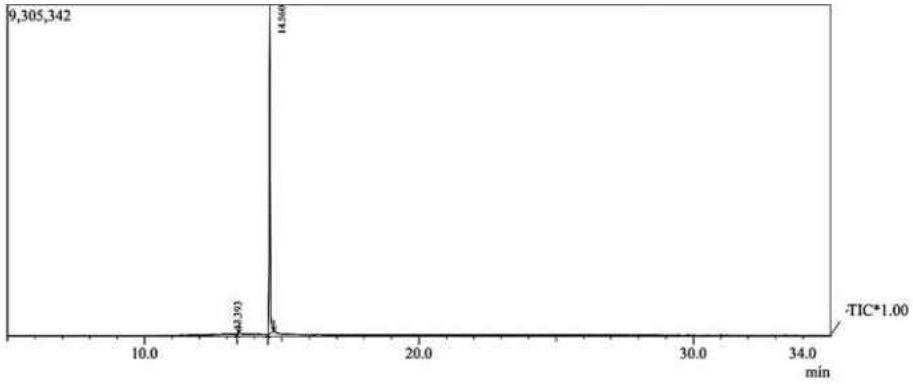

Peak Report TIC

Peak#	R.Time	I.Time	F.Time	Area	Area%	Height	Height%	A/H	Mark	Name
1	13.393	13.365	13.435	171240	0.70	92302	0.99	1.86		Pyrrolidine[2,1-c]-2H,5H-1,4-be
2	14.560	14.485	14.709	24152632	99.30	9221747	99.01	2.62		Pyrrolidine-2-carboxylic acid, m
				24323872	100.00	9314049	100.00			

Line#:2 R.Time:14.6(Scan#:1367)
MassPeaks:303
RawMode:Averaged 14.6-14.6(1366-1368) BasePeak:70(4286381)
BG Mode:Calc. from Peak Group 1 - Event 1

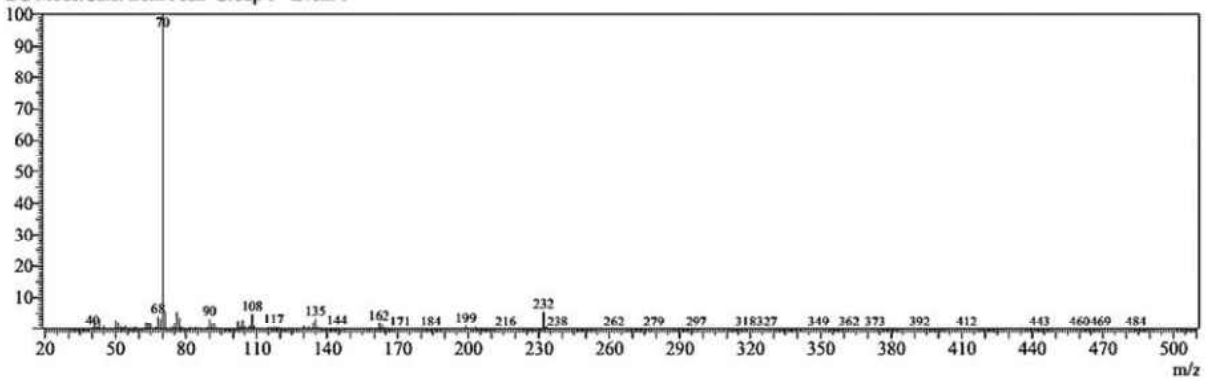

Appendix B4: IR Spectrum for Compound **2** in Chloroform

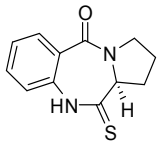

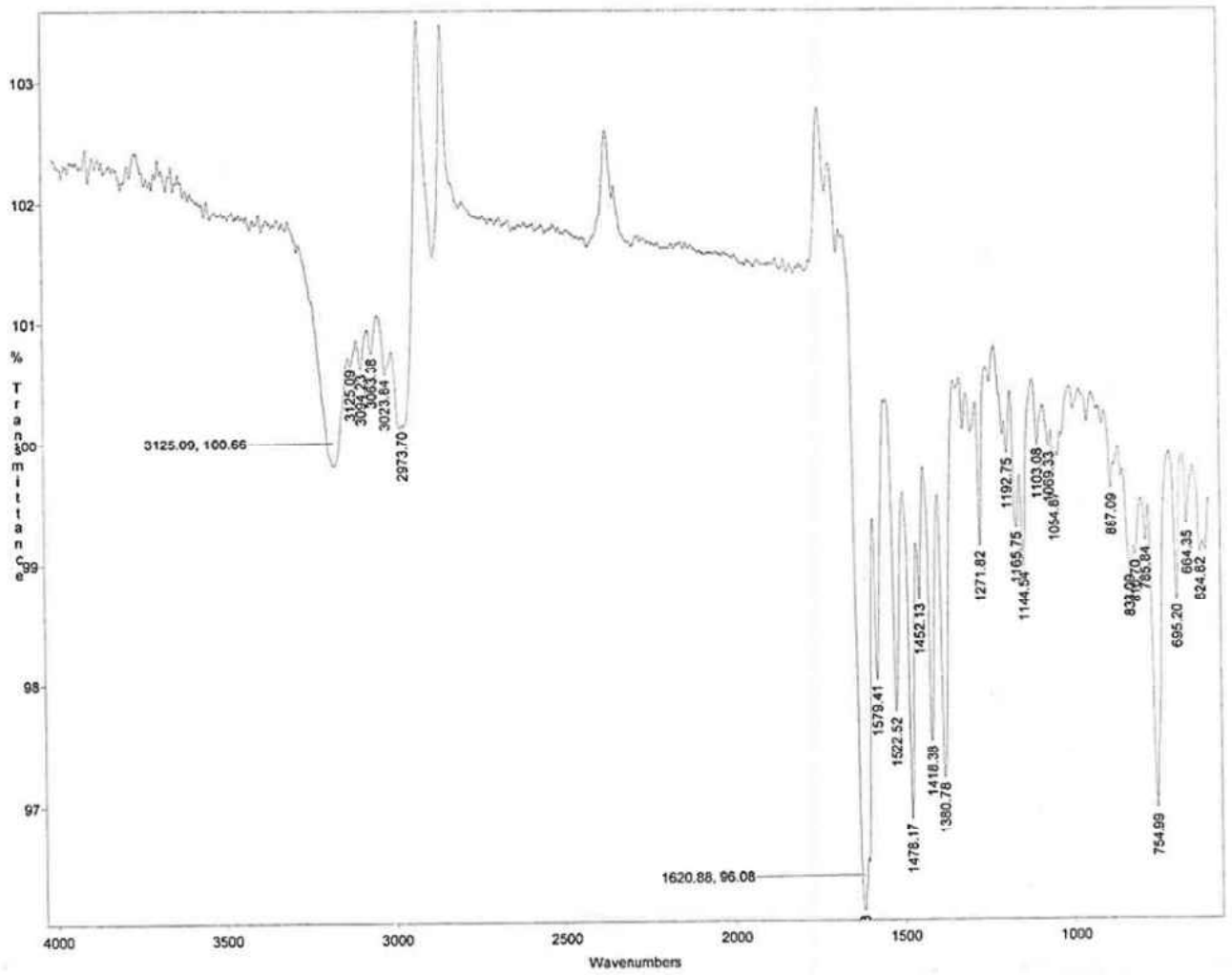

Appendix C1: ^{1}HNMR Spectrum for Compound **3** in Chloroform-d

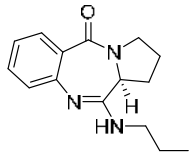

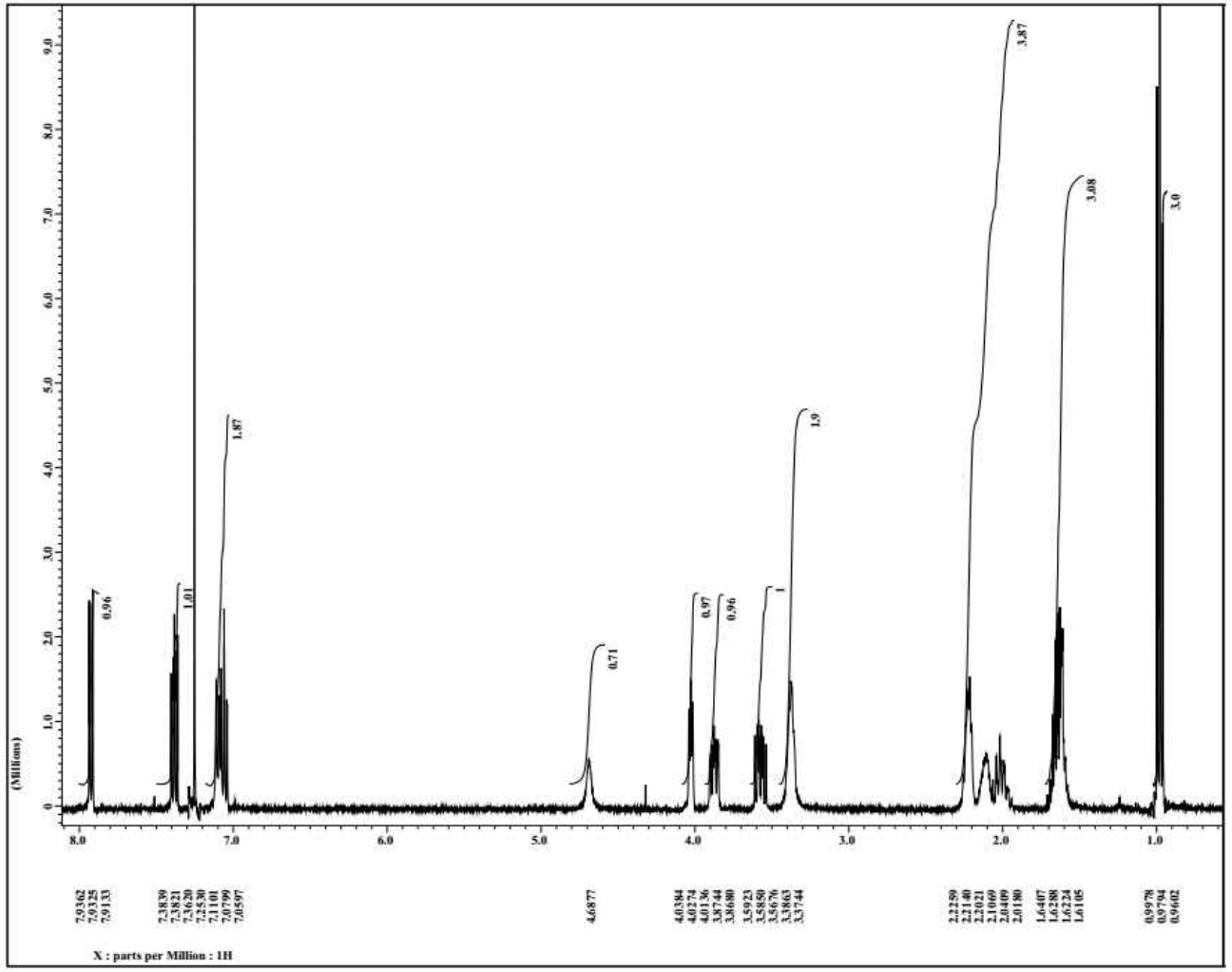

Appendix C2: ^{13}CNMR Spectrum for Compound **3** in Chloroform-d

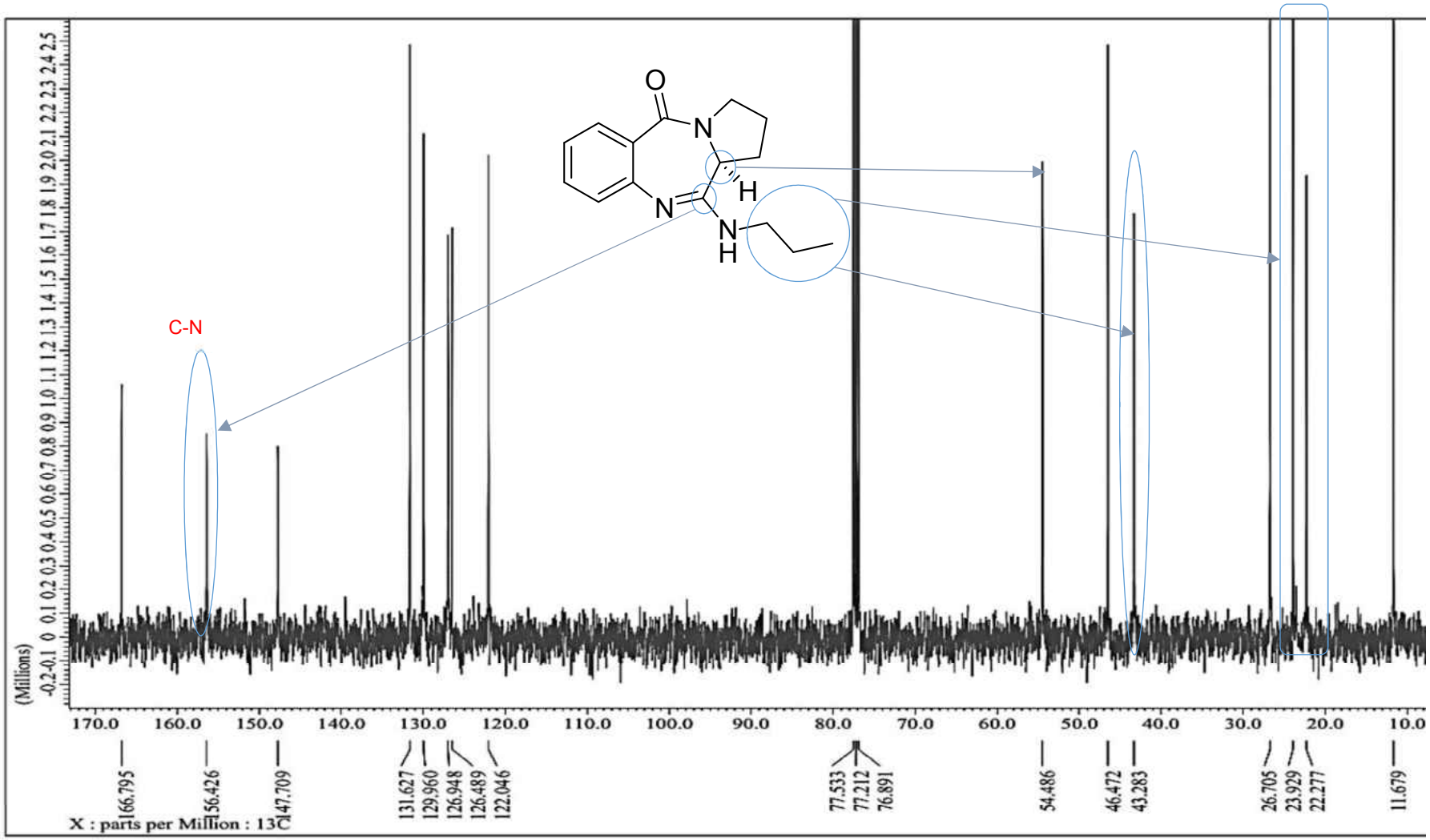

Appendix C3: GC-MS Spectrum for Compound **3** in Chloroform

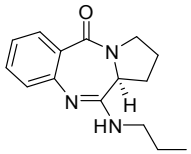

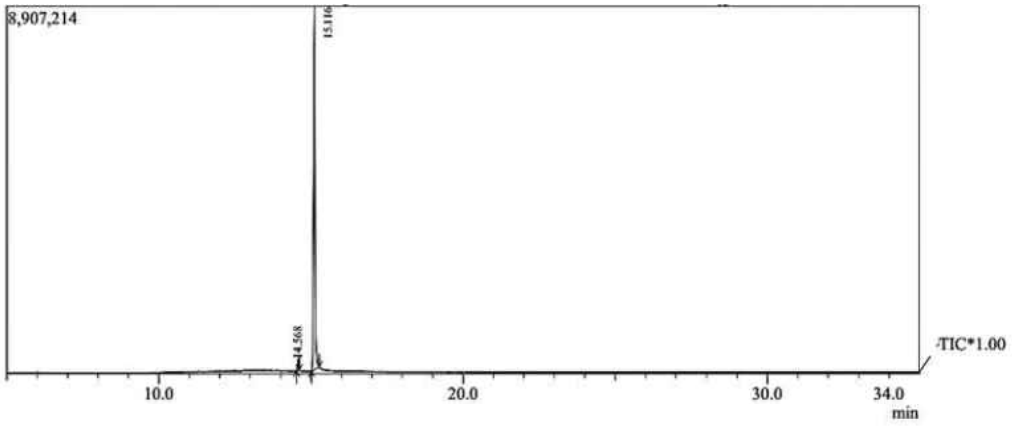

Peak Report TIC

Peak#	R.Time	I.Time	F.Time	Area	Area%	Height	Height%	A/H	Mark	Name
1	14.568	14.534	14.611	481511	1.44	258930	2.86	1.86		Di-n-octyl phthalate
2	15.116	15.017	15.269	32856332	98.56	8805909	97.14	3.73		Pyrrolidine[2,1-c]-2H,5H-1,4-be
				33337843	100.00	9064839	100.00			

Line#:2 R.Time:15.1(Scan#:1446)
MassPeaks:308
RawMode:Averaged 15.1-15.1(1445-1447) BasePeak:70(1806224)
BG Mode:Calc. from Peak Group 1 - Event 1

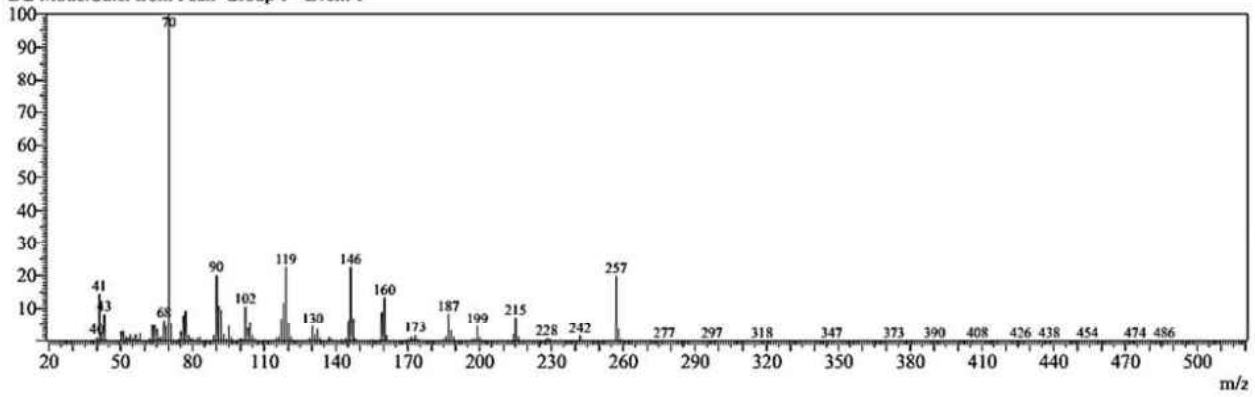

Appendix C4: IR Spectrum for Compound **3** in Chloroform

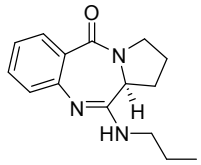

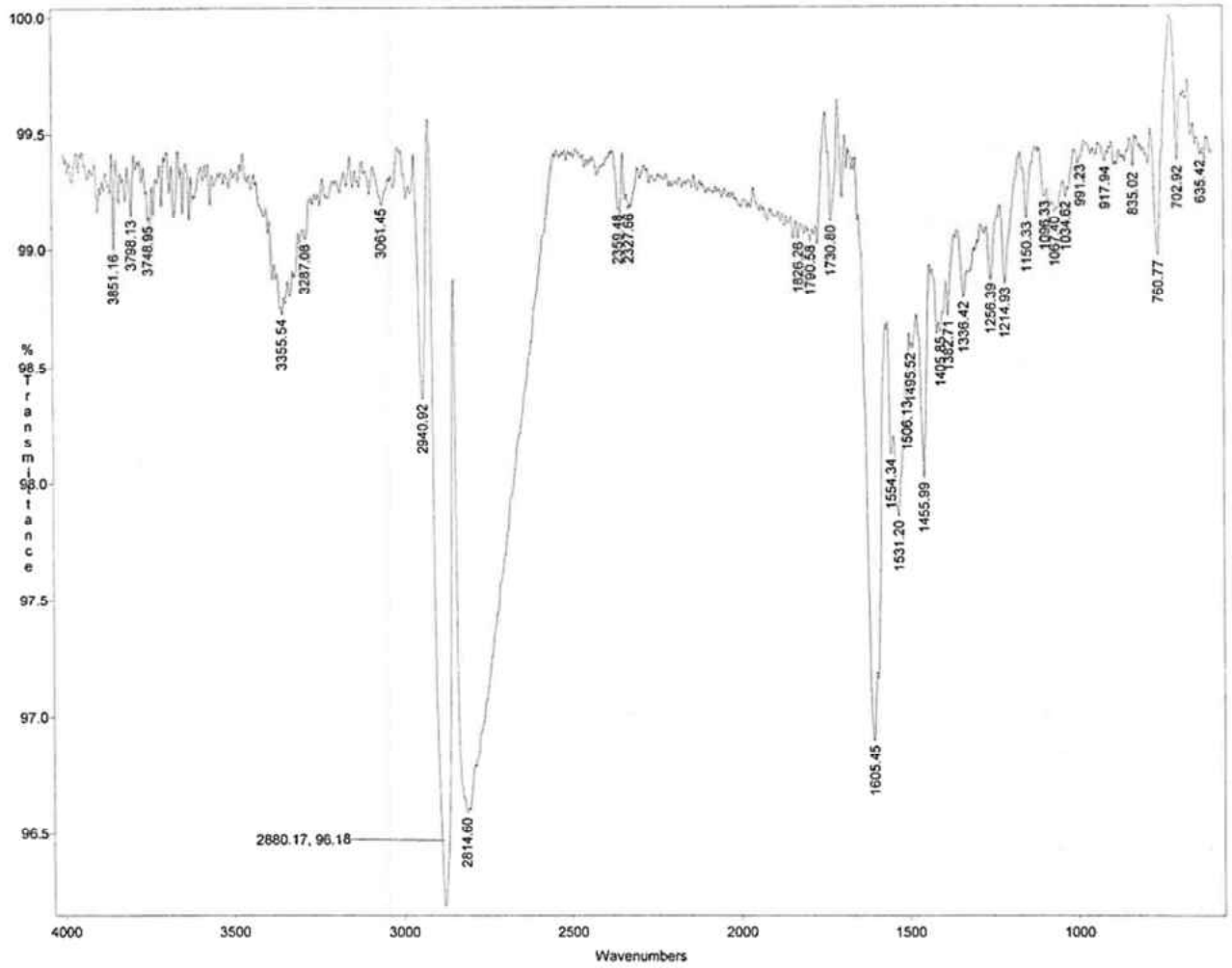

Appendix D1: ^{1}H NMR Spectrum for Compound **4** in Chloroform-d

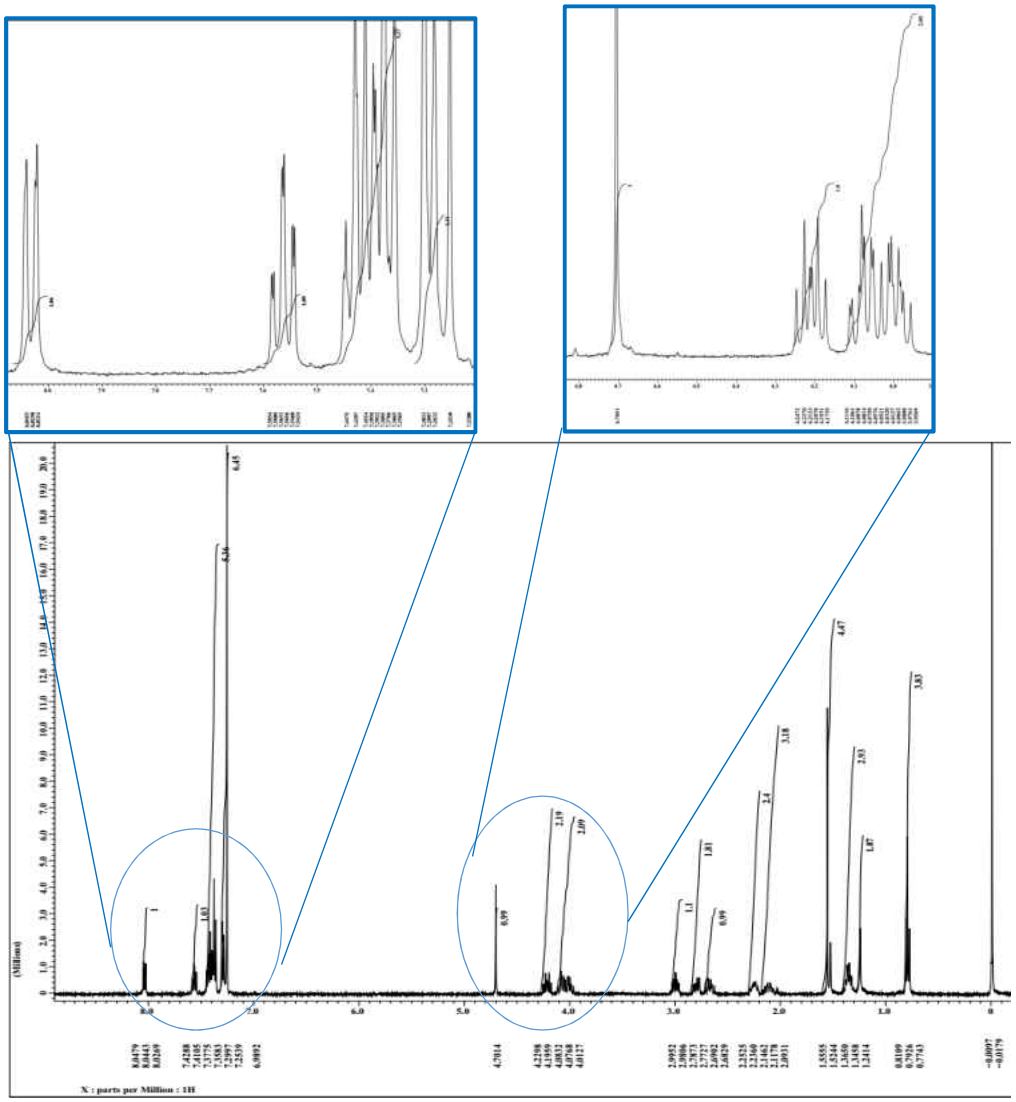

Appendix D2: ^{13}C NMR Spectrum for Compound **4** in Chloroform-d

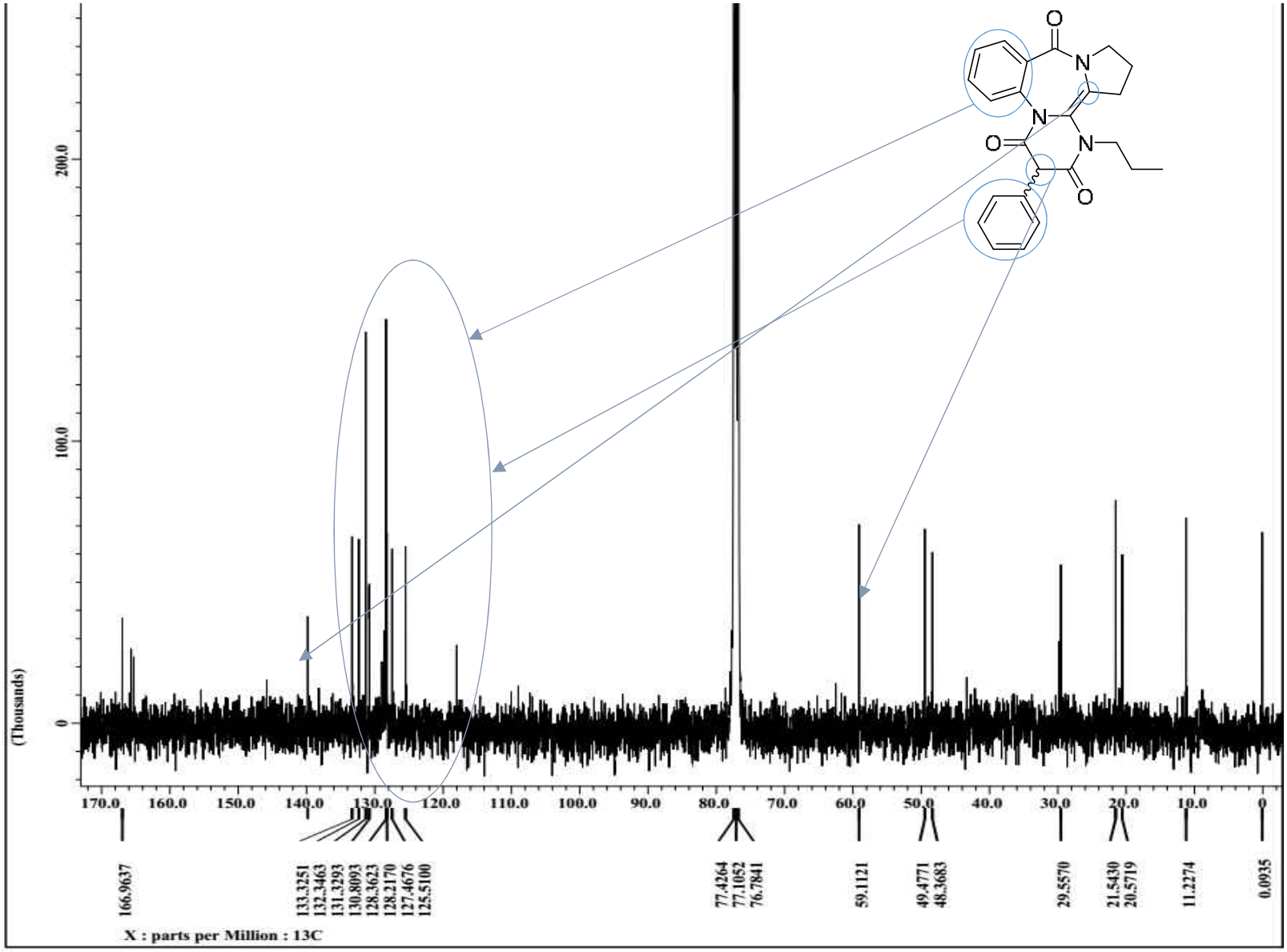

Appendix D3: GC-MS Spectrum for Compound **4** in Acetone

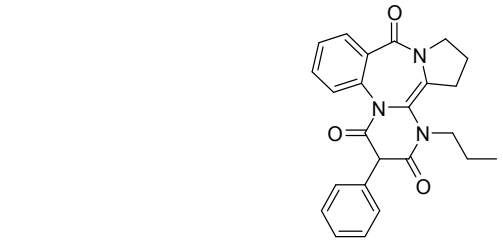

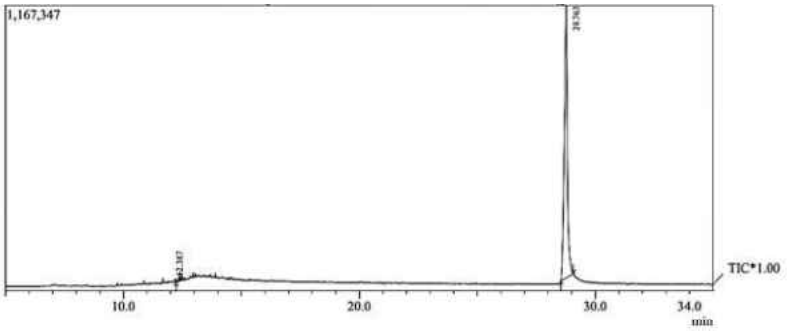

Peak Report TIC

Peak#	R.Time	I.Time	F.Time	Area	Area%	Height	Height%	A/H	Mark	Name
1	12.387	12.238	12.413	68366	0.66	16771	1.48	4.08		Cholest-5-en-3-ol (3.beta.)-, 9-o
2	28.763	28.534	29.080	10311306	99.34	1114854	98.52	9.25		2-(1-Methyl-2-nitro-ethyl)-3,4-d
				10379672	100.00	1131625	100.00			

Line#:2 R.Time:28.8(Scan#:3396)
MassPeaks:376
RawMode:Averaged 28.8-28.8(3395-3397) BasePeak:118(129740)
BG Mode:Calc. from Peak Group 1 - Event 1

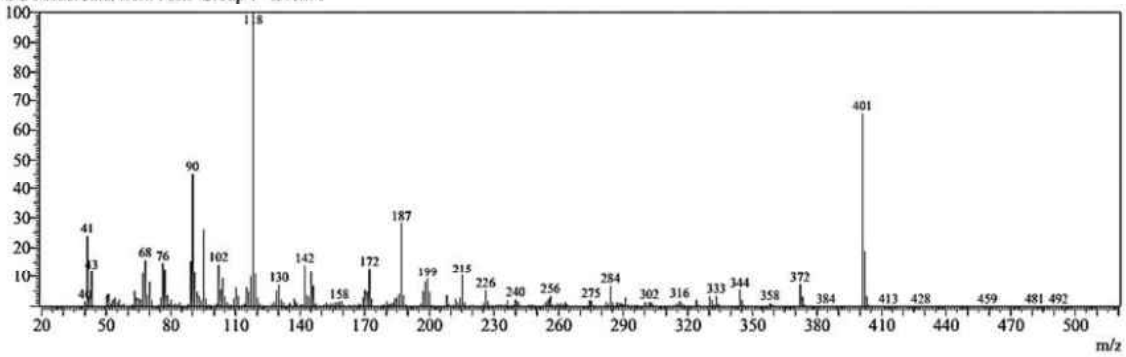

Appendix D4: IR Spectrum for Compound **4** in Chloroform

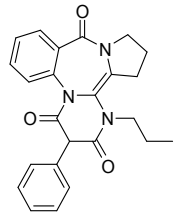

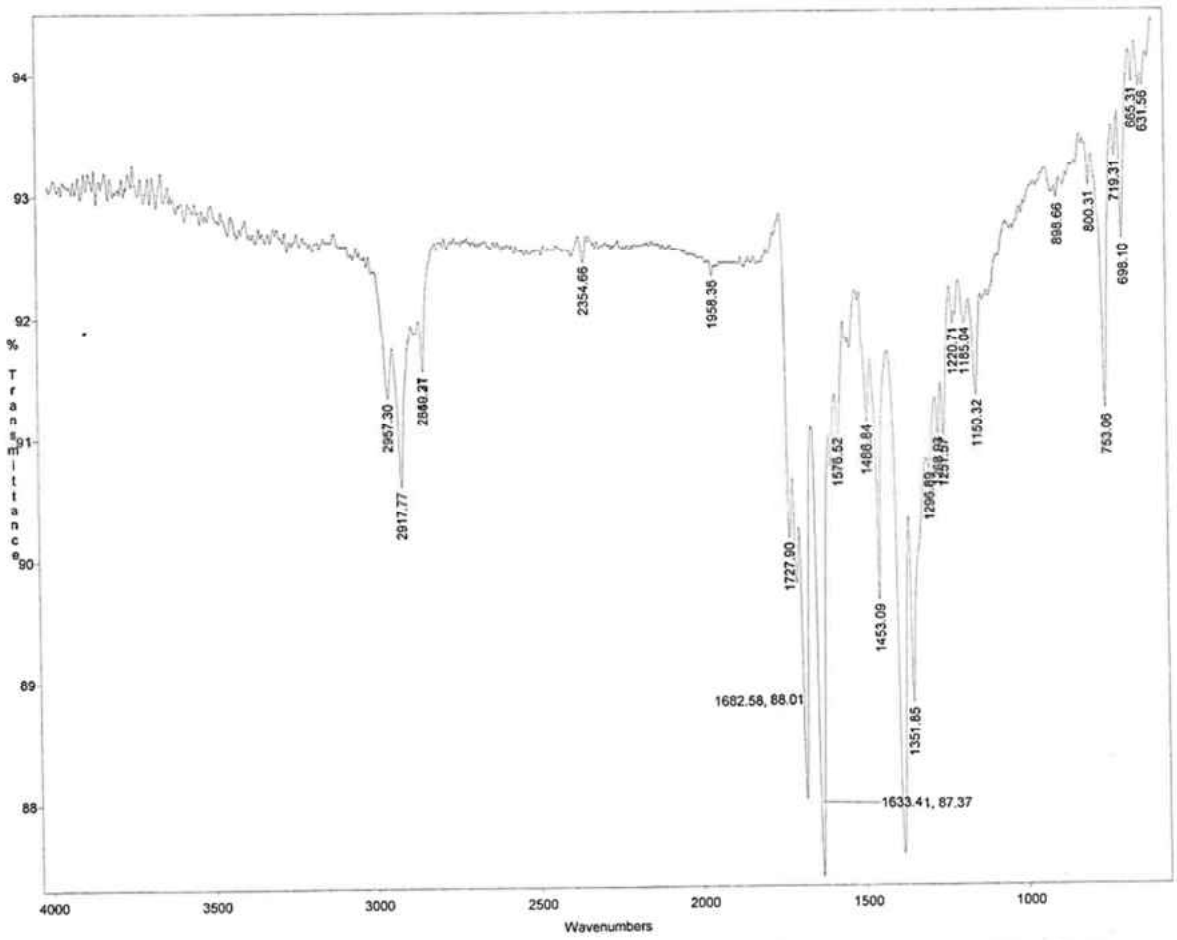

Appendix E1: ^{1}H NMR Spectrum for Compound **5** in Chloroform-d

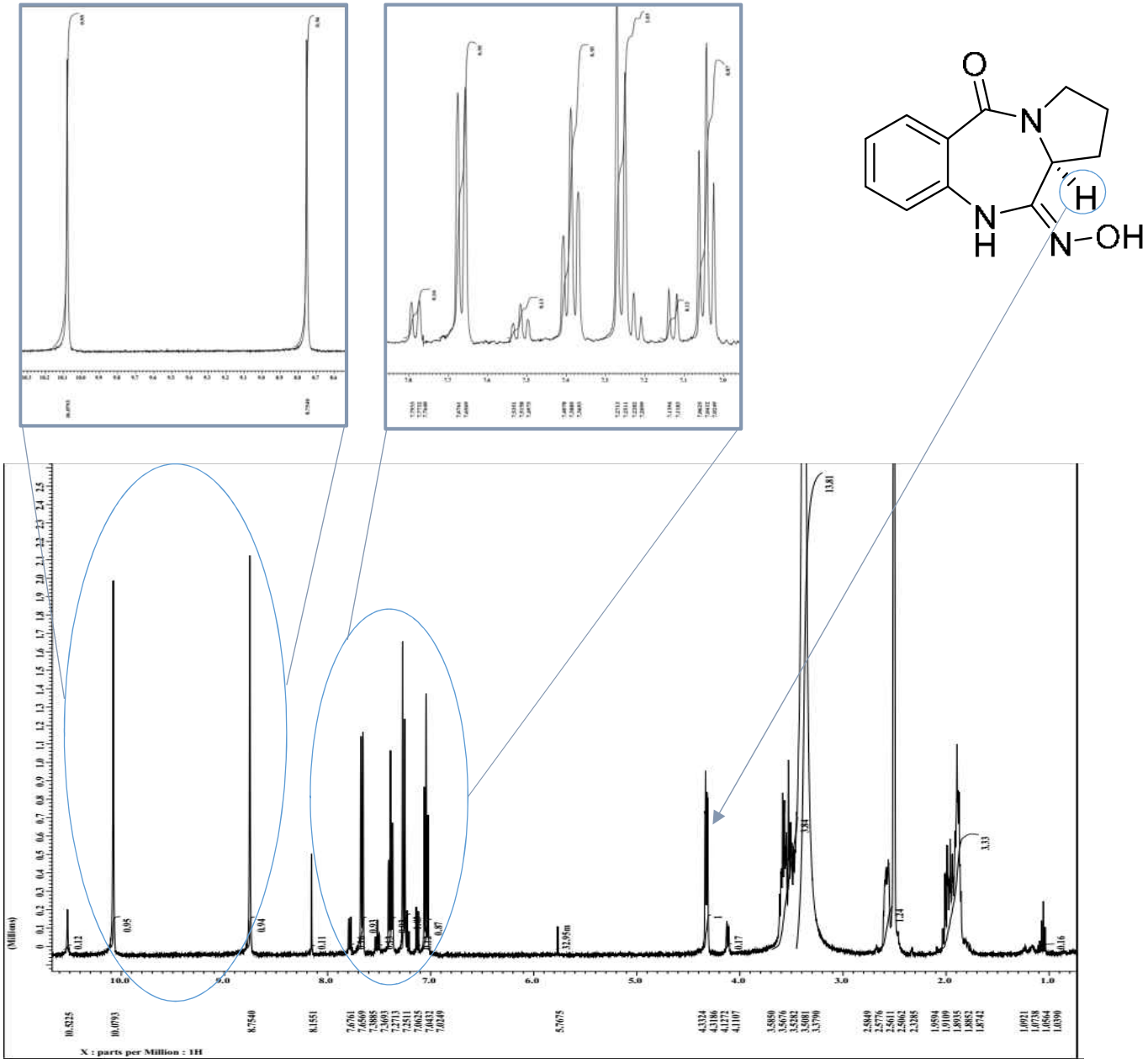

Appendix E2: ^{13}C NMR Spectrum for Compound **5** in Chloroform-d

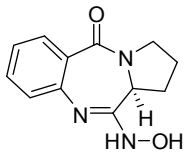

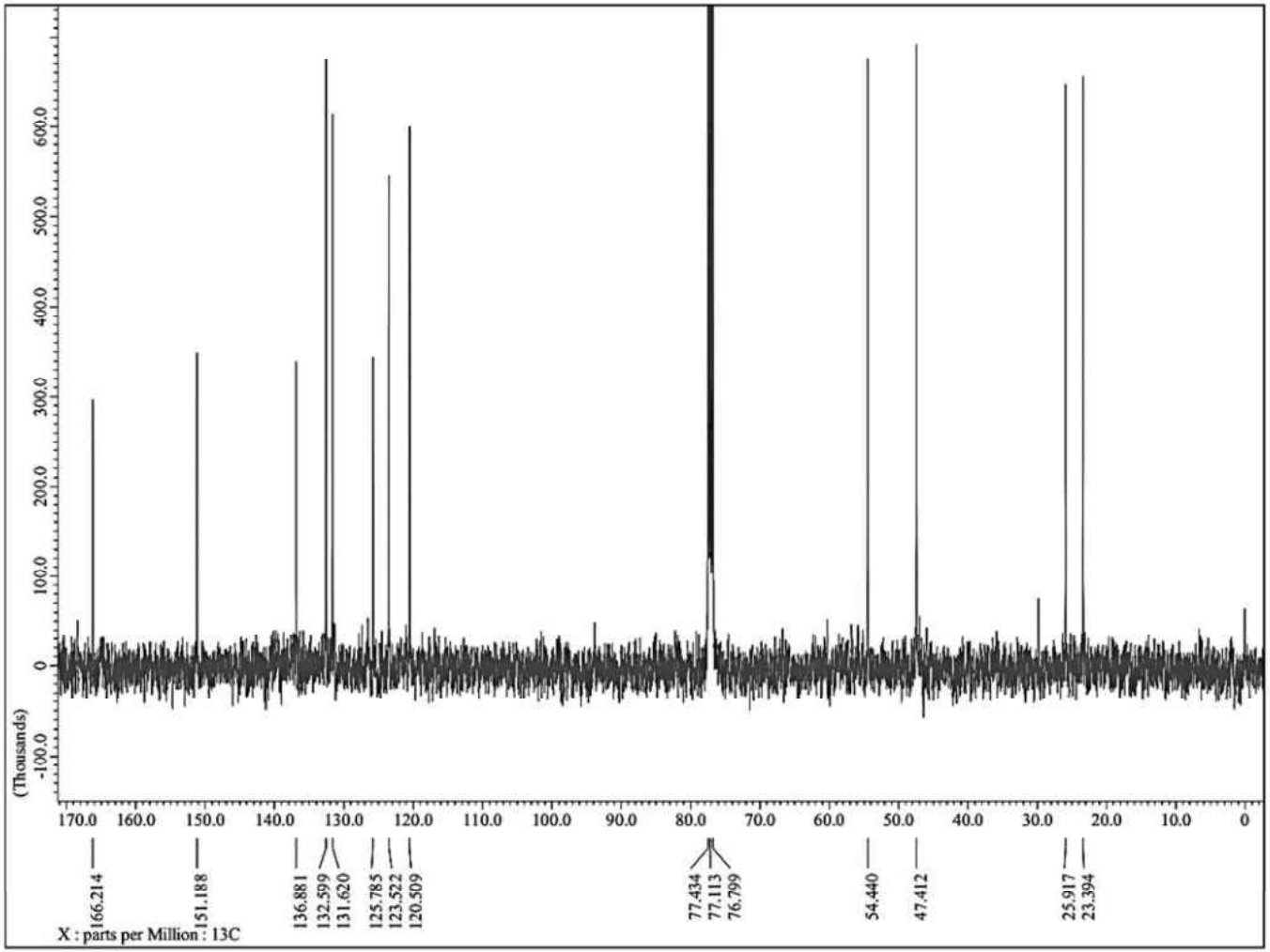

Appendix E4: GC-MS Spectrum for Compound **5** in Chloroform

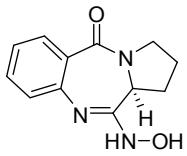

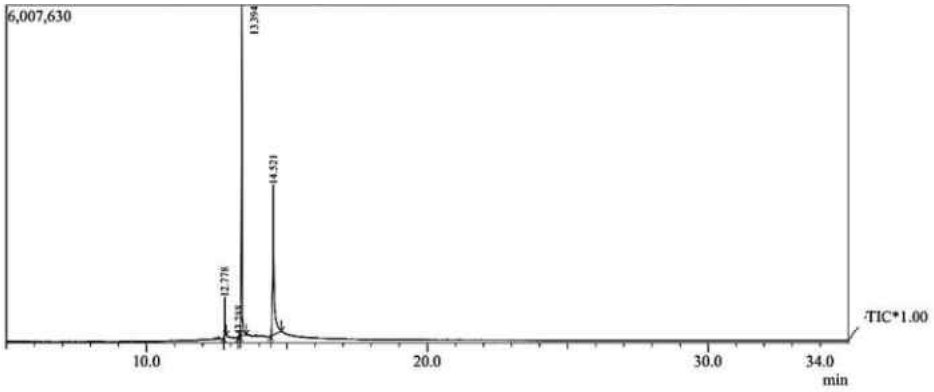

Peak Report TIC

Peak#	R.Time	I.Time	F.Time	Area	Area%	Height	Height%	A/H	Mark	Name
1	12.778	12.749	12.840	1207570	5.01	721418	7.73	1.67		3-Quinolinamine (CAS)
2	13.288	13.260	13.344	144310	0.60	43245	0.46	3.34		4-Aminonicotinonitrile
3	13.394	13.344	13.554	12002853	49.76	5888783	63.13	2.04	V	Pyrrolidine[2,1-c]-2H,5H-1,4-be
4	14.521	14.429	14.800	10766796	44.64	2674194	28.67	4.03		Pyrrolidine[2,1-c]-2H,5H-1,4-be
				24121529	100.00	9327640	100.00			

Line#:4 R.Time:14.5(Scan#:1361)
MassPeaks:310
RawMode:Averaged 14.5-14.5(1360-1362) BasePeak:70(444620)
BG Mode:Calc. from Peak Group 1 - Event 1

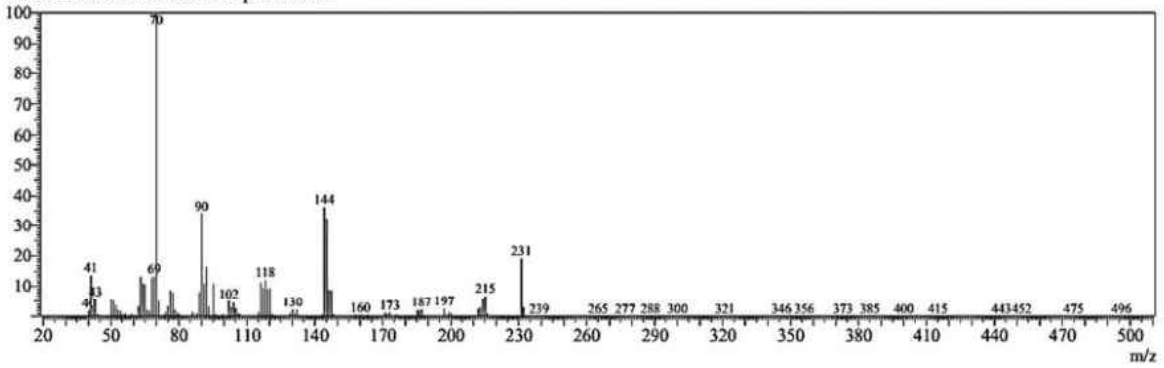

Appendix E4: IR Spectrum for Compound **5** in Chloroform

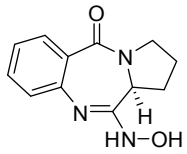

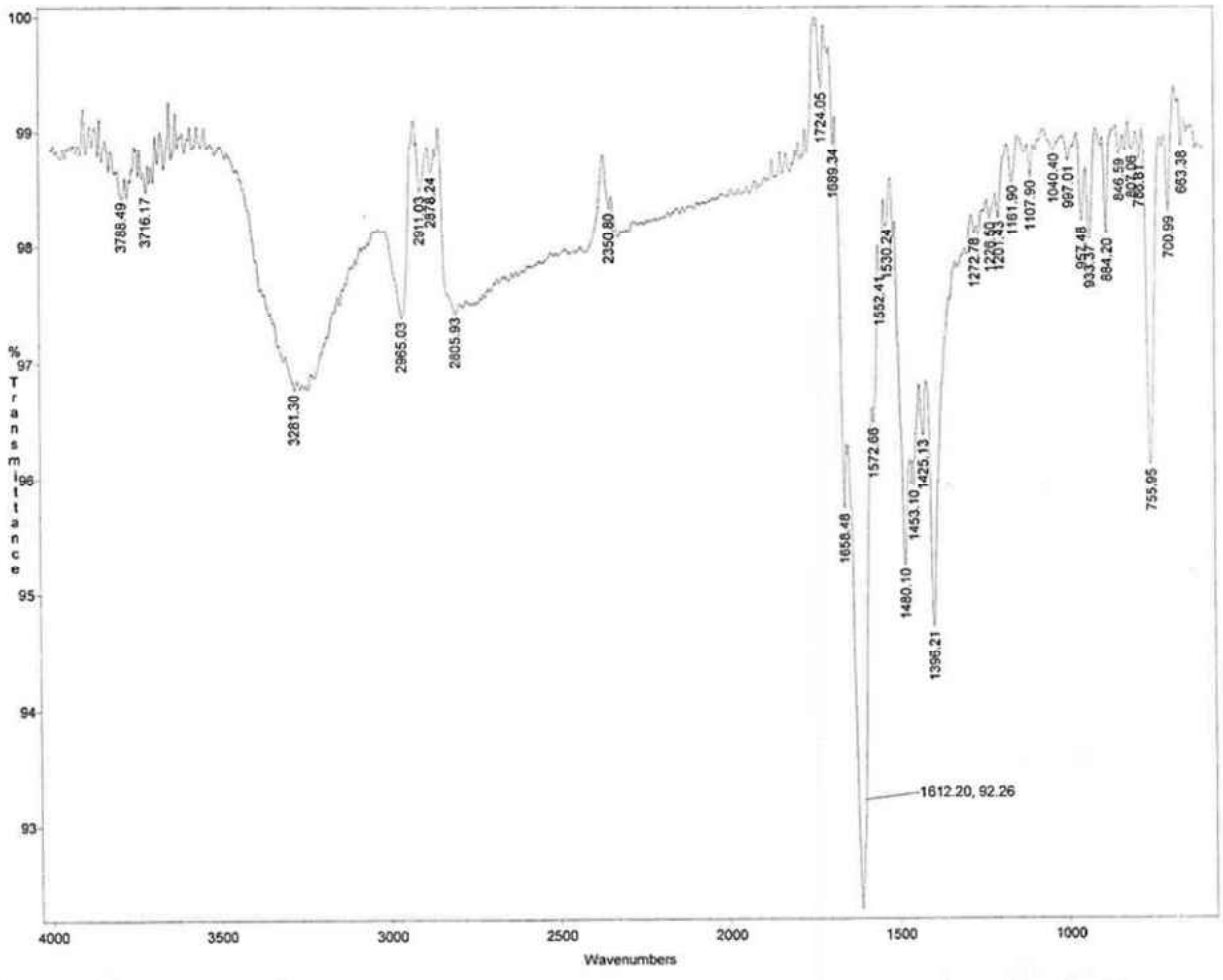

Appendix F1: ^{1}H NMR Spectrum for Compound **6** in Chloroform-d

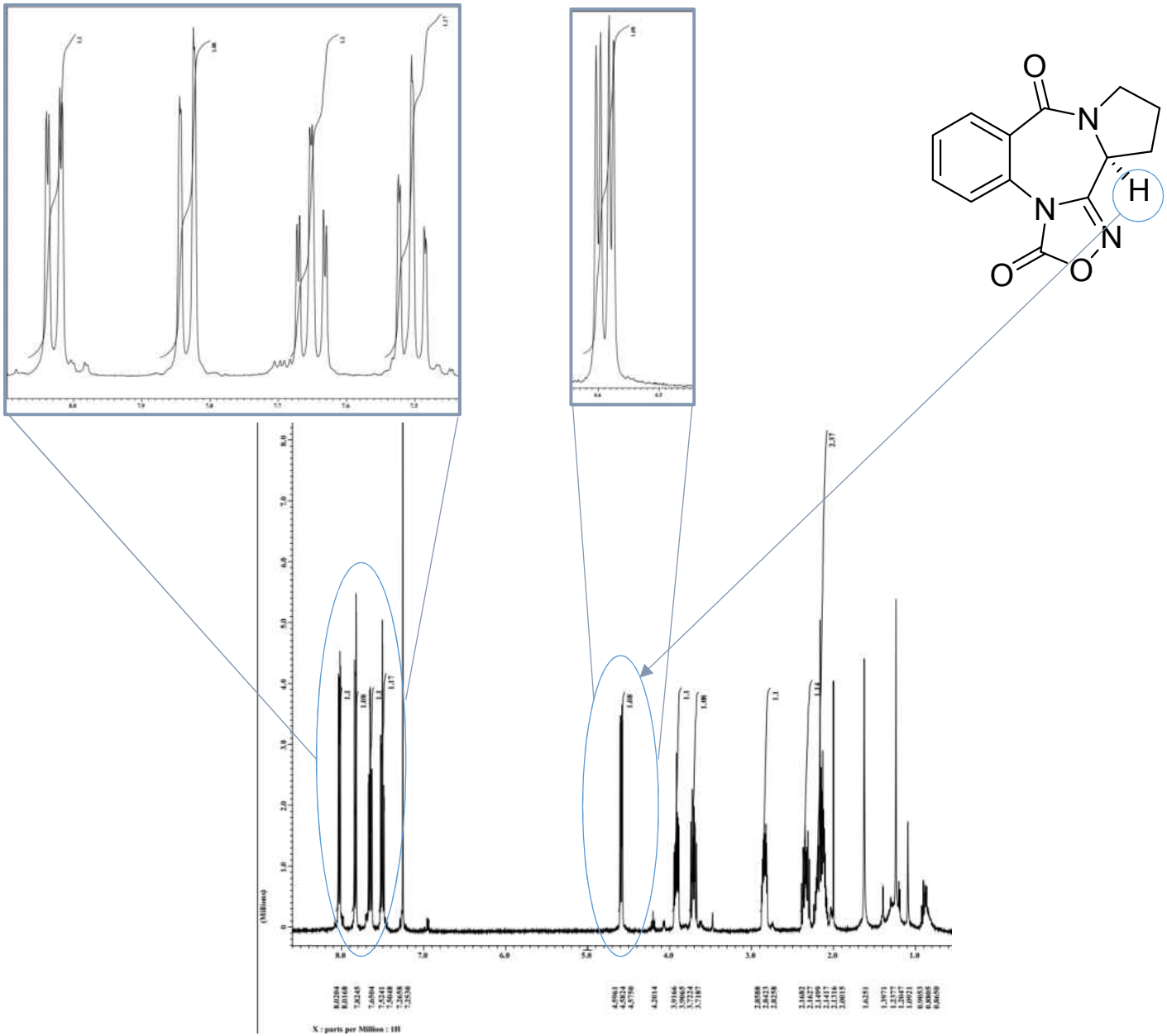

Appendix F2: ^{13}C NMR Spectrum for Compound **6** in Chloroform-d

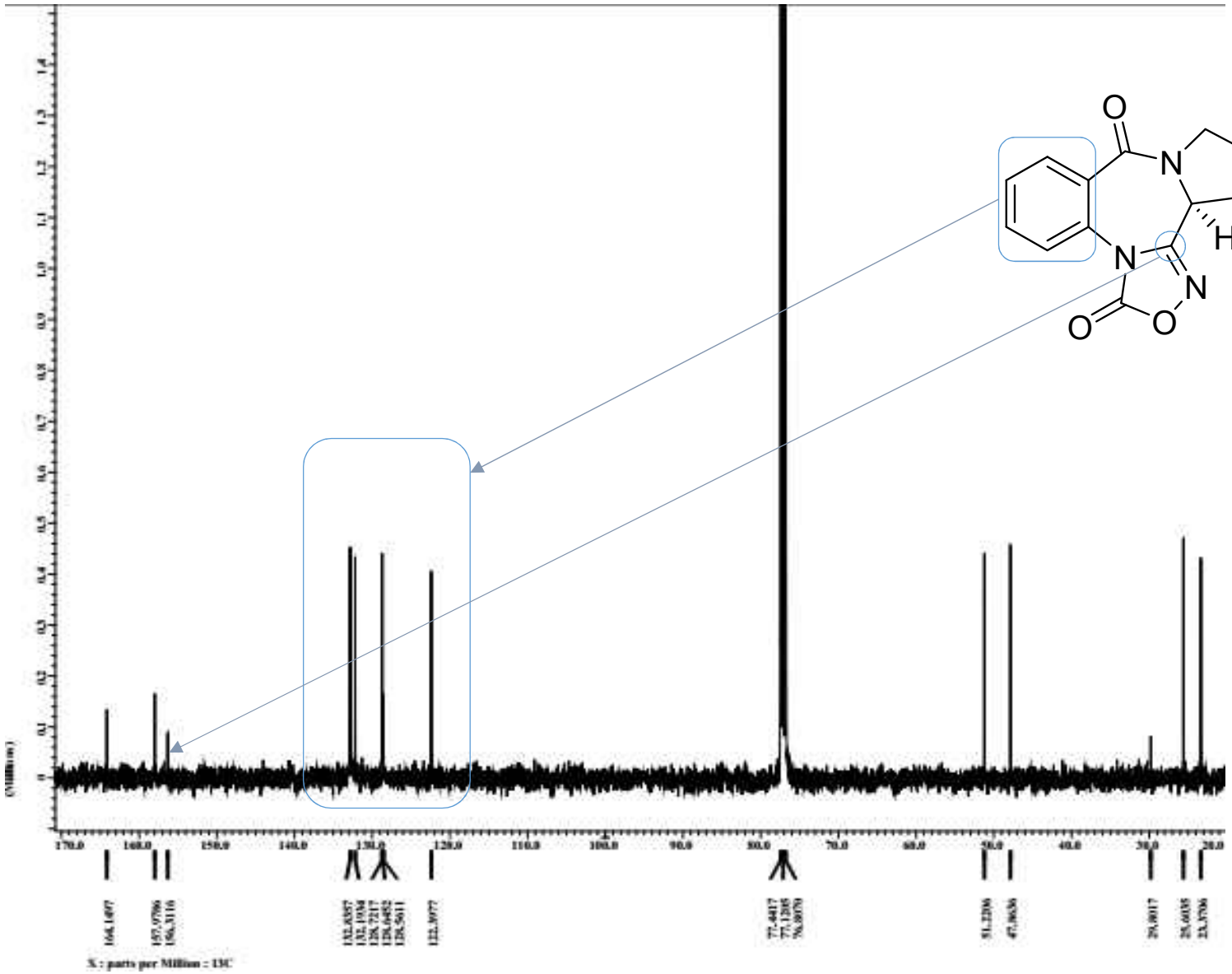

Appendix F3: GC-MS Spectrum for Compound **6** in Chloroform

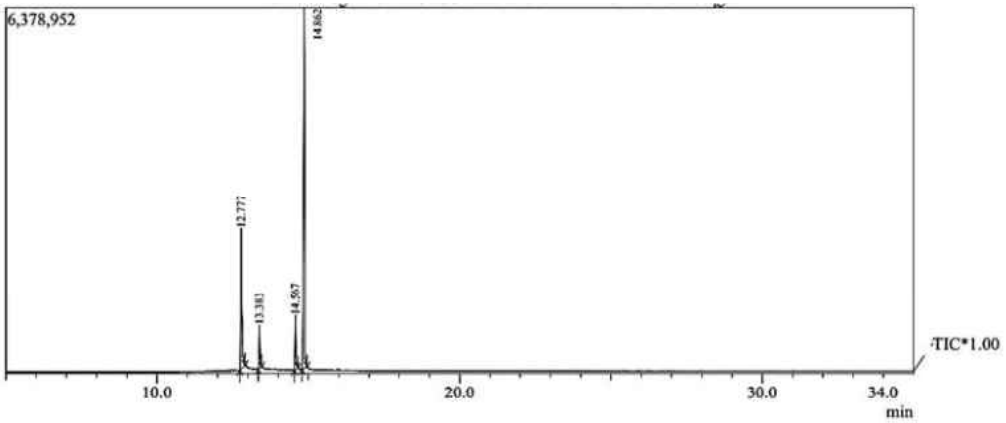

Peak Report TIC

Peak#	R.Time	I.Time	F.Time	Area	Area%	Height	Height%	A/H	Mark	Name
1	12.777	12.735	12.910	6135869	23.77	2448799	23.52	2.51		3-Quinolinamine (CAS)
2	13.383	13.344	13.456	1477618	5.72	742153	7.13	1.99		Pyrrolidine[2,1-c]-2H,5H-1,4-be
3	14.567	14.527	14.660	1950819	7.56	929844	8.93	2.10		Di-n-octyl phthalate
4	14.862	14.786	14.961	16246796	62.94	6289632	60.42	2.58		3-Quinolinamine (CAS)
				25811102	100.00	10410428	100.00			

Line#:4 R.Time:14.9(Scan#:1410)
MassPeaks:292
RawMode:Averaged 14.9-14.9(1409-1411) BasePeak:144(969790)
BG Mode:Calc. from Peak Group 1 - Event 1

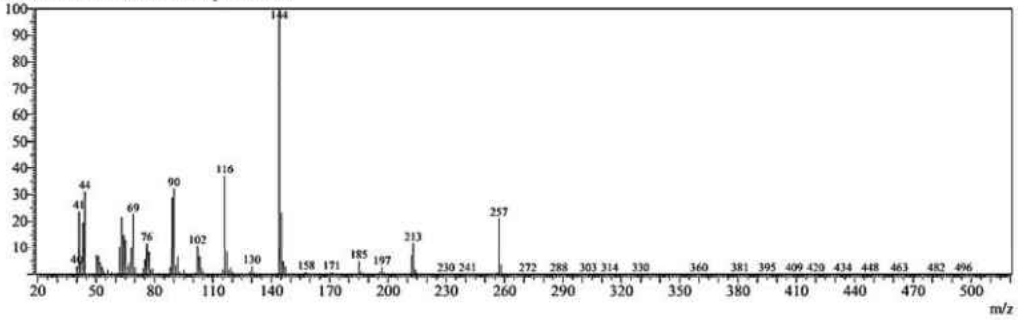

F4: IR Spectrum for Compound **6** in Chloroform

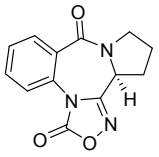

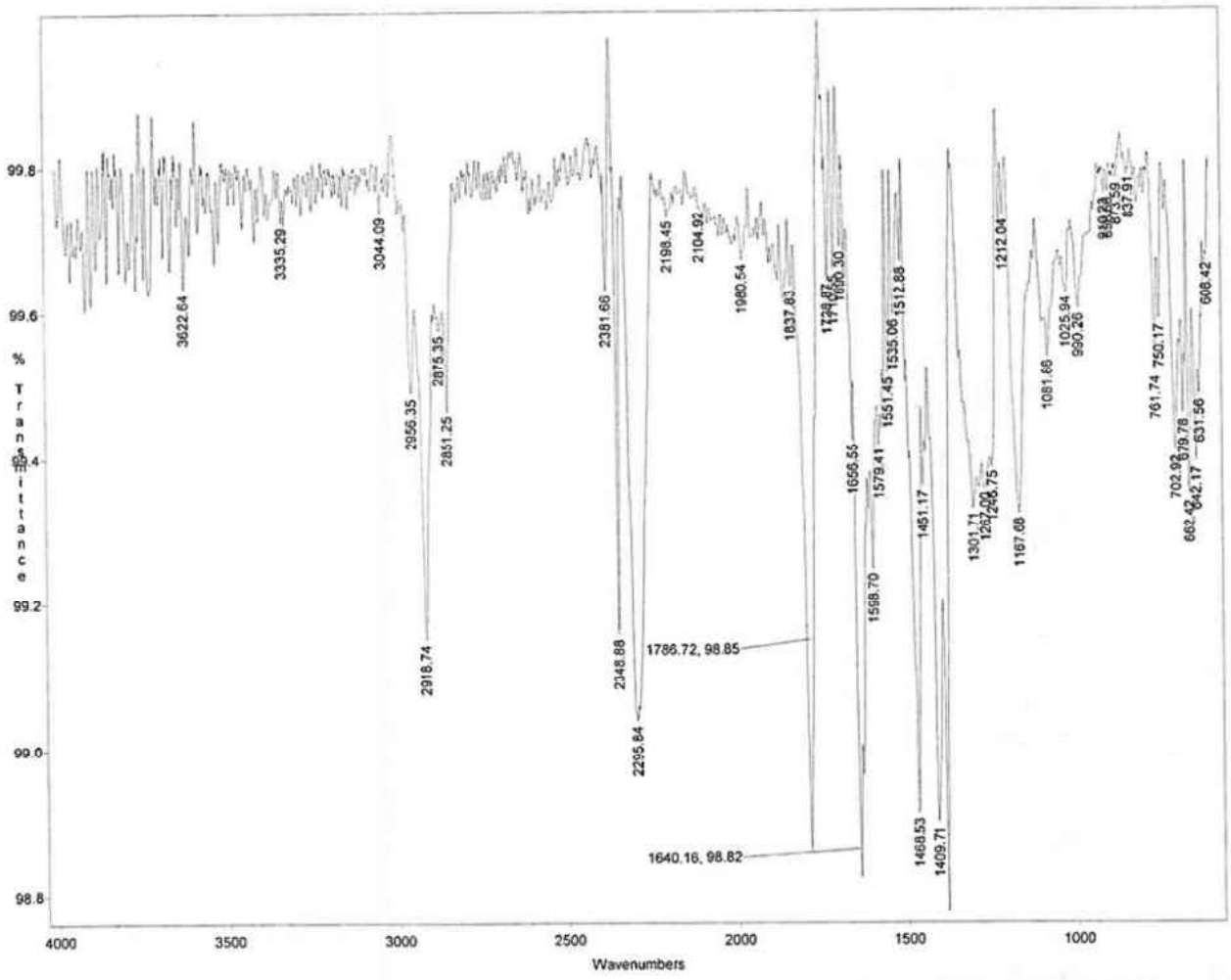

Appendix G1: ^{1}C NMR Spectrum for Compound **7** in Chloroform-d

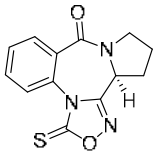

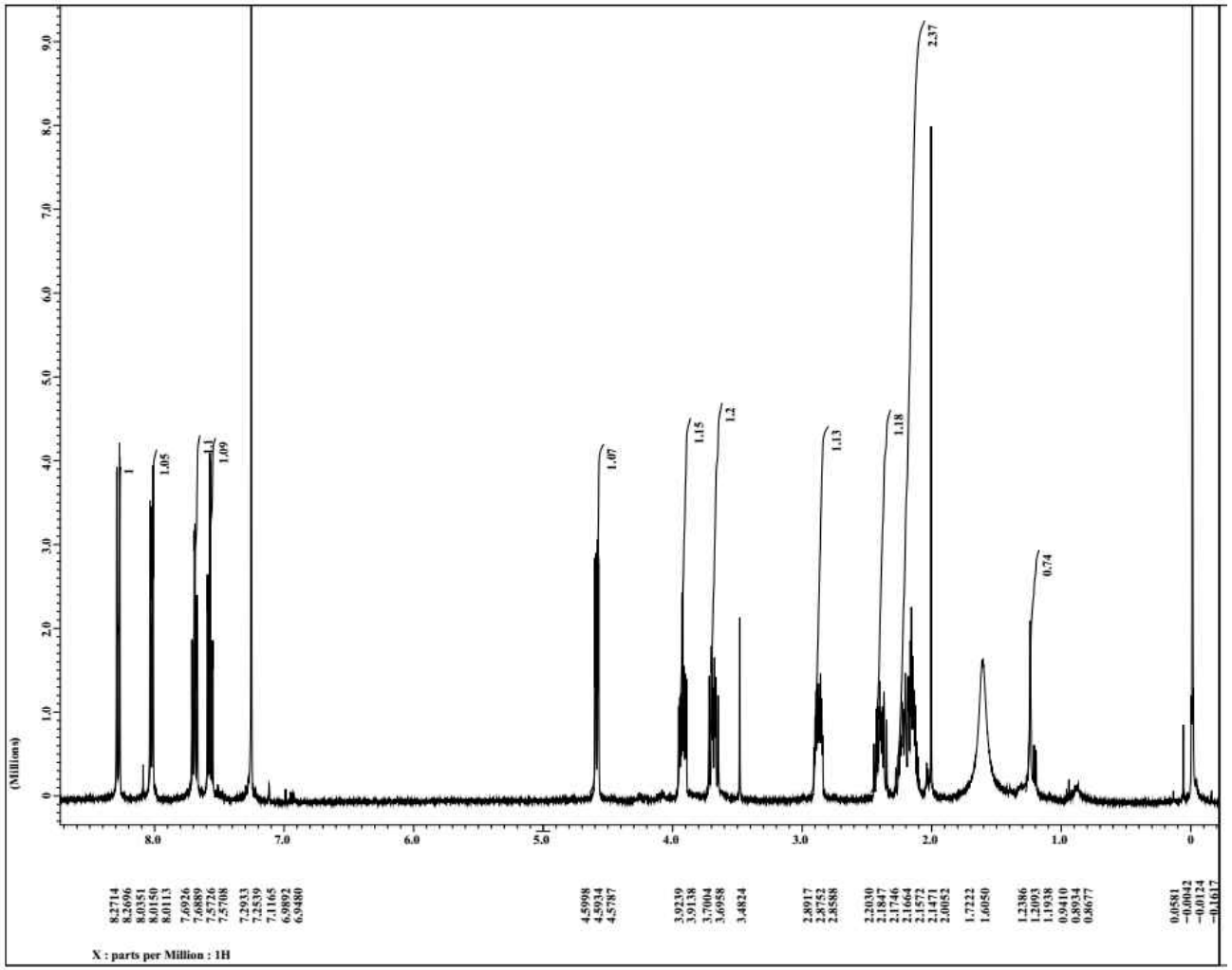

Appendix G2: ^{13}C NMR Spectrum for Compound **7** in Chloroform-d

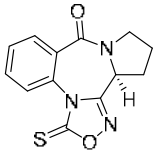

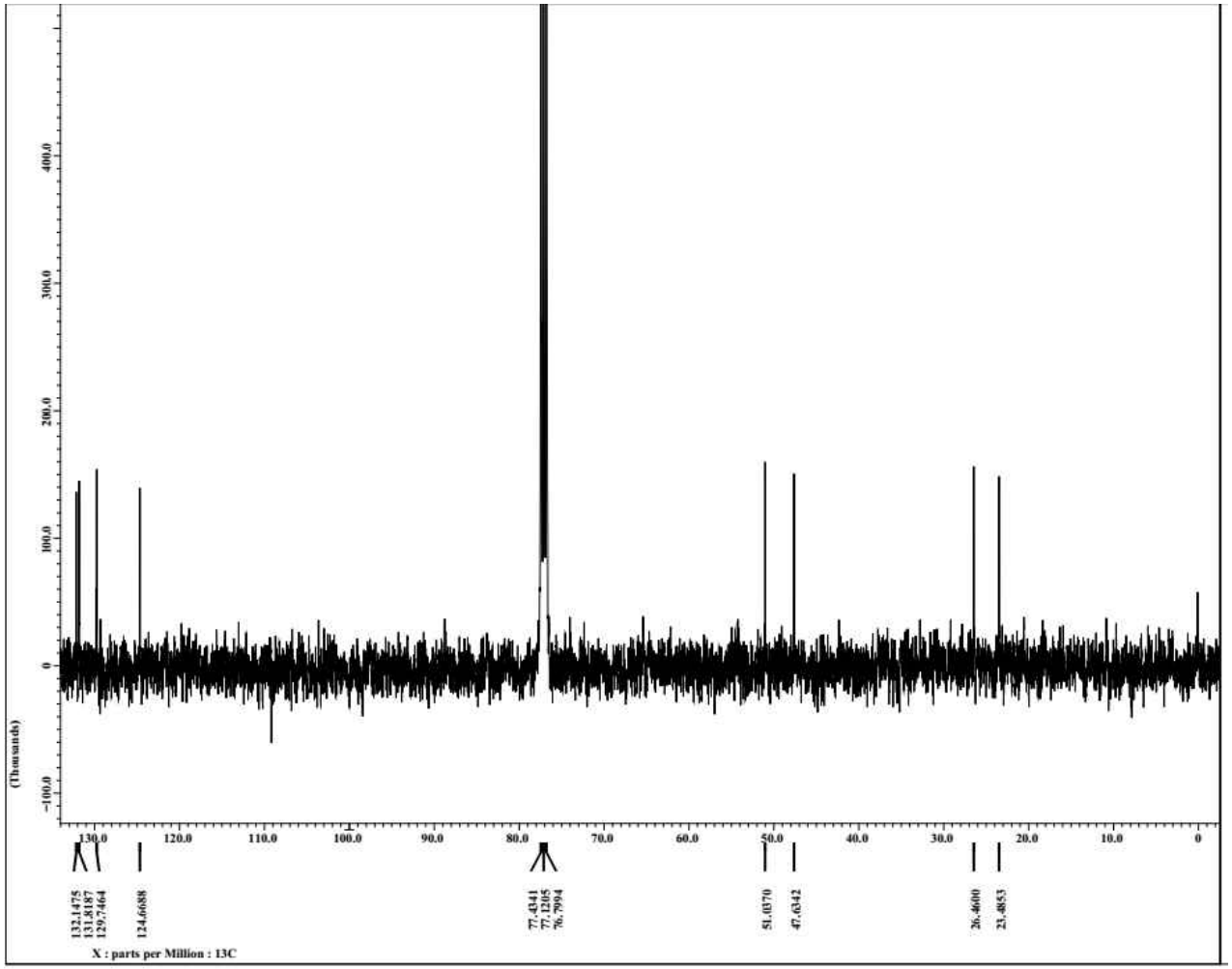

Appendix G3: GC-MS Spectrum for Compound **7** in Chloroform

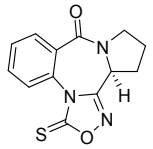

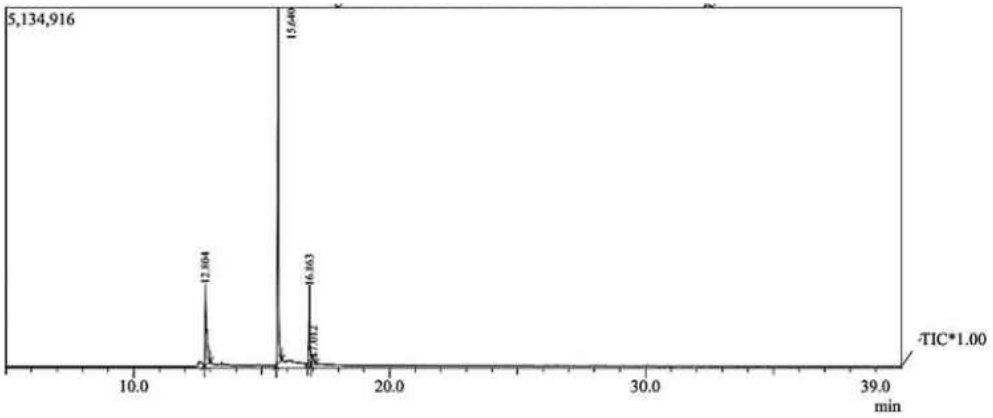

Peak Report TIC

Peak#	R.Time	I.Time	F.Time	Area	Area%	Height	Height%	A/H	Mark	Name
1	12.804	12.763	12.994	4413308	19.00	1139789	15.40	3.87		3-Quinolinamine (CAS)
2	15.640	15.563	15.780	14749099	63.49	5068738	68.49	2.91		Acetamide, trifluoro-, N-(2'-acet
3	16.863	16.788	16.928	3451189	14.86	1109077	14.99	3.11		1H-Indole-2,3-dione, 1-(pentafl
4	17.012	16.928	17.117	618045	2.66	83251	1.12	7.42	V	2-Pyrrolidinone, 1-methyl-5-(1-r
				23231641	100.00	7400855	100.00			

Line#:2 R.Time:15.6(Scan#:1521)
MassPeaks:331
RawMode:Averaged 15.6-15.6(1520-1522) BasePeak:43(463027)
BG Mode:Calc. from Peak Group 1 - Event 1

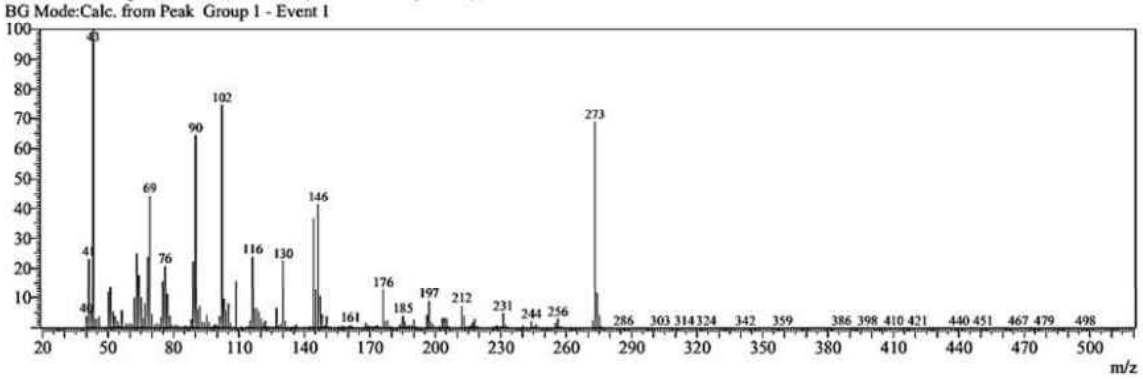

Appendix G4: IR Spectrum for Compound **7** in Chloroform

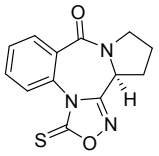

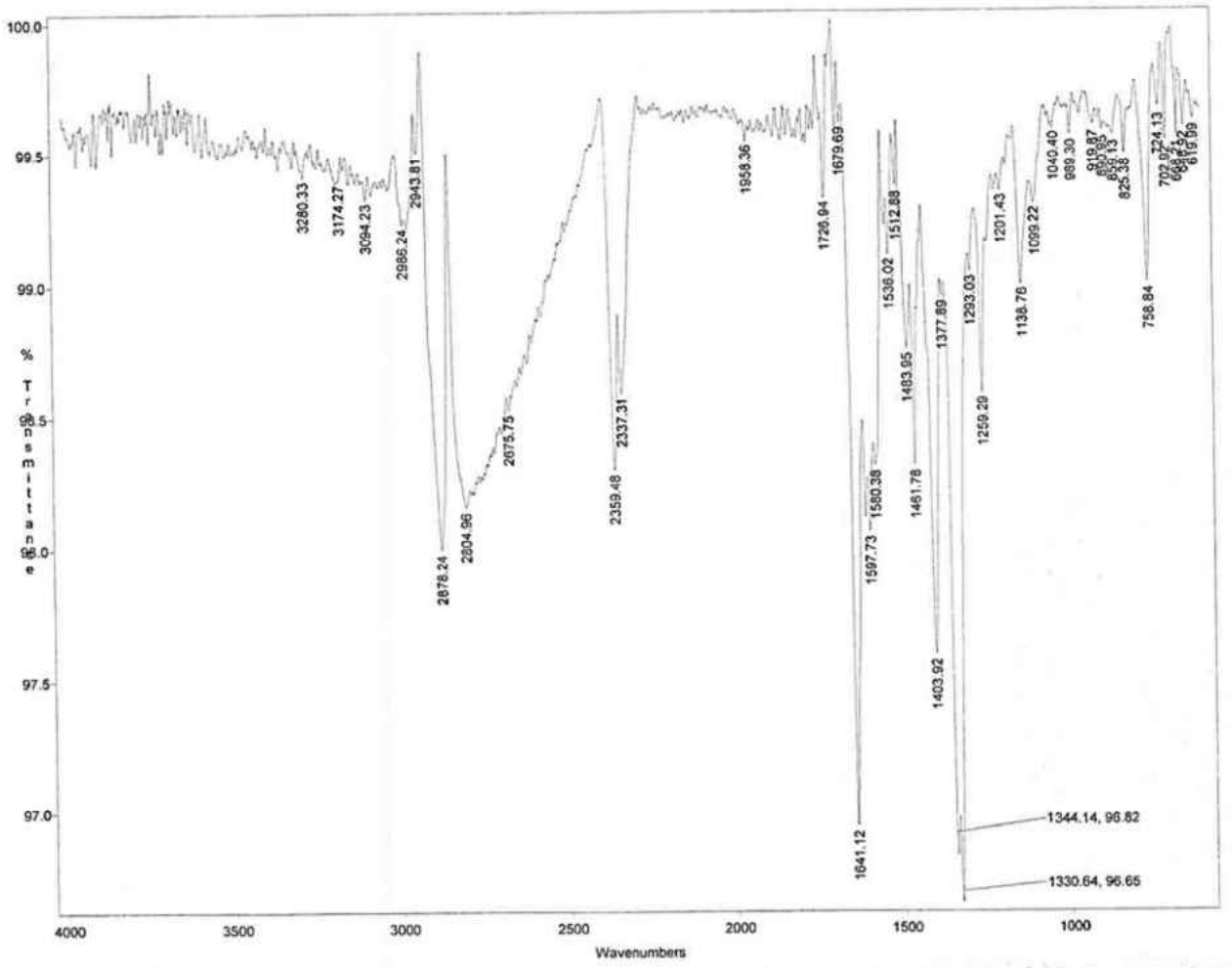

Appendix H1: ^{1}H NMR Spectrum for Compound **8** in Chloroform-d

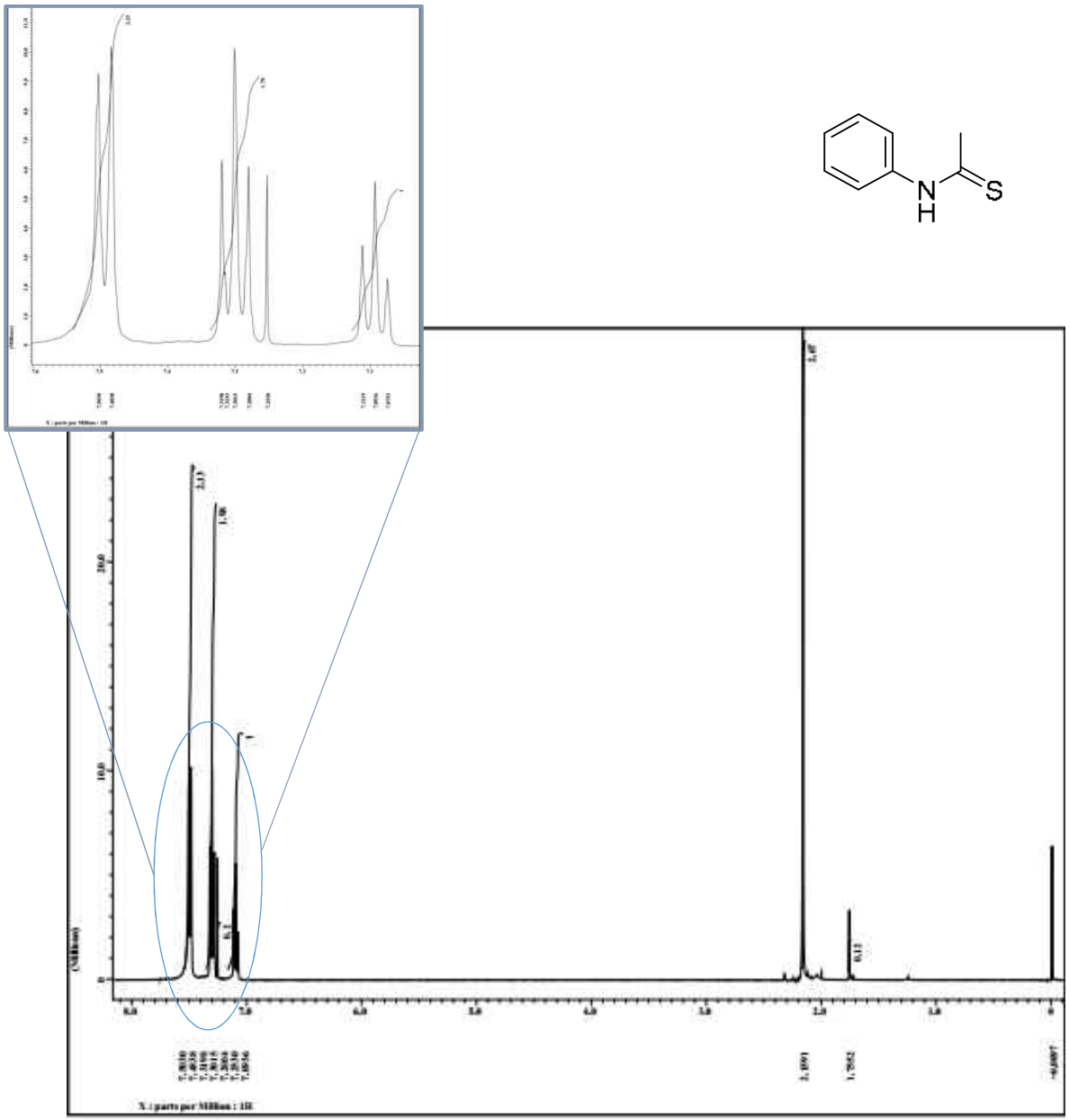

Appendix H2: ^{13}C NMR Spectrum for Compound **8** in Chloroform-d

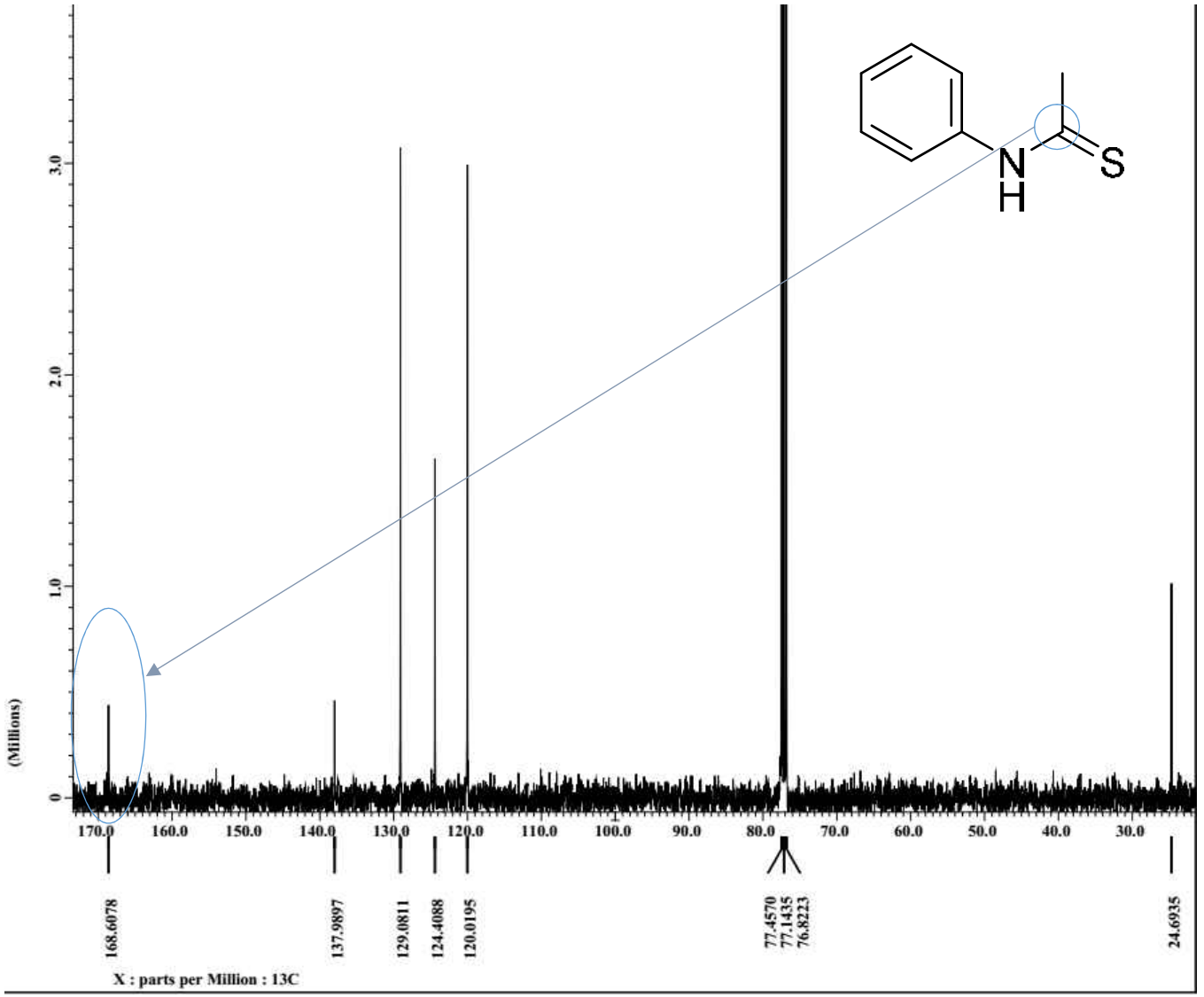

Appendix H3: GC-MS Spectrum for Compound **8** in Chloroform

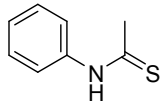

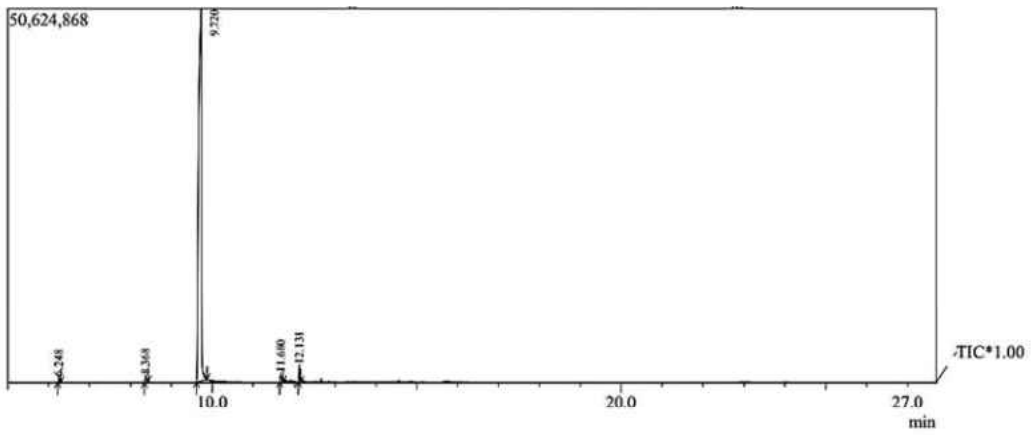

Peak Report TIC

Peak#	R.Time	I.Time	F.Time	Area	Area%	Height	Height%	A/H	Mark	Name
1	6.248	6.218	6.295	1271959	0.50	726992	1.31	1.75		Sydnone, 4-methyl-3-phenyl-
2	8.368	8.339	8.430	2008015	0.79	915796	1.65	2.19		Acetamide, N-phenyl-
3	9.720	9.606	9.872	246119067	96.60	50380016	90.73	4.89		Ethanethioamide, N-phenyl-
4	11.680	11.650	11.741	2200402	0.86	1227835	2.21	1.79		tetrakis (Dimethylsilylcarbodiin
5	12.131	12.098	12.161	3174303	1.25	2275354	4.10	1.40		1-trans-(2-phenylethenyl)-3-tran
				254773746	100.00	55525993	100.00			

Line#:3 R.Time:9.7(Scan#:675)
MassPeaks:270
RawMode:Averaged 9.7-9.7(674-676) BasePeak:93(7529181)
BG Mode:Calc. from Peak Group 1 - Event 1

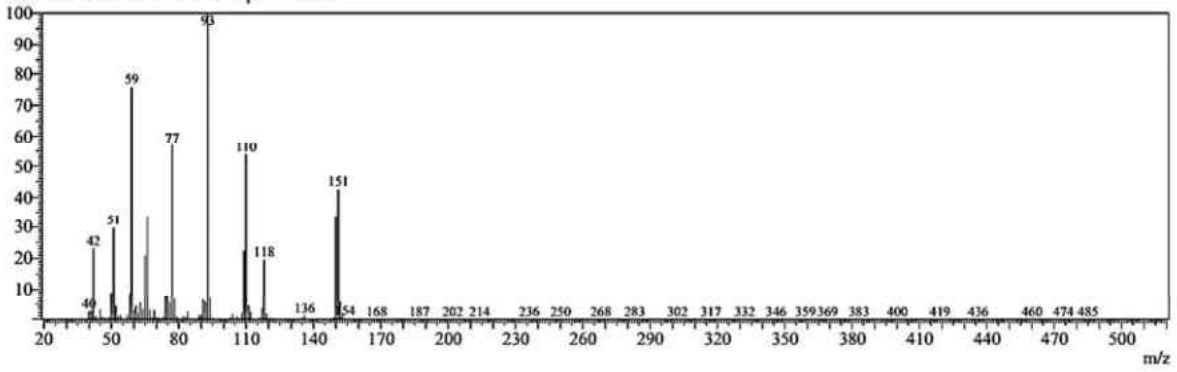

Appendix H4: IR Spectrum for Compound **8** in Chloroform

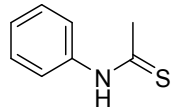

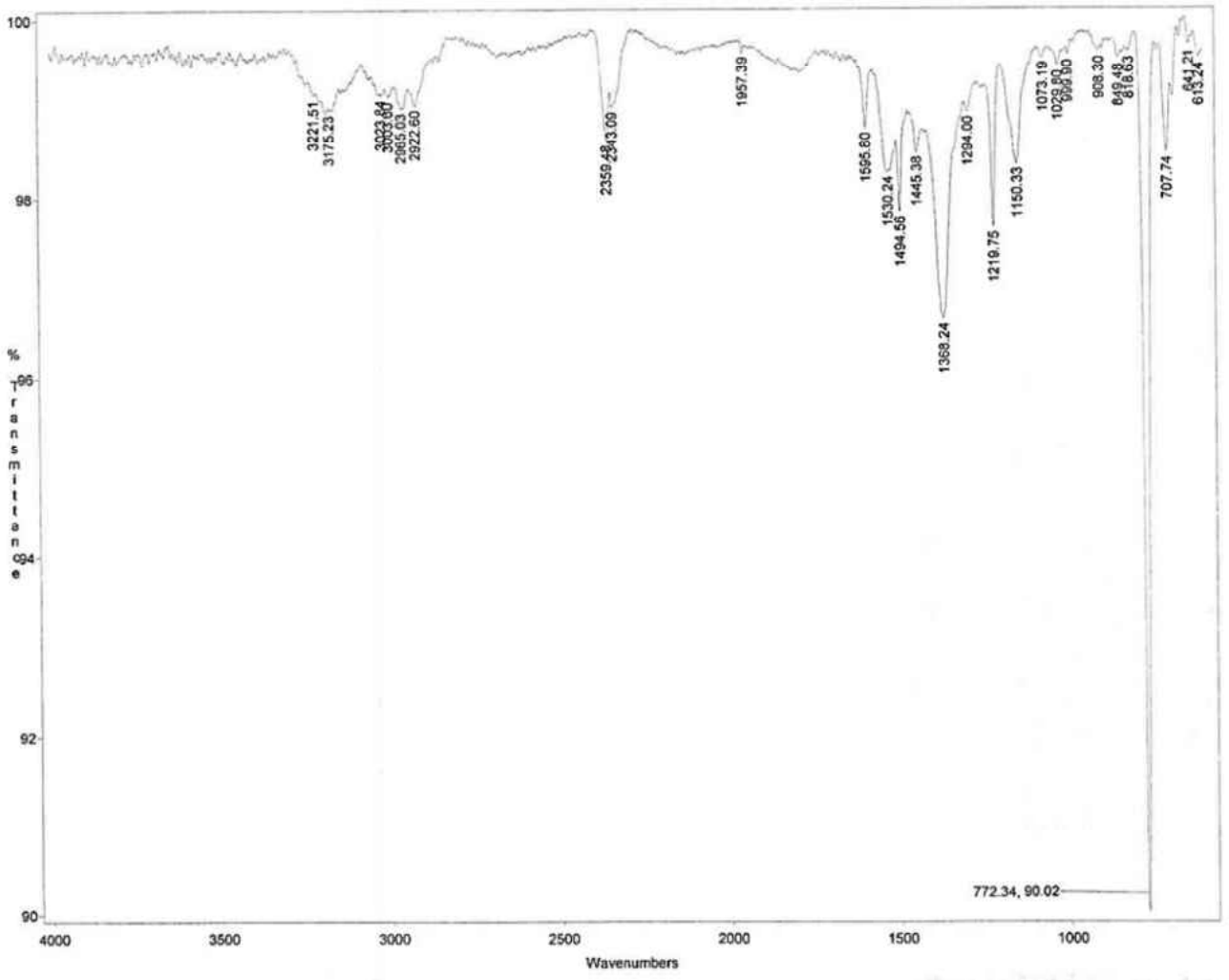

Appendix I1: ^{1}H NMR Spectrum for Compound **9** in Chloroform-d

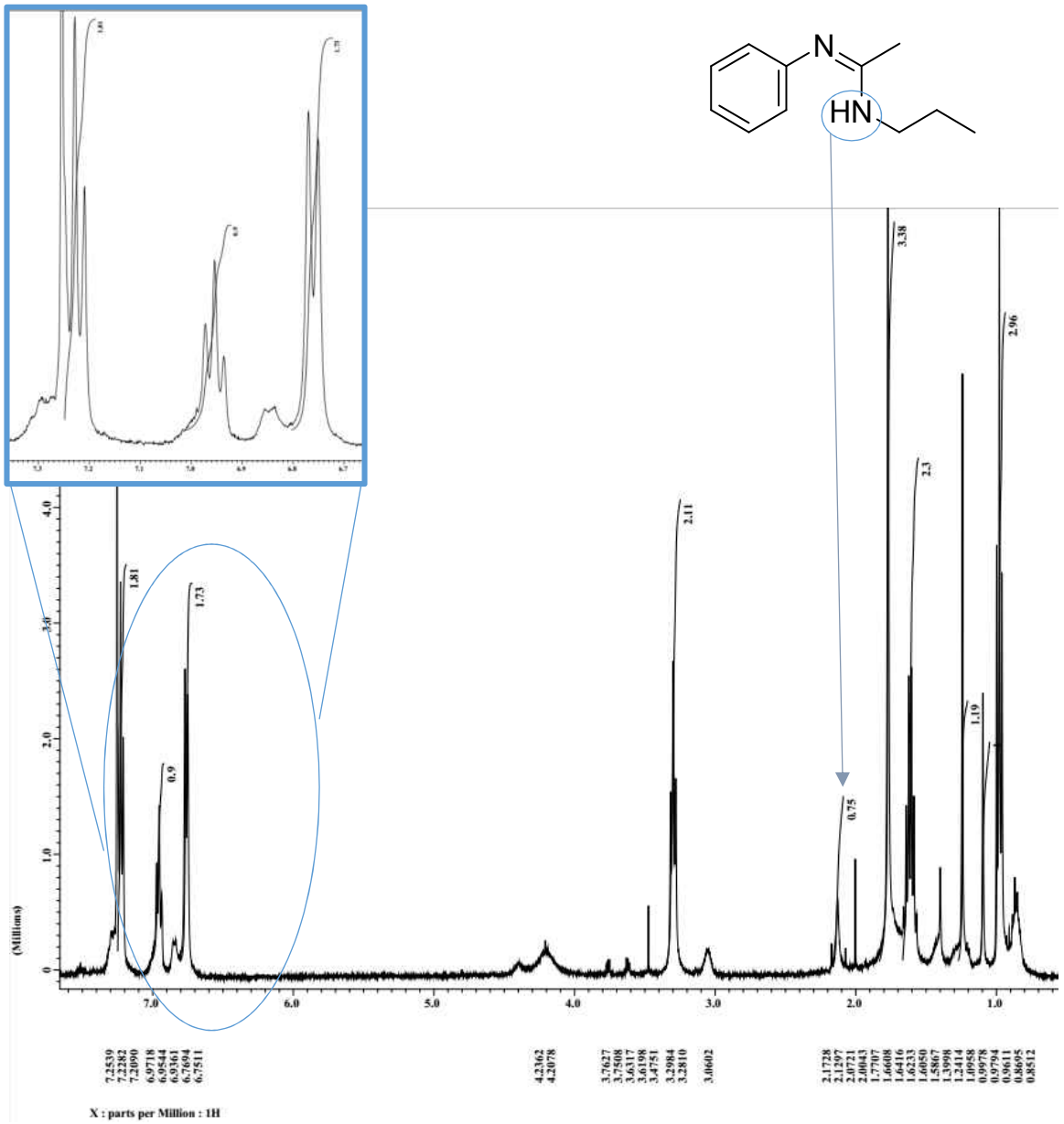

Appendix I2: ^{13}C NMR Spectrum for Compound **9** in Chloroform-d

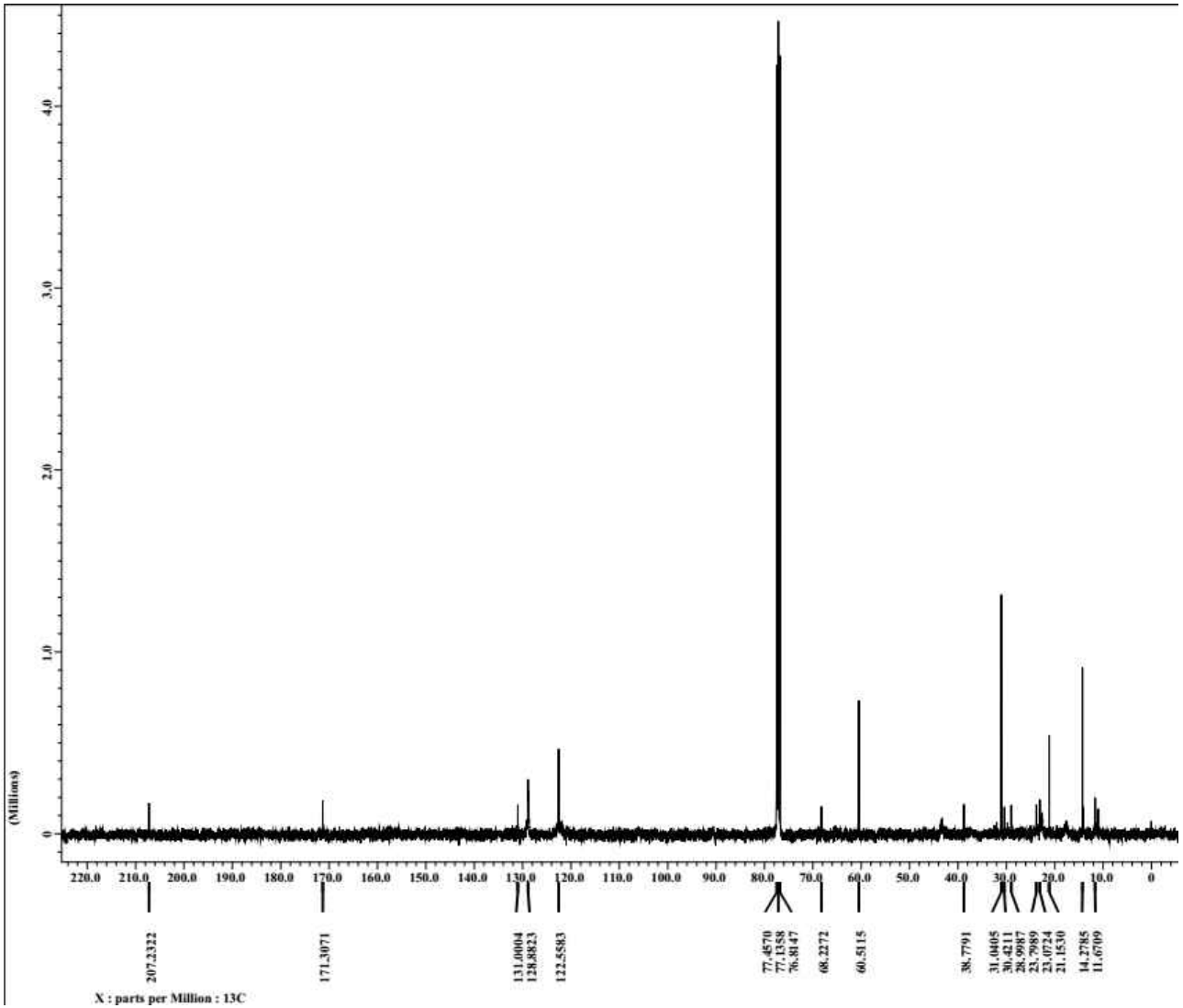

Appendix I3: GC-MS Spectrum for Compound **9** in Chloroform-d

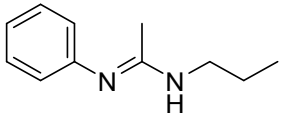

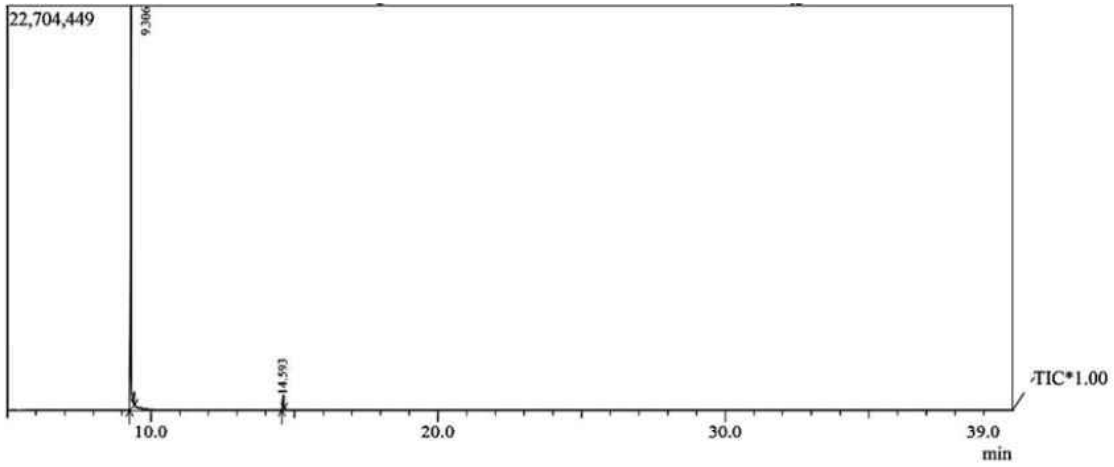

Peak Report TIC

Peak#	R.Time	I.Time	F.Time	Area	Area%	Height	Height%	A/H	Mark	Name
1	9.306	9.256	9.431	50059682	96.84	22600874	96.65	2.21		Thiourea,1-(3-hydroxypropyl)-3
2	14.593	14.555	14.646	1635722	3.16	782383	3.35	2.09		Di-n-octyl phthalate
				51695404	100.00	23383257	100.00			

Line#:1 R.Time:9.3(Scan#:616)
MassPeaks:272
RawMode:Averaged 9.3-9.3(615-617) BasePeak:77(3366871)
BG Mode:Calc. from Peak Group 1 - Event 1

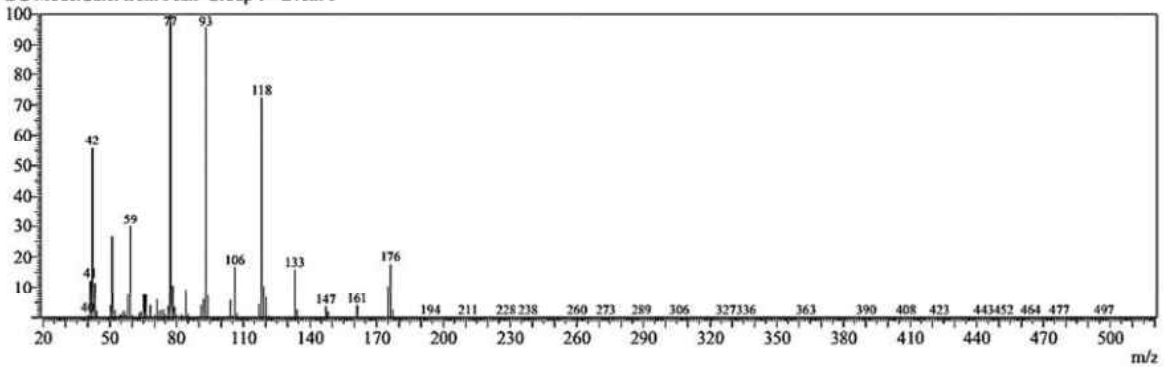

Appendix I4: IR Spectrum for Compound **9** in Chloroform-d

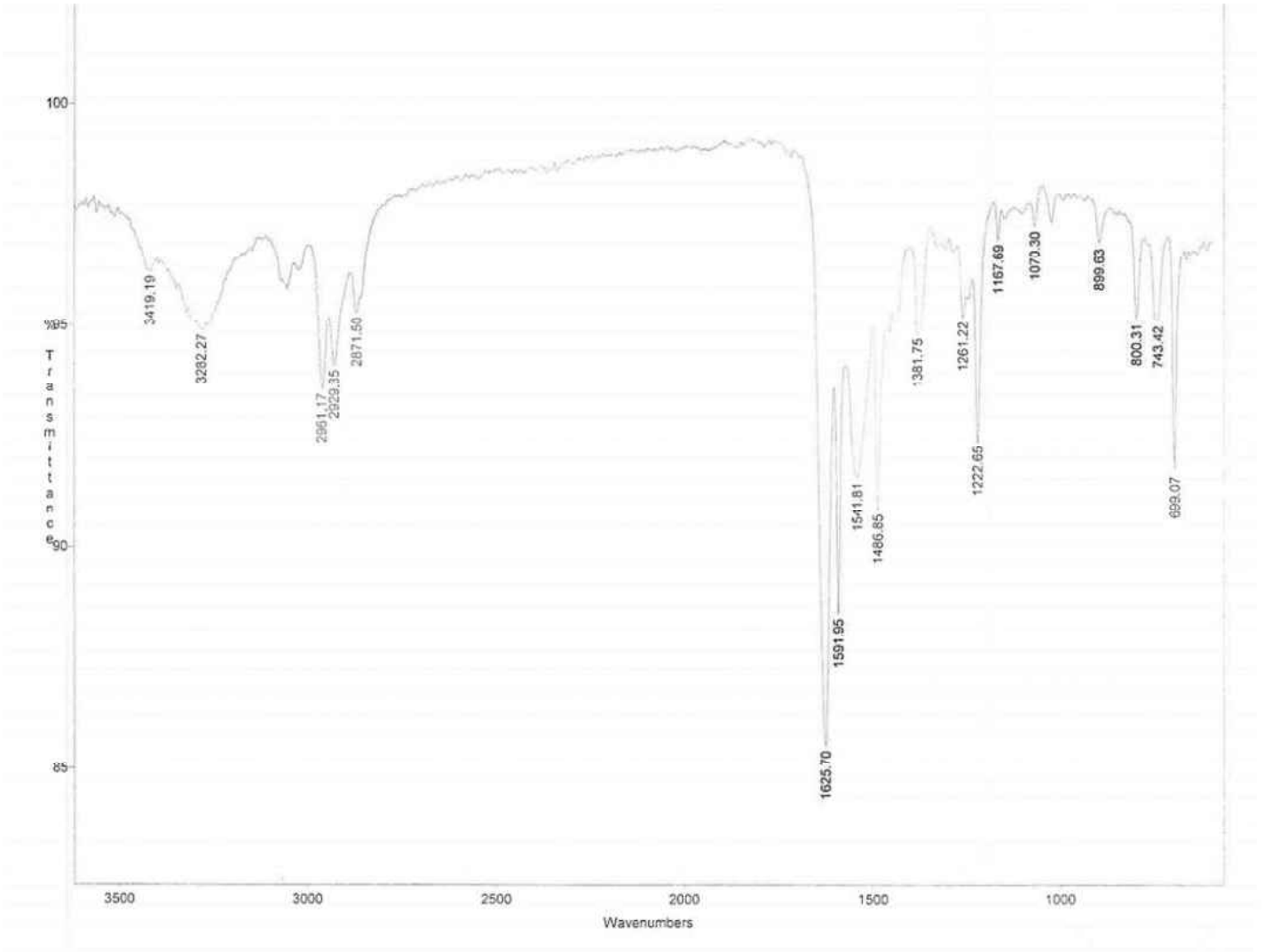

Appendix J1: ^{1}H NMR Spectrum for Compound **10** in Chloroform-d

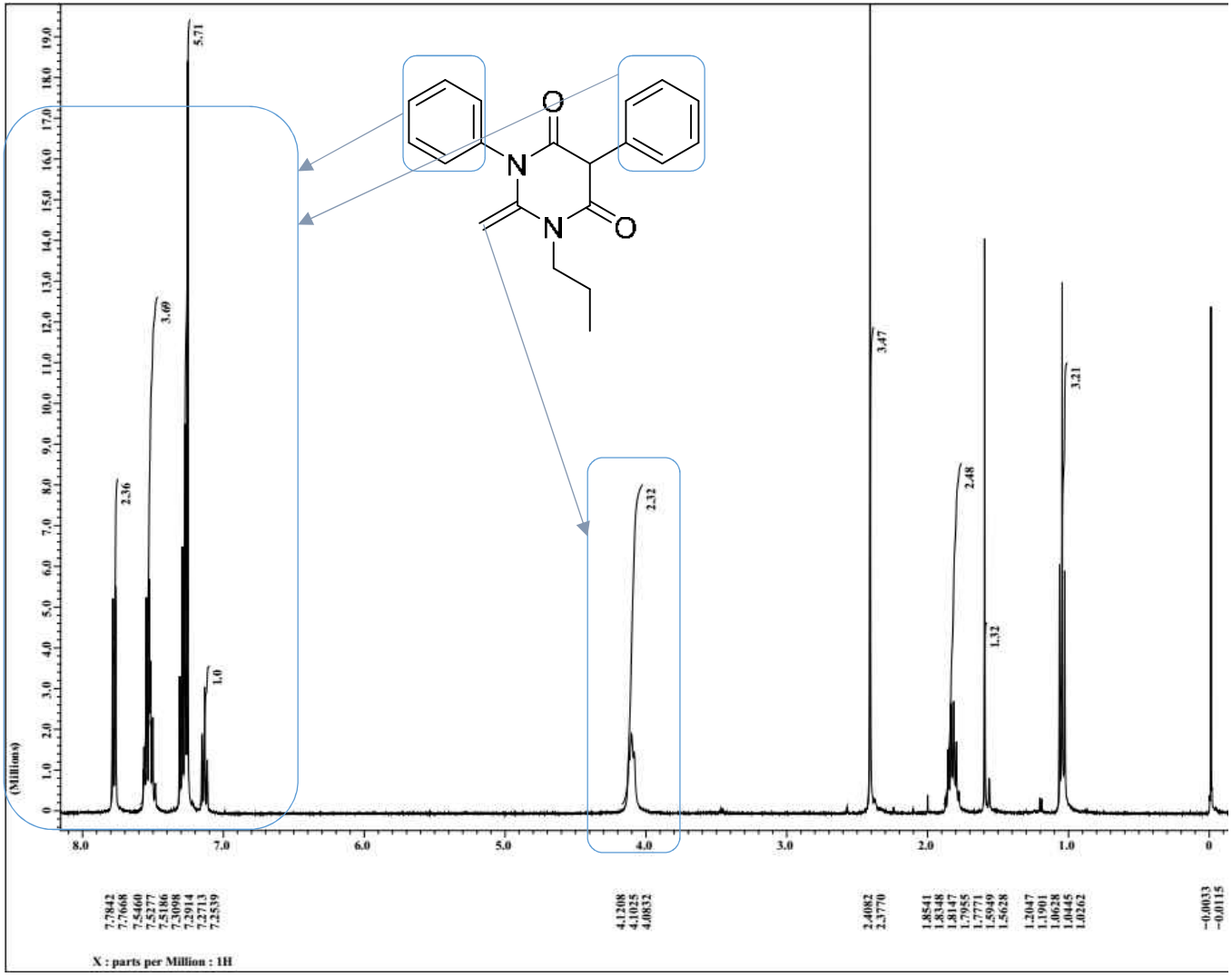

Appendix J2: ^{13}C NMR Spectrum for Compound **10** in Chloroform-d

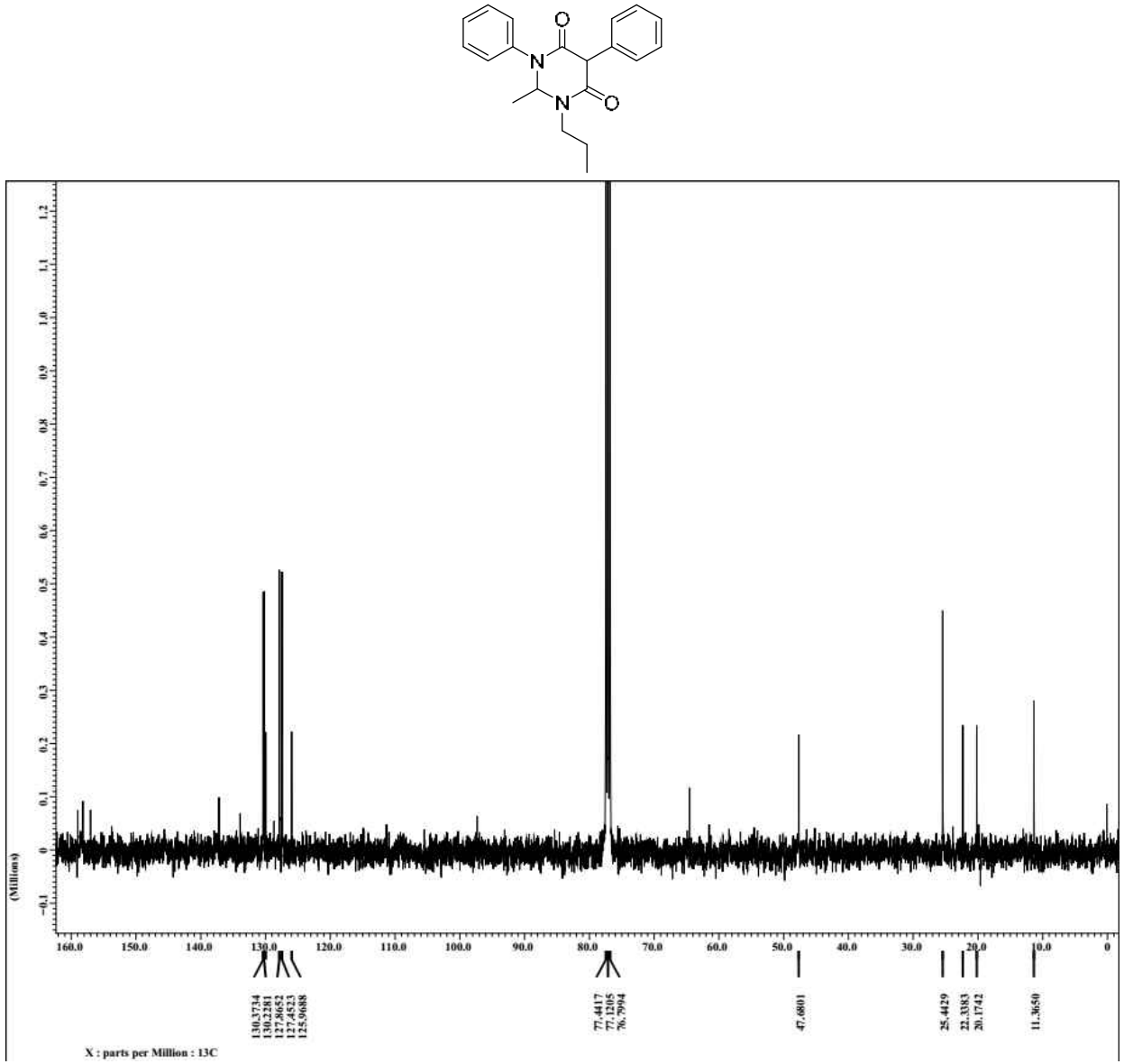

Appendix J3: GC-MS Spectrum for Compound **10** in Chloroform

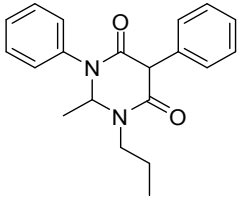

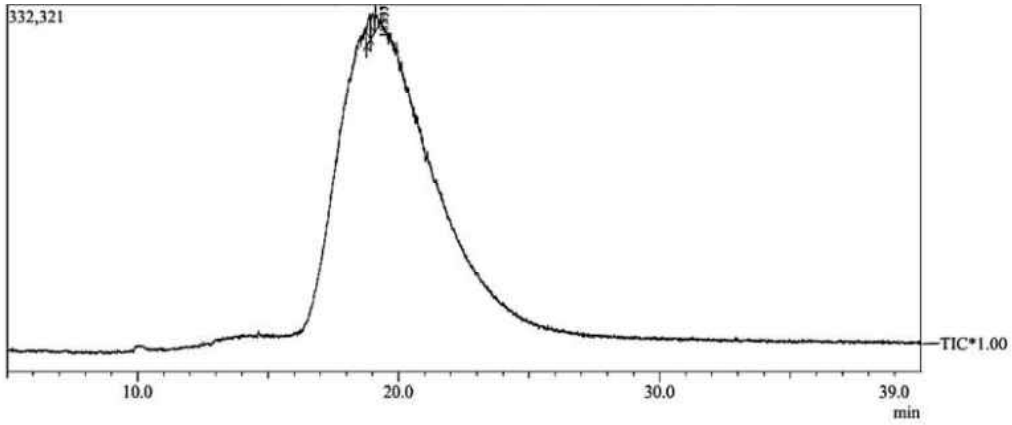

Peak Report TIC

Peak#	R.Time	I.Time	F.Time	Area	Area%	Height	Height%	A/H	Mark	Name
1	18.895	18.769	18.923	168033	51.15	23878	55.52	7.04	V	4-Cyano-N-acetylaniline
2	18.937	18.923	19.084	160490	48.85	19127	44.48	8.39	V	1(2H)-Naphthalenone, 3,4-dihyd
				328523	100.00	43005	100.00			

Line#:2 R.Time:18.9(Scan#:1992)
MassPeaks:243
RawMode:Averaged 18.9-18.9(1991-1993) BasePeak:90(1406)
BG Mode:Calc. from Peak Group 1 - Event 1

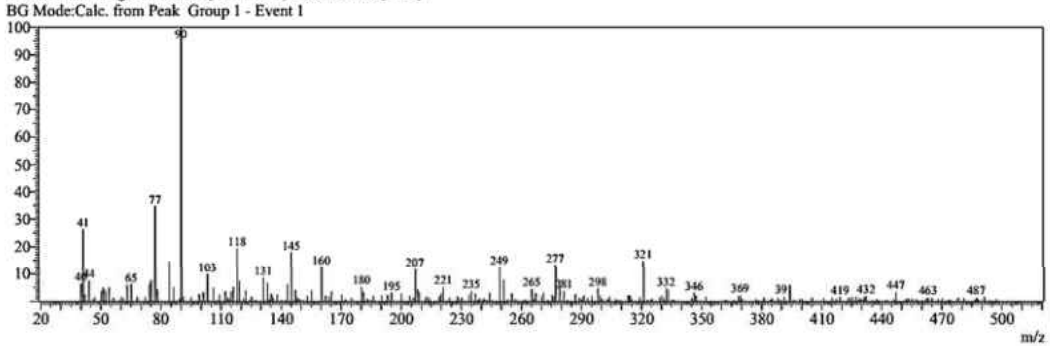

Appendix J4: IR Spectrum for Compound **10** in Chloroform

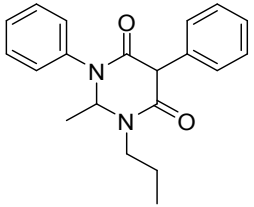

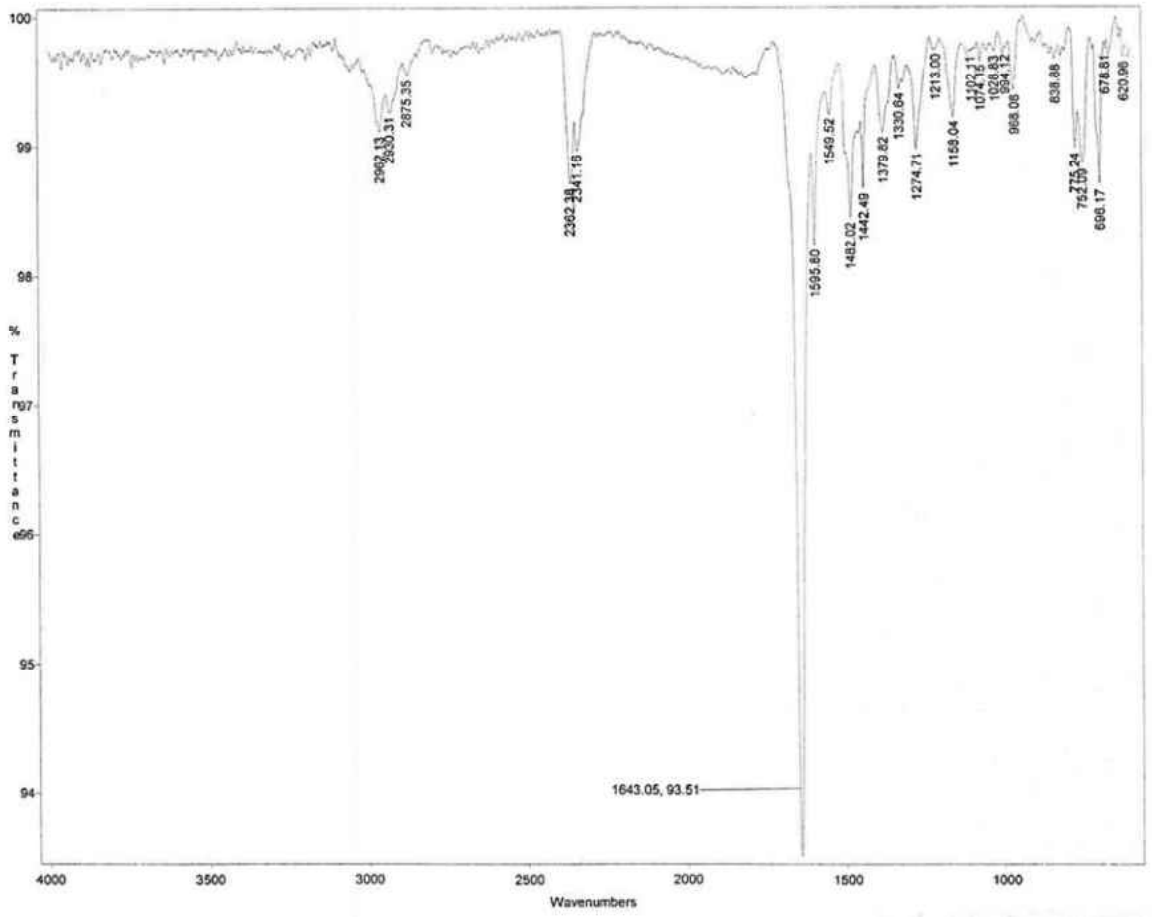

Appendix K1: ^{1}H NMR Spectrum for Compound **11** in Chloroform-d

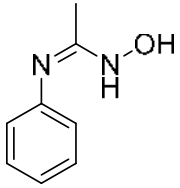

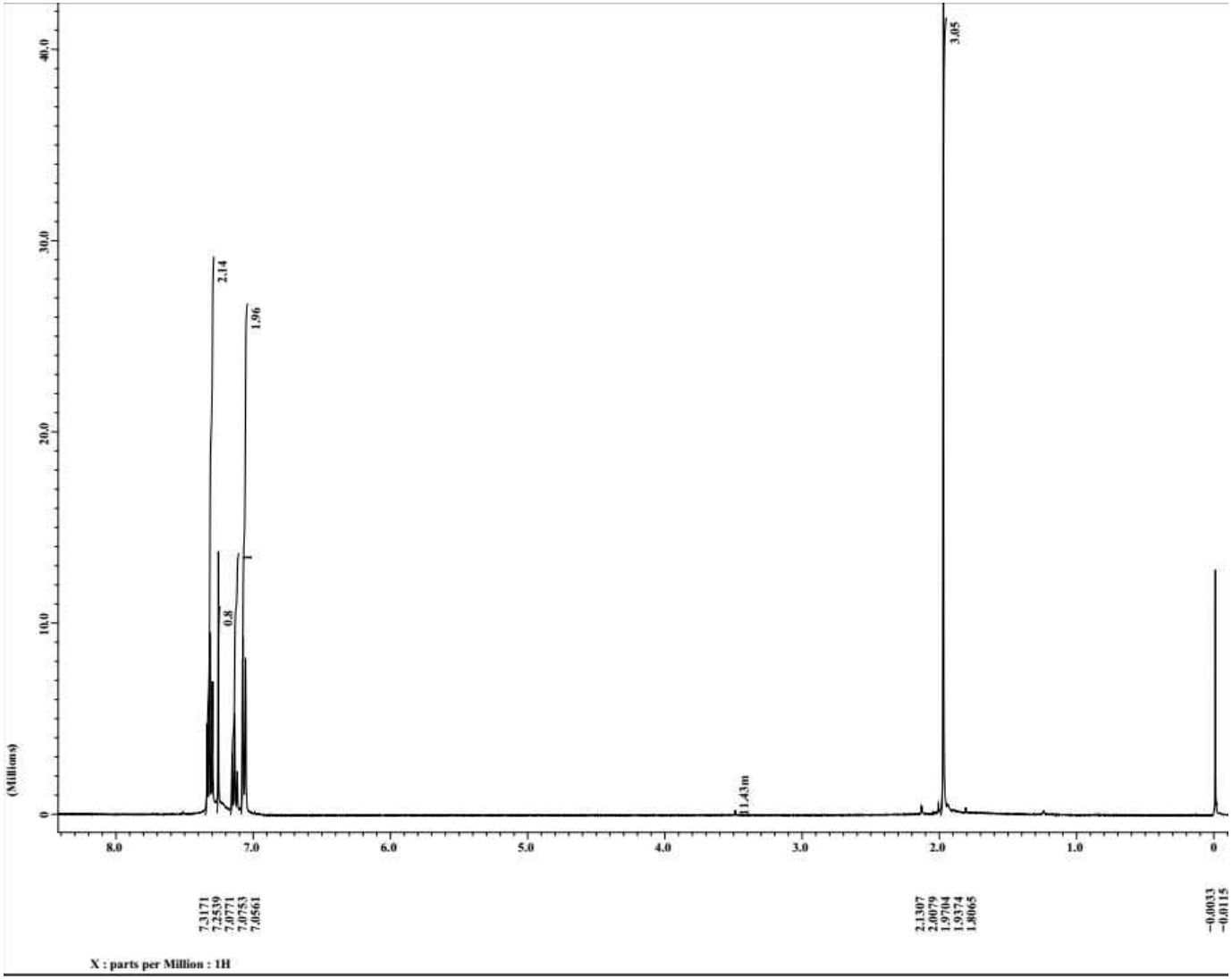

Appendix K2: ^{13}C NMR Spectrum for Compound **11** in Chloroform-d

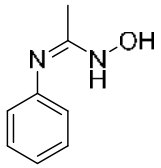

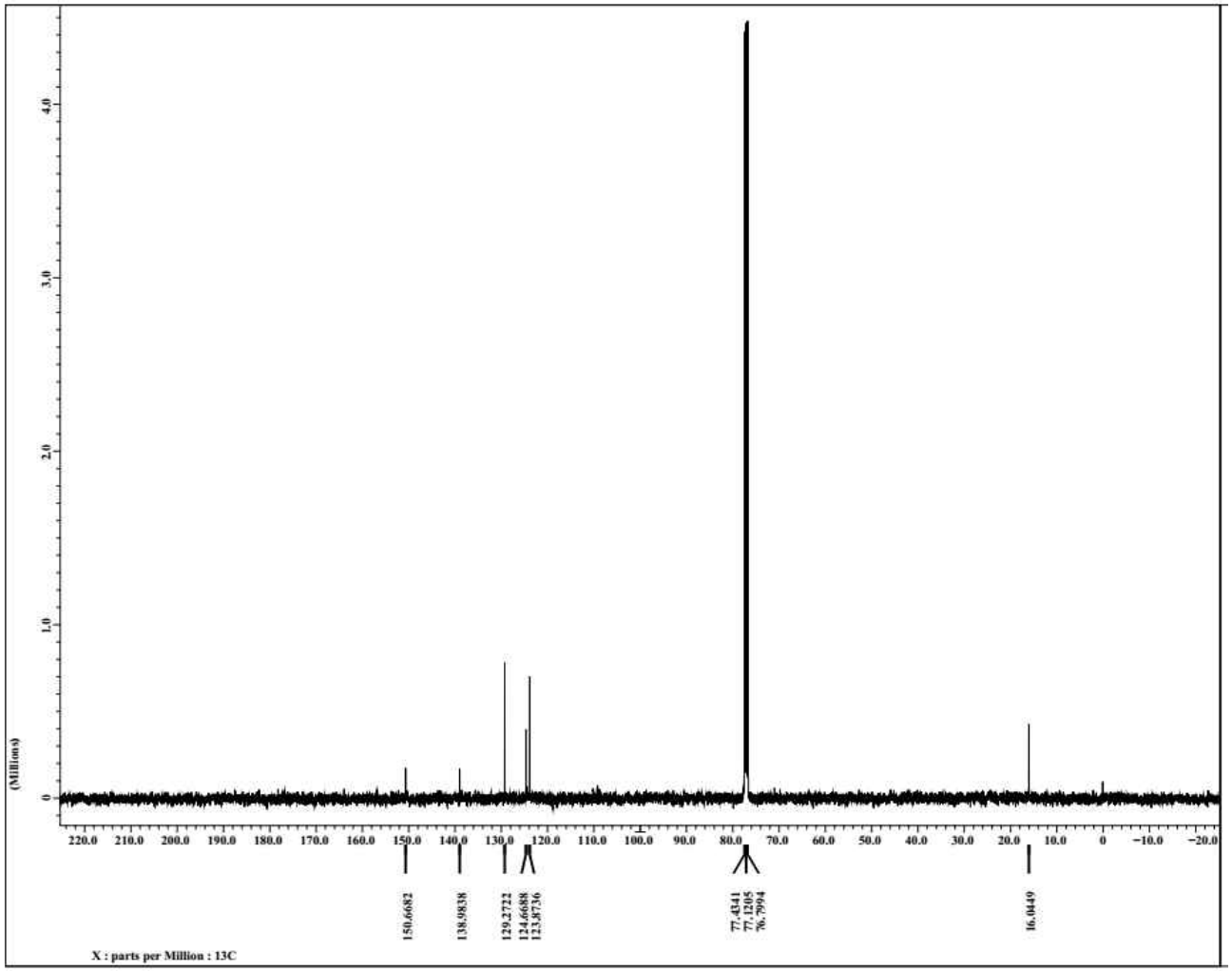

Appendix K3: GC-MS Spectrum for Compound **11**

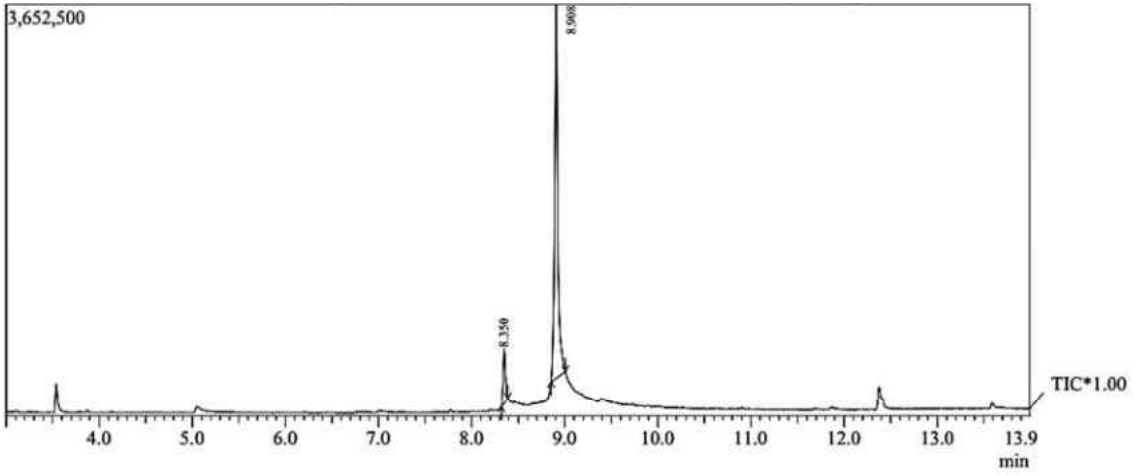

Line#:2 R.Time:8.9(Scan#:845)
MassPeaks:260
RawMode:Averaged 8.9-8.9(844-846) BasePeak:93(502372)
BG Mode:Calc. from Peak Group 1 - Event 1

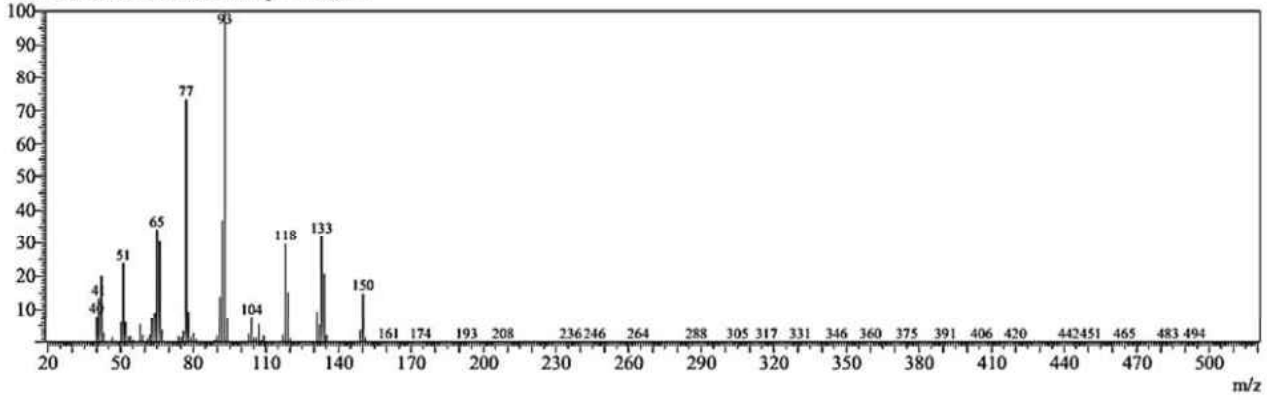

Appendix K4: IR Spectrum for Compound **11** in Chloroform

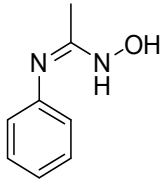

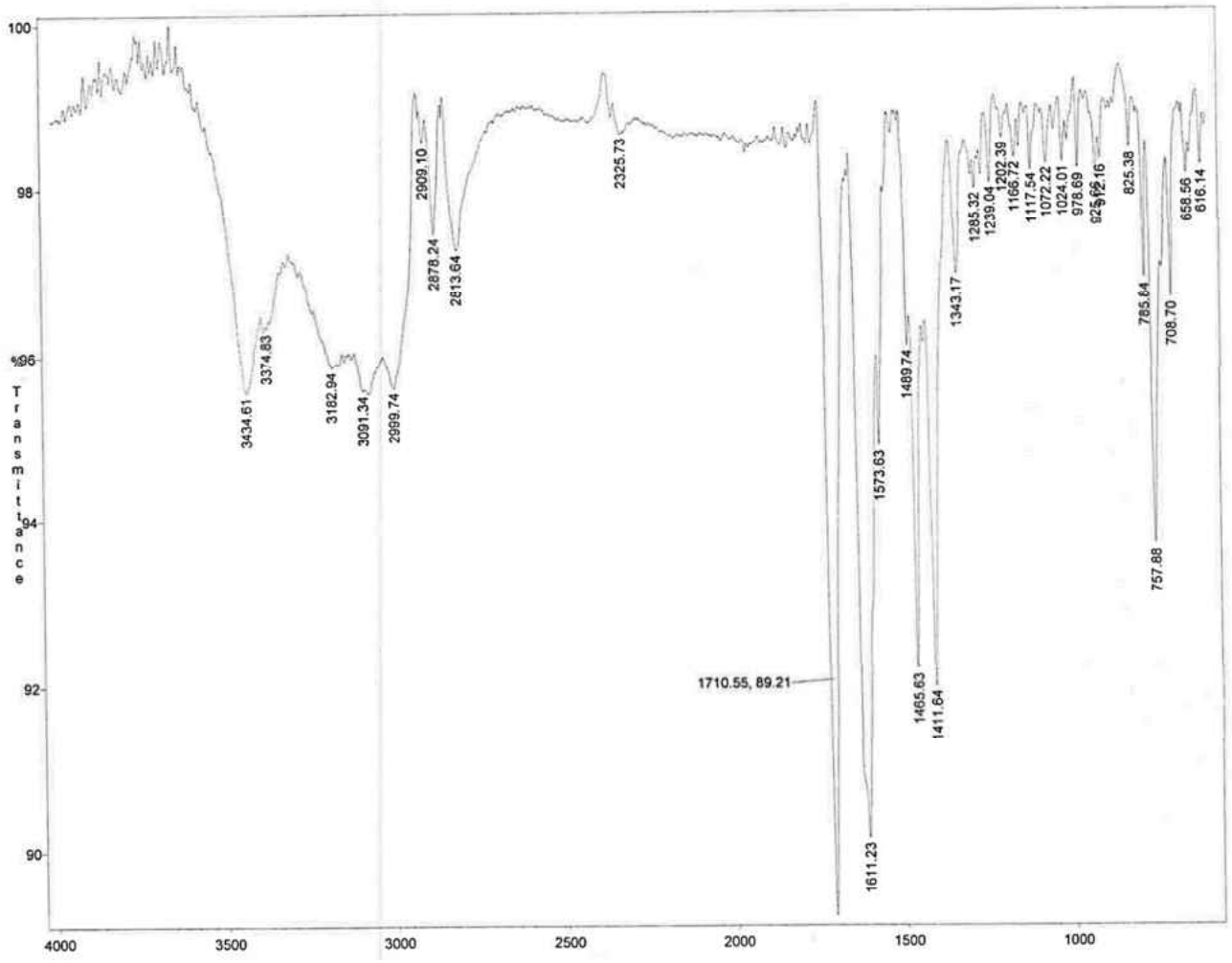

Appendix L1: ^{1}H NMR Spectrum for Compound **12** in Chloroform-d

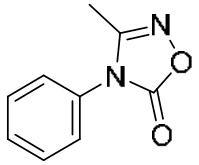

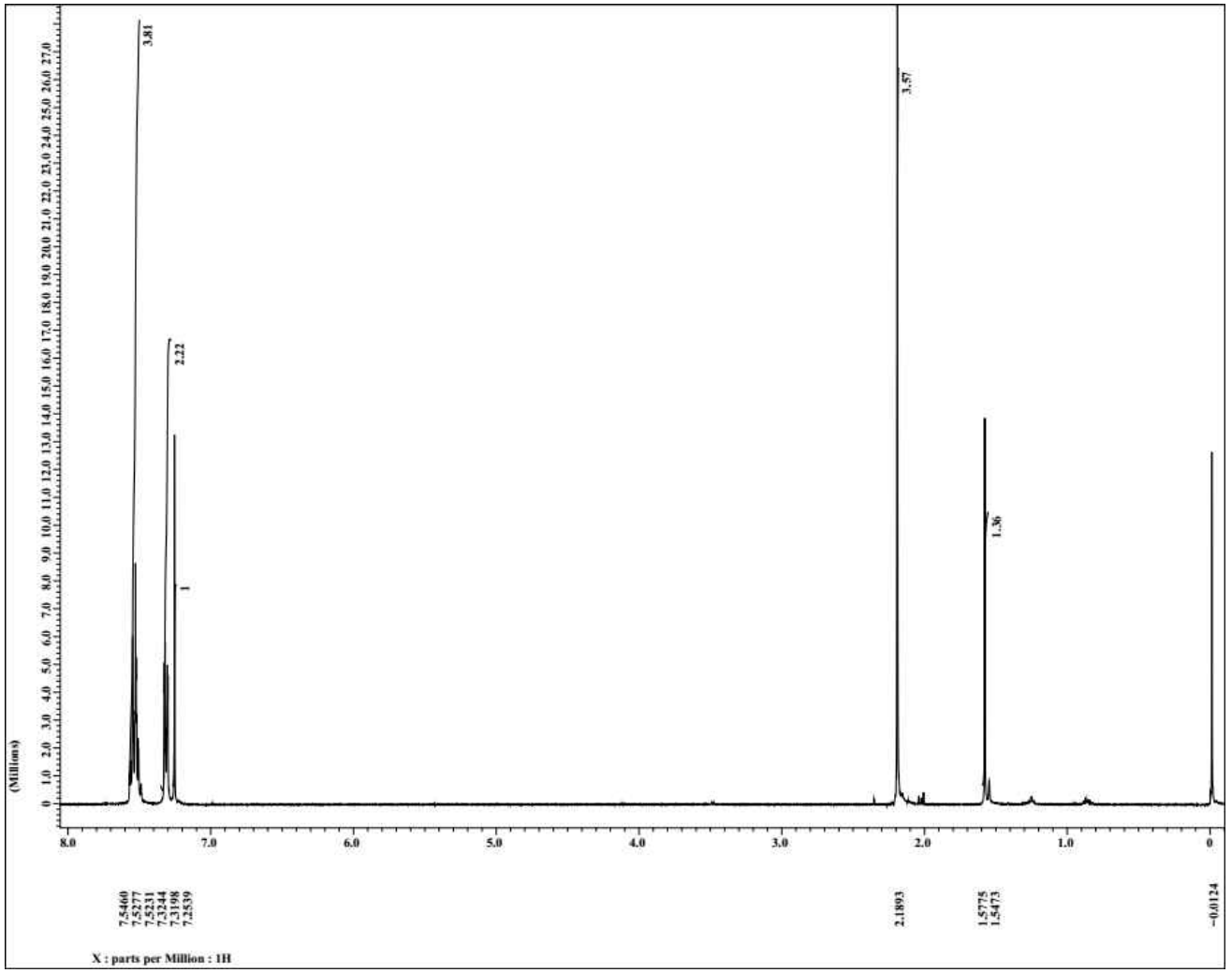

Appendix L2: ^{13}C NMR Spectrum for Compound **12** in Chloroform-d

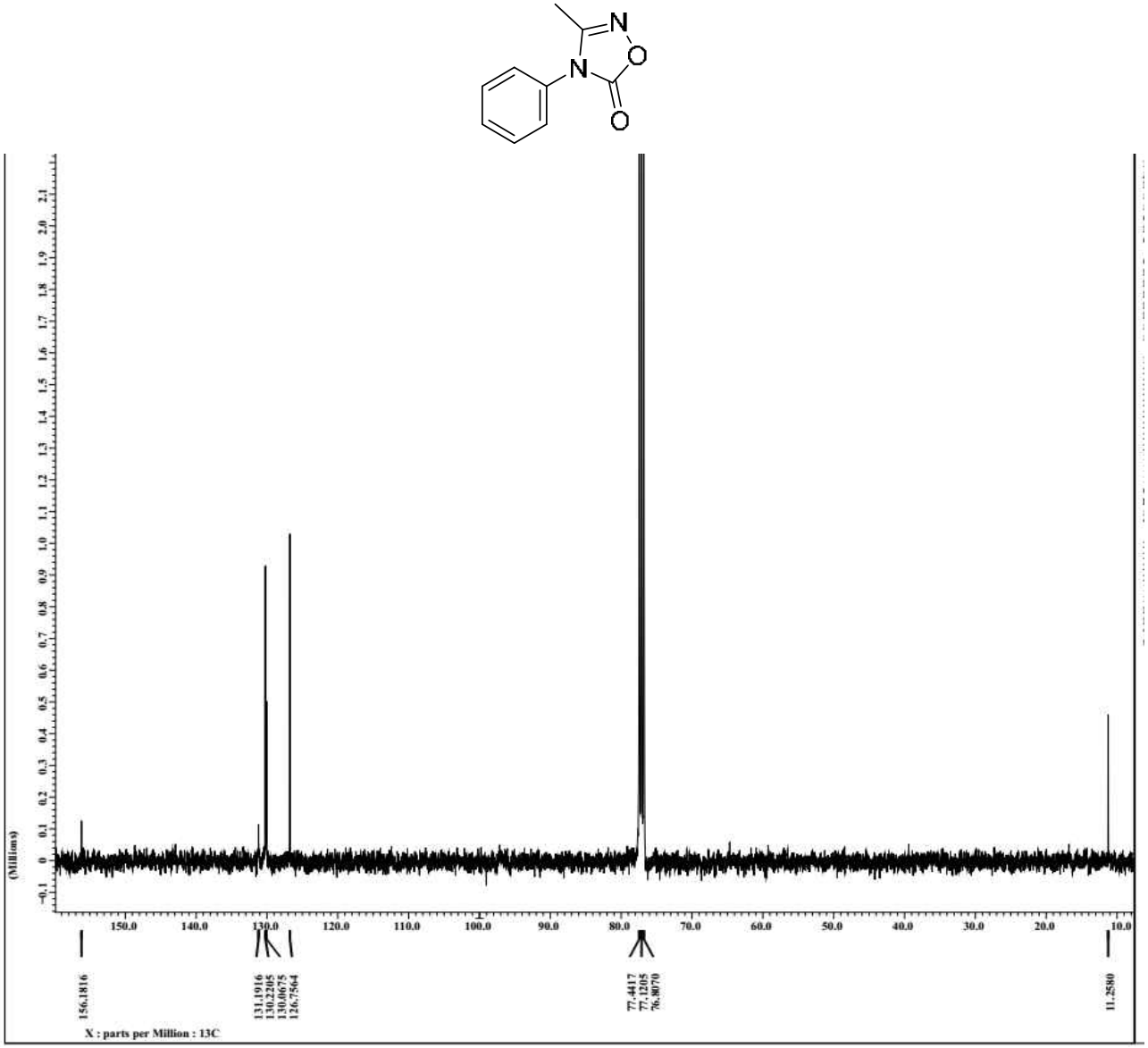

Appendix L3: GC-MS Spectrum for Compound **12** in Chloroform

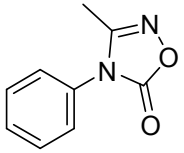

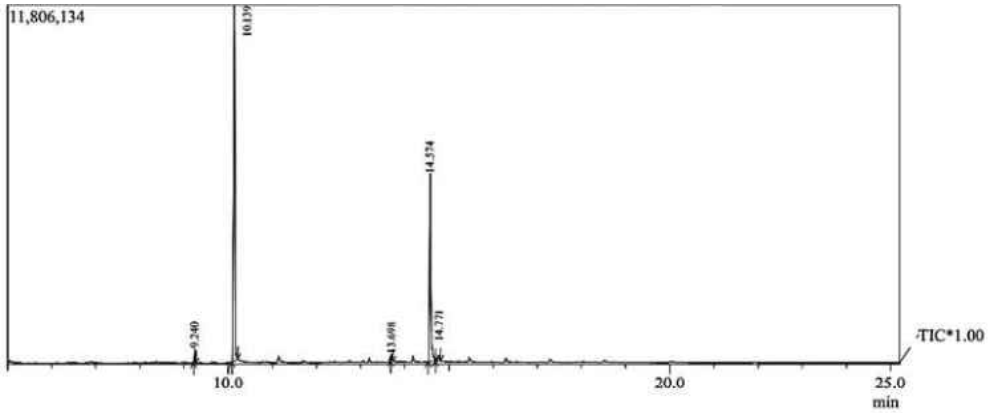

Peak Report TIC

Peak#	R.Time	I.Time	F.Time	Area	Area%	Height	Height%	A/H	Mark	Name
1	9.240	9.214	9.270	608706	1.48	468374	2.49	1.30		Phenol, 2,6-bis(1,1-dimethylethy
2	10.139	10.082	10.215	26207026	63.78	11695676	62.30	2.24		1-Phenyl-5-(methylamino)-1H-t
3	13.698	13.680	13.736	365441	0.89	224731	1.20	1.63	V	Hexanedioic acid, bis(2-ethylhe
4	14.574	14.527	14.695	13479602	32.81	6202188	33.04	2.17		Di-n-octyl phthalate
5	14.771	14.695	14.814	427395	1.04	182279	0.97	2.34	V	Heneicosane
				41088170	100.00	18773248	100.00			

Line#:2 R.Time:10.1(Scan#:735)
MassPeaks:259
RawMode:Averaged 10.1-10.1(734-736) BasePeak:77(1450824)
BG Mode:Calc. from Peak Group 1 - Event 1

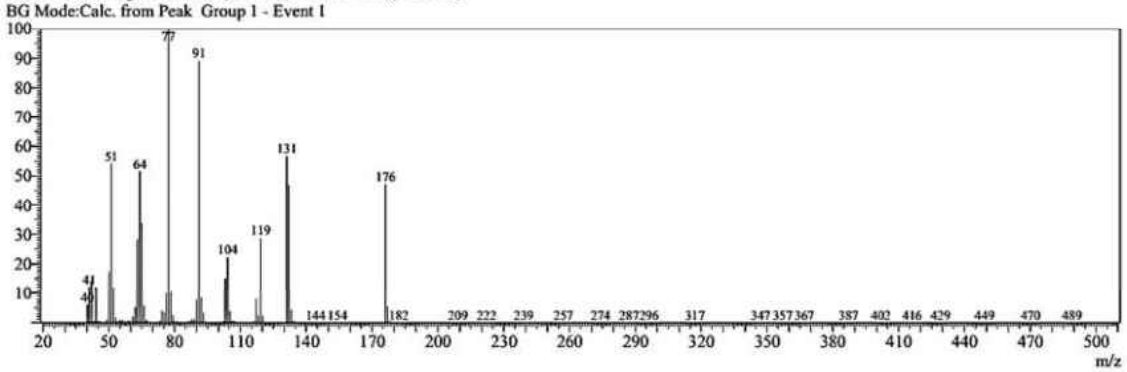

Appendix L4: 1H NMR Spectrum for Compound **12** in Chloroform-d

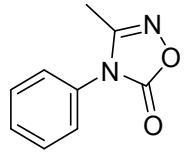

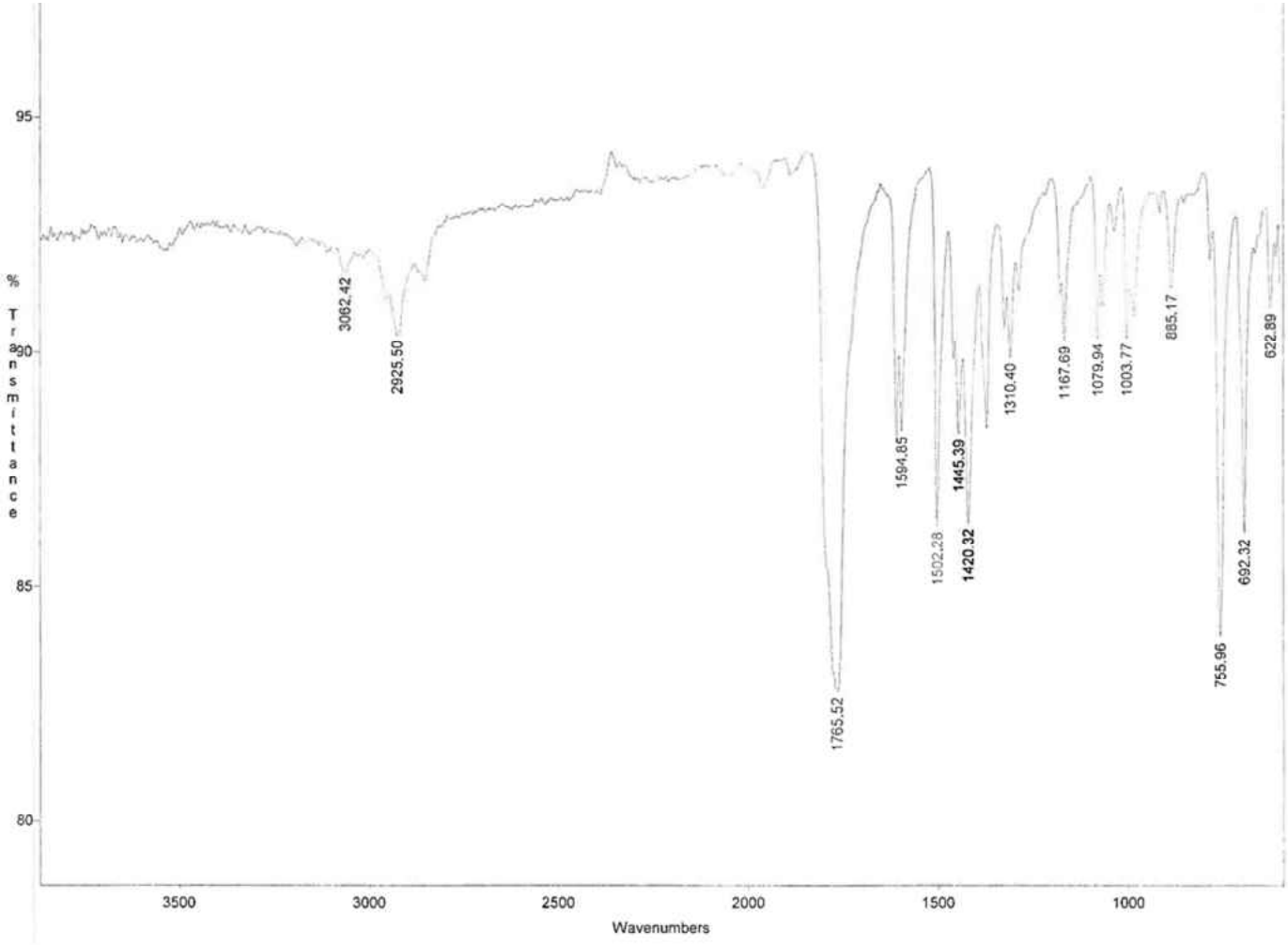

Appendix M1: ^{1}H NMR Spectrum for Compound **13** in Chloroform-d

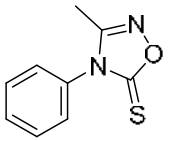

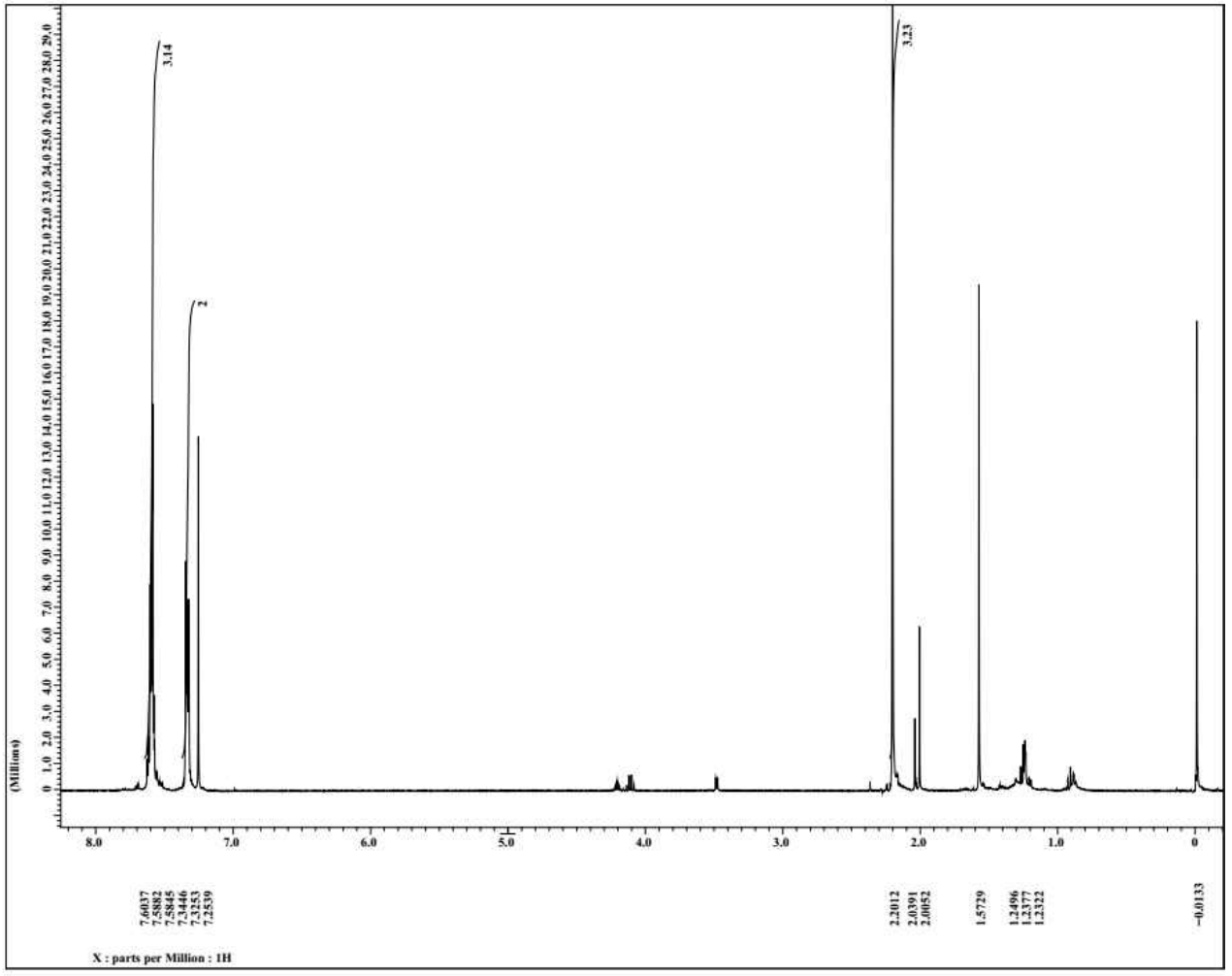

Appendix M2: ^{13}C NMR Spectrum for Compound **13** in Chloroform-d

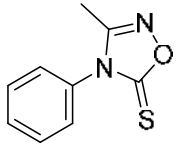

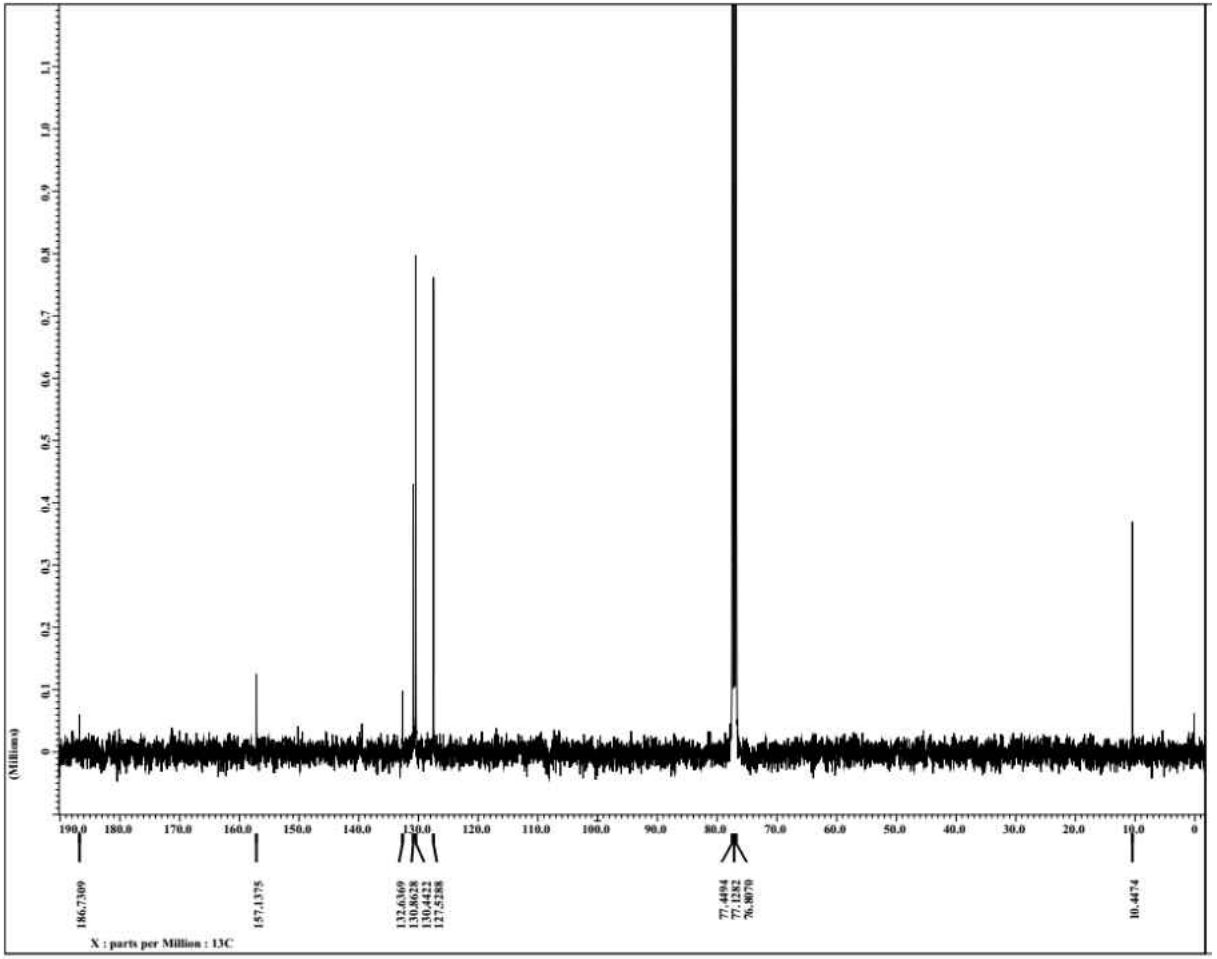

Appendix M3: GC-MS Spectrum for Compound **13** in Chloroform

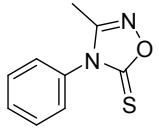

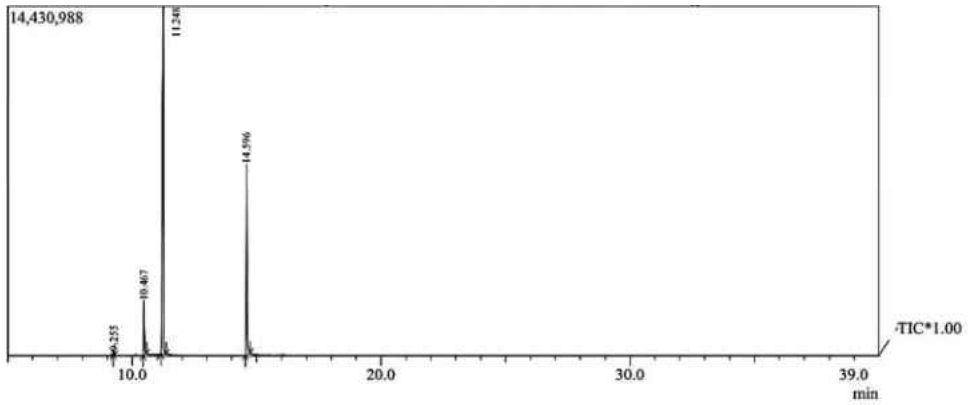

Peak Report TIC

Peak#	R.Time	I.Time	F.Time	Area	Area%	Height	Height%	A/H	Mark	Name
1	9.255	9.228	9.291	197962	0.30	154460	0.63	1.28		Phenol, 2,6-bis(1,1-dimethyleth
2	10.467	10.425	10.579	4907874	7.33	2221283	9.03	2.21		Urea, N-phenyl-N'-1,2,3-thiadia
3	11.248	11.160	11.370	45625658	68.11	14336972	58.29	3.18		1,2,3,4-Thiatriazol-5-amine, N-p
4	14.596	14.548	14.744	16256334	24.27	7883260	32.05	2.06		Di-n-octyl phthalate
				66987828	100.00	24595975	100.00			

Line#:3 R.Time:11.3(Scan#:894)
MassPeaks:289
RawMode:Averaged 11.2-11.3(893-895) BasePeak:77(1408182)
BG Mode:Calc. from Peak Group 1 - Event 1

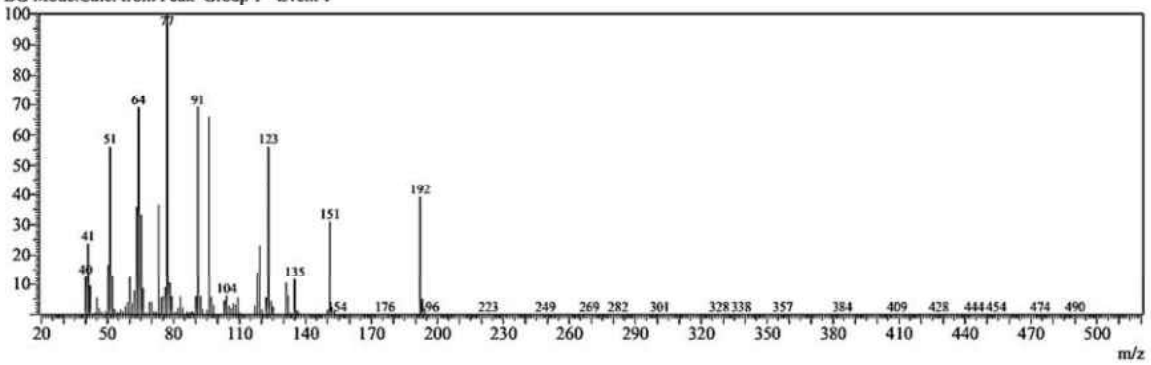

Appendix M4: IR Spectrum for Compound **13** in Chloroform

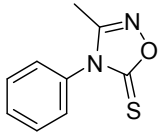

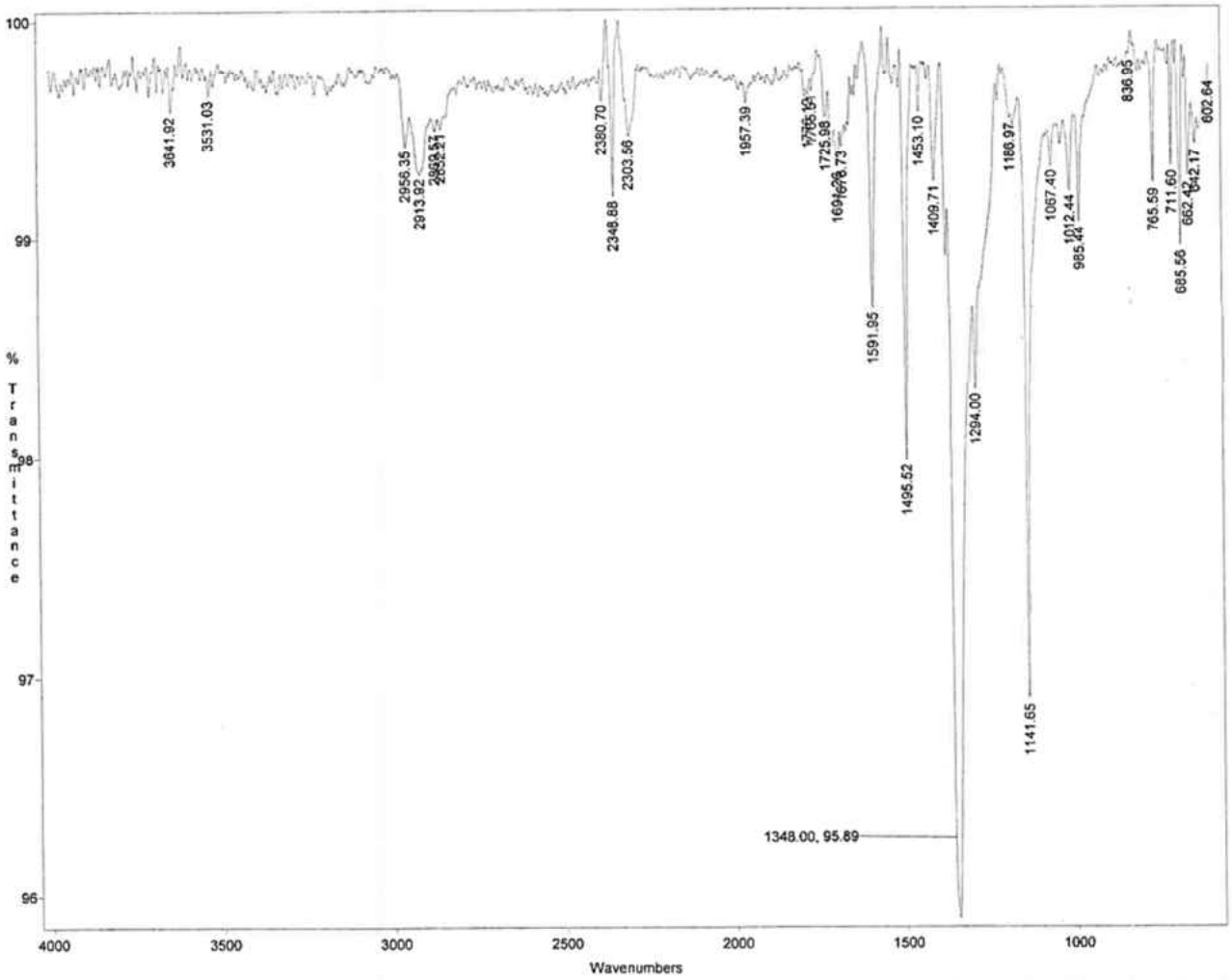

Appendix N1: Crystal data, structure refinement, Bond lengths [Å] and angles [°] for **6**

Table 7: Crystal data and structure refinement for **6**.

Identification code	6	
Empirical formula	$C_{13}H_{11}N_3O_3$	
Formula weight	257.25	
Temperature	100.00(10) K	
Wavelength	0.71073 Å	
Crystal system	Monoclinic	
Space group	I 1 2 1	
Unit cell dimensions	*a* = 14.6877(6) Å	□= 90°.
	b = 6.8905(3) Å	□= 91.751(4) °.
	c = 11.5288(5) Å	□ = 90°.
Volume	1166.23(8) Å^3	
Z	4	
Density (calculated)	1.465 Mg/m^3	
Absorption coefficient	0.107 mm^{-1}	
F (000)	536	
Crystal size	0.2255 x 0.1477 x 0.108 mm^3	
Theta range for data collection	3.445 to 32.367°.	
Index ranges	-21<=h<=21, -9<=k<=10, -16<=l<=16	
Reflections collected	10951	
Independent reflections	3882 [R(int) = 0.0435]	
Completeness to theta = 30.000°	99.7 %	
Absorption correction	Semi-empirical from equivalents	
Max. and min. transmission	1.00000 and 0.95967	
Refinement method	Full-matrix least-squares on F^2	
Data / restraints / parameters	3882 / 1 / 172	
Goodness-of-fit on F^2	1.028	
Final R indices [I>2sigma(I)]	R1 = 0.0518, wR2 = 0.0954	
R indices (all data)	R1 = 0.0631, wR2 = 0.1003	
Absolute structure parameter	-0.9(7)	
Extinction coefficient	n/a	
Largest diff. peak and hole	0.262 and -0.227 e.Å^{-3}	

Table 8: Bond lengths [Å] and angles [°] for **6**.

O(1)-C(1)	1.226(3)	N(2)-C(8)	1.369(3)	C(5)-C(6)	1.382(4)
O(2)-C(10)	1.202(3)	N(2)-C(10)	1.386(3)	C(6)-C(7)	1.386(3)
O(3)-N(3)	1.441(3)	N(3)-C(8)	1.288(3)	C(8)-C(9)	1.495(3)
O(3)-C(10)	1.358(3)	C(1)-C(2)	1.508(3)	C(9)-C(11)	1.525(3)
N(1)-C(1)	1.348(3)	C(2)-C(3)	1.398(3)	C(11)-C(12)	1.528(3)
N(1)-C(9)	1.468(3)	C(2)-C(7)	1.401(3)	C(12)-C(13)	1.526(3)
N(1)-C(13)	1.470(3)	C(3)-C(4)	1.379(4)		
N(2)-C(7)	1.424(3)	C(4)-C(5)	1.386(4)		

C(10)-O(3)-N(3)	109.94(17)	N(1)-C(9)-C(11)	103.83(17)
C(1)-N(1)-C(9)	125.75(18)	C(8)-C(9)-C(11)	113.24(19)
C(1)-N(1)-C(13)	122.07(18)	O(2)-C(10)-O(3)	124.2(2)
C(9)-N(1)-C(13)	112.18(17)	O(2)-C(10)-N(2)	130.2(2)
C(8)-N(2)-C(7)	126.35(18)	O(3)-C(10)-N(2)	105.6(2)
C(8)-N(2)-C(10)	107.0(2)	C(9)-C(11)-C(12)	103.84(18)
C(10)-N(2)-C(7)	126.6(2)	C(13)-C(12)-C(11)	103.43(19)
C(8)-N(3)-O(3)	103.95(18)	N(1)-C(13)-C(12)	103.09(1)
O(1)-C(1)-N(1)	121.8(2)		
O(1)-C(1)-C(2)	119.7(2)		
N(1)-C(1)-C(2)	118.52(18)		
C(3)-C(2)-C(1)	116.0(2)		
C(3)-C(2)-C(7)	117.5(2)		
C(7)-C(2)-C(1)	126.4(2)		
C(4)-C(3)-C(2)	121.4(2)		
C(3)-C(4)-C(5)	120.0(2)		
C(6)-C(5)-C(4)	120.0(2)		
C(5)-C(6)-C(7)	119.8(2)		
C(2)-C(7)-N(2)	121.28(19)		
C(6)-C(7)-N(2)	117.4(2)		
C(6)-C(7)-C(2)	121.3(2)		
N(2)-C(8)-C(9)	119.90(19)		
N(3)-C(8)-N(2)	113.47(19)		
N(3)-C(8)-C(9)	126.6(2)		
N(1)-C(9)-C(8)	107.49(17)		

VITA

JOSEPH OSAMUDIAMEN OSAZEE

Education:

B.Sc. Microbiology (Honors; Second Class Upper Division) University of Benin, Benin City, Nigeria, 2008

M.Sc. Environmental Plant Physiology, University of Benin, Benin City, Nigeria, 2014

M.S. Chemistry East Tennessee State University, Johnson City, Tennessee, 2016

Professional Experience:

Graduate Teaching Assistant, East Tennessee State University College of Arts & Sciences, 2015 – 2016

Publications:

Mgbeze, G. C. and Osazee, J. O. "Assessment of Floristic, microbial composition and growth of *Sphenostylis stenocarpa* (Hochst ex A. Rich) in soil from Two Dumpsites in Benin city, Nigeria", *Journal of Basic & Applied Sciences*, 2014, *10,* 357–365.

Ikhajiagbe, B., Chijioke – Osuji, C. C. and Osazee, J. O., "Heavy metal contents and microbial diversity of waste engine oil – polluted soil in some public and commercial centers in Benin City metropolis, Nigeria", *The Bioscientist,* 2014*, 2(1),* 41-53.

Daniel, E.O., Osazee, J.O. and Iseh, E.C., "Total Microbial count and nutritional analysis of four weaning foods sold in Benin City", *NISEB Journal,* 2013, *13 (3&4)*, 61 – 64.

Osazee, J. O., Daniel, O. E., Ogunsan, F. E., and Elimian, O. K., "*In-vitro* screening of antibacterial potentials of *Aspilia africana* leaves", *The Bioscientist,* 2013, *1(2)*, 140 – 146.

Elimian, O. K., Daniel, O. E., Adesanmi, E. A., and Osazee, J. O., "Comparative analysis of A*geratum conyzoides* L. and

Ocimum gratissimum extracts on some clinical bacterial isolates", *Asian Journal of Plant Science and Research*, 2013, *3(5),* 65 – 69.

Osazee, J. O., Obayagbona, N. O. and Daniel, E. O., "Microbiological and Physiochemical Analyses of Top soils obtained from four municipal waste dumpsites in Benin City, Nigeria", *International Journal of Microbiology and Mycology*, 2013, *1(1),* 23 – 30.

Presentations:

Osazee, J. O., and Shilabin, A. G., "Synthesis and Molecular docking of Pyrrolobenzodiazepine derivatives as potential non-β-lactam β-lactamase inhibitors", 71st SWRM/ 67th SERMACS, Memphis, TN 38103, USA, November 4-9, 2015. Abstr: General Biological Chemistry – 277

Osazee, J. O. and Shilabin, A. G., "Fragment-Based Design and Evaluation of Pyrrolo[2,1-C][1,4]benzodiazepine Derivatives as Novel Non-β-lactam β-Lactamase Inhibitors", Appalachian Student Research Forum, Johnson City, TN 37604, USA, April 8 – 9, 2015. Abstr: Natural Sciences – 68

Aibangbee, J., Osazee, J. O., Galau, B. P., Osazee, O. J. and Daniel, E. O., "Antibiotic susceptibility, plasmid isolation and curing of some foodborne pathogens", Appalachian Student Research Forum, Johnson City, TN 37604, USA, April 8 – 9, 2015. Abstr: Biomedical and Health Sciences – 48.

Honors and Awards:

First Prize for Master Student Poster Presentation (Natural Sciences – Group B) at the 2015 Appalachian Student Research Forum.